



**Calhoun: The NPS Institutional Archive**  
**DSpace Repository**

---

Theses and Dissertations

1. Thesis and Dissertation Collection, all items

---

1972

# Automatic control systems for longitudinal motion of semisubmerged ships.

Monell, Gilbert Finley.

Monterey, California. Naval Postgraduate School

---

<http://hdl.handle.net/10945/16007>

---

*Downloaded from NPS Archive: Calhoun*



Calhoun is the Naval Postgraduate School's public access digital repository for research materials and institutional publications created by the NPS community. Calhoun is named for Professor of Mathematics Guy K. Calhoun, NPS's first appointed -- and published -- scholarly author.

**Dudley Knox Library / Naval Postgraduate School**  
**411 Dyer Road / 1 University Circle**  
**Monterey, California USA 93943**

<http://www.nps.edu/library>

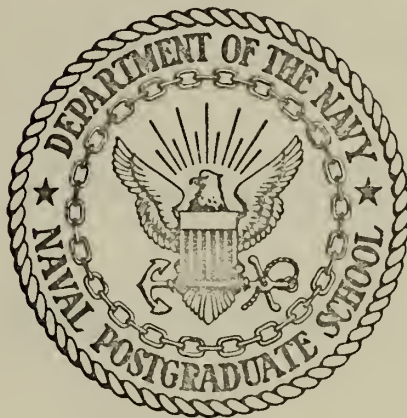
AUTOMATIC CONTROL SYSTEMS FOR  
LONGITUDINAL MOTION OF SEMISUBMERGED SHIPS

Gilbert Finley Monell

LIBRARY  
U.S. Naval Postgraduate School  
Monterey, California 93940

# NAVAL POSTGRADUATE SCHOOL

## Monterey, California



# THESIS

AUTOMATIC CONTROL SYSTEMS  
FOR  
LONGITUDINAL MOTION OF SEMISUBMERGED SHIPS

by

Gilbert Finley Monell, Jr.

Thesis Advisor:

D. E. Kirk

September 1972

*Approved for public release; distribution unlimited.*

1149341



Automatic Control Systems  
for  
Longitudinal Motion of Semisubmerged Ships

by

Gilbert Finley Monell, Jr.  
Lieutenant, United States Navy  
BSEE, Purdue University, 1966

Submitted in partial fulfillment of the  
requirements for the degree of

ELECTRICAL ENGINEER

from the

NAVAL POSTGRADUATE SCHOOL  
September 1972

Thesis  
M 673  
c. 1

# ABSTRACT

Optimal control theory is used to develop three automatic control systems for the longitudinal motion of a semisubmerged ship. A linearized mathematical model of the ship motion is used and the control problem is treated as a linear regulator. Simulations of the ship's longitudinal motions, utilizing the three control systems, are compared for various sea conditions. It is concluded that if the wave forces and moments are known or are estimated as functions of time, a suboptimal controller is the best controller. However, if a frequency domain approach is used to estimate the wave forces and moments, the complexity of a suboptimal controller approaches that of an optimal controller and the difference between the two is negligible. Preliminary work on three techniques for estimating the forces and moments is presented.





## TABLE OF CONTENTS

I.	INTRODUCTION	7
II.	PROBLEM FORMULATION	10
	A. NON-DIMENSIONALITY	10
	B. SEMISUBMERGED SHIP FORM USED FOR THEORETICAL ANALYSIS	11
	C. COORDINATE SYSTEM	11
	1. $X_S$ - Axis	14
	2. $Y_S$ - Axis	15
	3. $Z_S$ - Axis	15
	4. Angles of Rotation	15
	D. LONGITUDINAL RESPONSE PROBLEM	15
III.	SIMULATION MODEL	17
	A. LINEARIZED EQUATIONS OF MOTION	17
	B. TRANSFER FUNCTIONS	20
	C. COMPUTER MODEL	22
	1. Analog Model	22
	2. Digital Model	25
IV.	CONTROL SYSTEMS FOR THE SEMISUBMERGED SHIP	28
	A. PERFORMANCE MEASURE	28
	B. CONTROL SYSTEM FOR THE SHIP IN A CALM SEA	29
	C. THE OPTIMAL CONTROL LAW FOR THE SHIP WHEN SUBJECTED TO WAVE FORCES	30
	D. A SUBOPTIMAL CONTROL LAW FOR THE SHIP WHEN SUBJECTED TO WAVE FORCES	35
	E. CONSTANT STATE FEEDBACK	38



V.	SIMULATION PROCEDURE	46
A.	WAVE MODEL	46
B.	COMMAND SIGNAL	48
VI.	RESULTS	53
A.	CASES INVESTIGATED	53
1.	Case I	56
2.	Case II	56
3.	Case III	56
4.	Case IV	56
5.	Case V	56
6.	Case VI	56
B.	THE EFFECT OF VARYING THE CONTROL WEIGHTING MATRIX (CASE I)	56
C.	CONSTRAINED CONTROL SURFACE DEFLECTIONS (CASE II)	57
D.	THE CONSTANT-GAIN CONTROLLER (CASE III)	64
E.	THE OPTIMAL CONTROLLER (CASE IV)	68
F.	THE SUBOPTIMAL CONTROLLER (CASE V)	68
G.	THE EFFECT OF INACCURATE ESTIMATION OF WAVE FORCES (CASE VI)	68
VII.	PRELIMINARY WORK ON WAVE ESTIMATORS	81
A.	AN INPUT-SIGNAL OBSERVER	81
B.	FAST-FOURIER TRANSFORM ESTIMATION	84
C.	STATE OBSERVER MODEL	85
VIII.	CONCLUSIONS	89
A.	THE CONTROLLER	89
B.	RECOMMENDATIONS FOR FURTHER STUDY	90
1.	Sea Conditions	90
2.	Control Dynamics	9



3. Measurement Noise	90
4. Wave Estimator	90
5. Weighting Matrices	91
6. Wave Contouring	91
APPENDIX A	92
APPENDIX B	94
COMPUTER PROGRAM	95
LIST OF REFERENCES	110
INITIAL DISTRIBUTION LIST	111
FORM DD 1473	112



## ACKNOWLEDGEMENT

A significant debt of gratitude is owed to Dr. D. E. Kirk, Naval Postgraduate School, for the many hours, ideas and assistance he extended in the preparation of this thesis. A special thanks goes to Dr. H. A. Titus, Naval Postgraduate School, for suggesting the area of investigation, and to Dr. D. T. Higdon, Naval Undersea Research and Development Center, for providing the specific problem areas and data of the semisubmerged ship.





## I. INTRODUCTION

In 1968 the need arose for a small, relatively inexpensive ship which could travel as fast as large Naval vessels and provide support for one of the Naval Undersea Research and Development Center (NUC) projects -- an unmanned undersea vehicle. The ensuing investigation conducted by NUC resulted in the semisubmerged ship concept shown in Fig. 1 [Ref. 1].

Referring to Fig. 1, the concept is described as follows:

- a. The two streamlined hulls provide the primary buoyancy and have less drag and experience smaller wave-induced forces than conventional ship hulls.
- b. A propeller is placed at the end of each hull where efficiency is increased by utilizing the boundary layer inflow.
- c. Two vertical, surface-piercing bouyant struts are attached to each hull, providing hydrostatic stability in pitch and heave due to the waterplane areas and spacing. Hydrodynamic stability in yaw is obtained from the hydrofoil behavior of the struts.
- d. The rudders are placed in the propeller slipstreams which provides additional rudder force and allows the rudders to induce forces on the aft struts.
- e. A horizontal tail surface provides pitch damping as well as pitch stability at high speeds.
- f. The superstructure, aside from providing the normal equipment and personnel spaces, provides the juncture for the



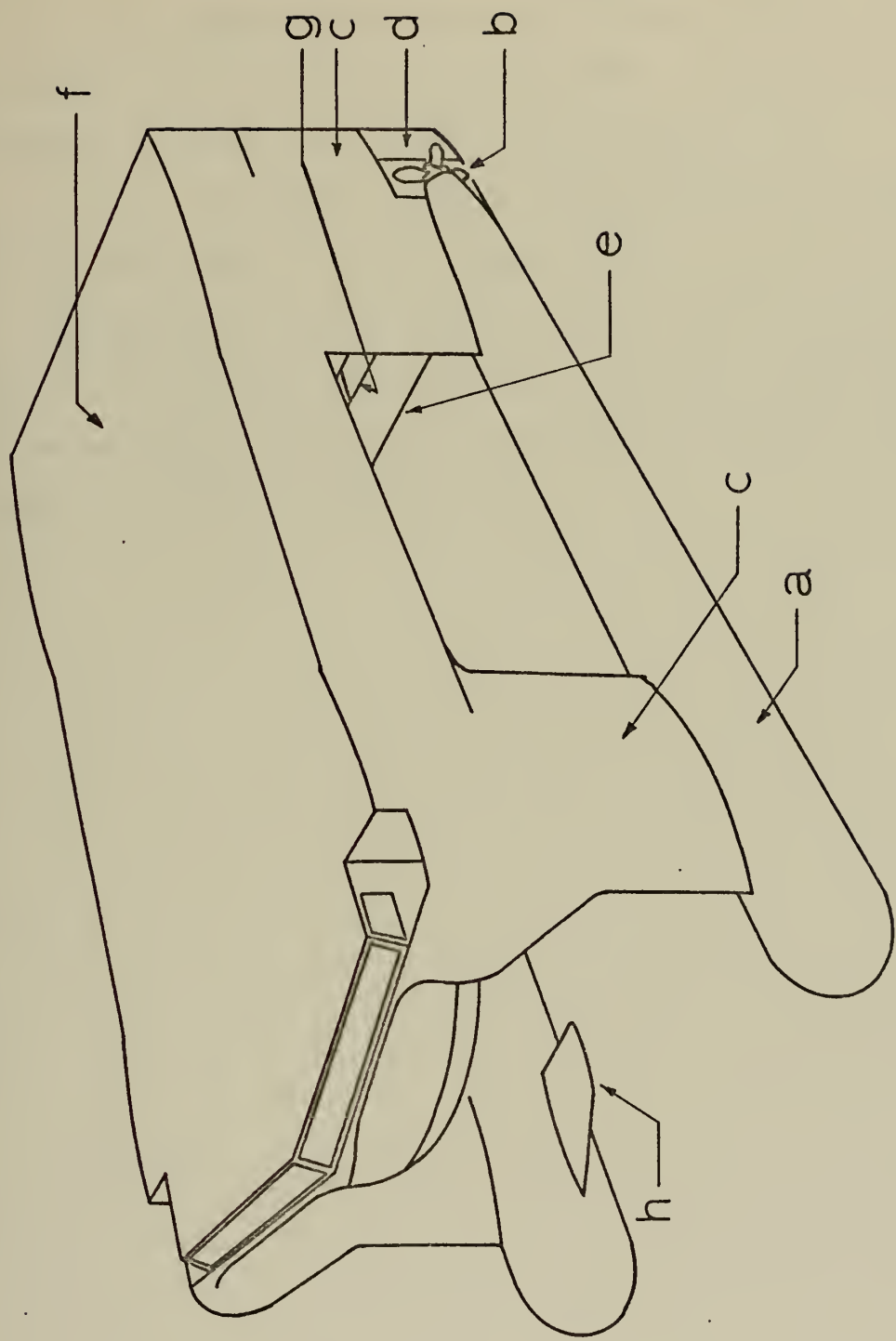


Figure 1. Semisubmerged Ship Concept.



rigid attachment of the two hull-strut systems. This rigid system provides stability in roll.

g. The elevator control surfaces incorporated in the horizontal tail surface allow a means of controlling the ship's response to waves when used in conjunction with

h. the canard control surfaces which are mounted on the forward part of the submerged hulls.

The purpose of this investigation was to consider various ways of controlling the elevator and canard surfaces and make recommendations concerning the method of control and areas requiring further investigation.



## II. PROBLEM FORMULATION

### A. NON-DIMENSIONALITY

The response of a ship to forces -- environmental and/or self-induced by control surface deflections -- can be determined from a system of equations which describe the ship. If the particular ship's displacement is changed, but the hull configuration is retained, it is necessary to determine a new system of equations in order to determine the ship's response. A non-dimensional system of equations however, will allow the response to be determined from this one system of equations and scaled to any particular displacement. The system of equations in this investigation are written in a non-dimensional form based on Froude number scaling.

$$\text{Froude number} = \frac{U}{\sqrt{g} \nabla^{1/3}} \quad (2.1)$$

where

$U$  = ship's forward velocity

$g$  = acceleration of gravity

$\nabla$  = ship's displacement volume

The dimensional values can be determined by multiplying the non-dimensional values by their appropriate factors as given in Table I. The symbol  $\rho$  indicates water density. The characteristic length,  $l_c$ , is the cube root of the displacement volume,  $\nabla$ . The ship's displacement weight is denoted by the symbol  $\Delta$ .



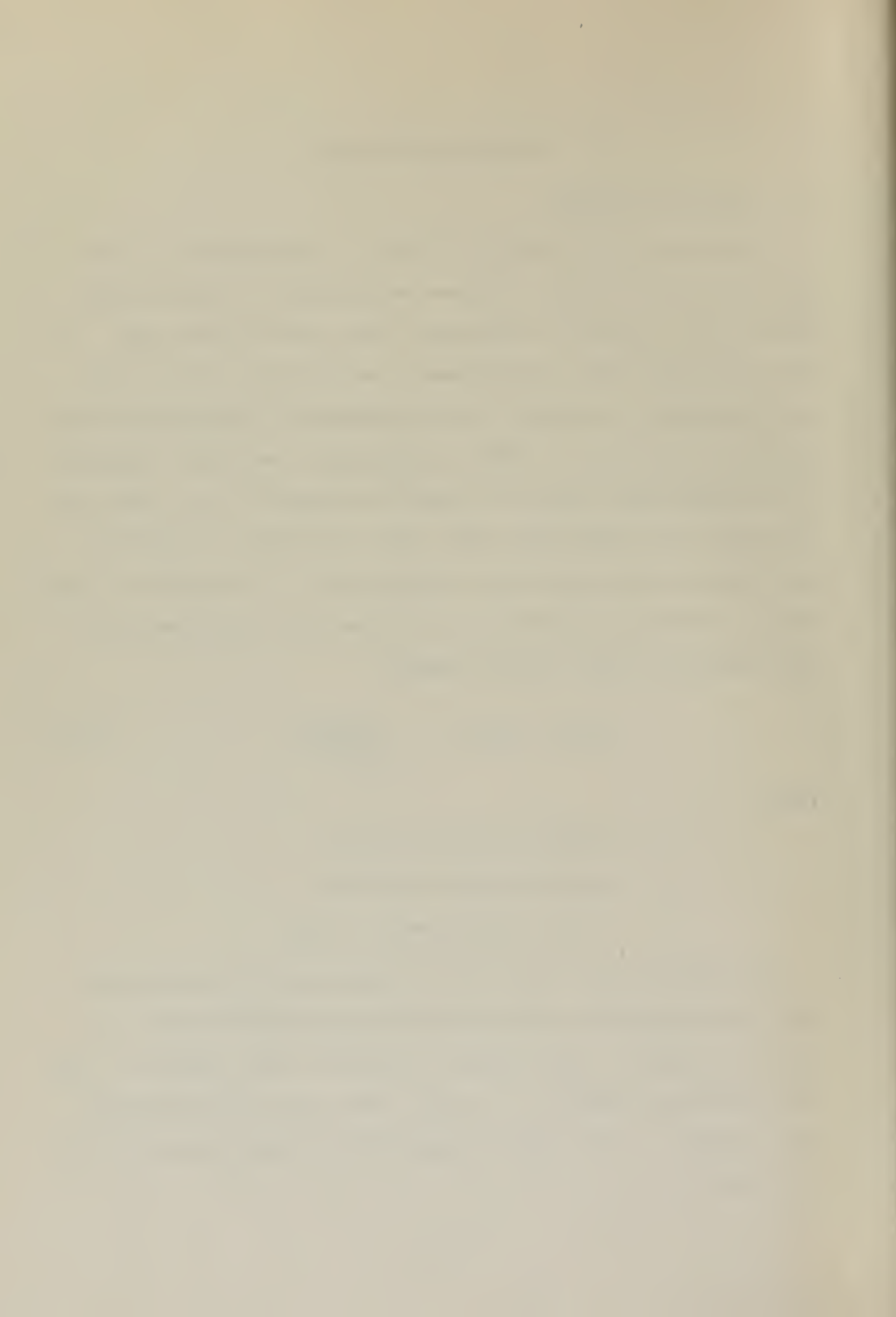


TABLE I  
CONVERSION FACTORS  
(Non-dimensional to Dimensional)

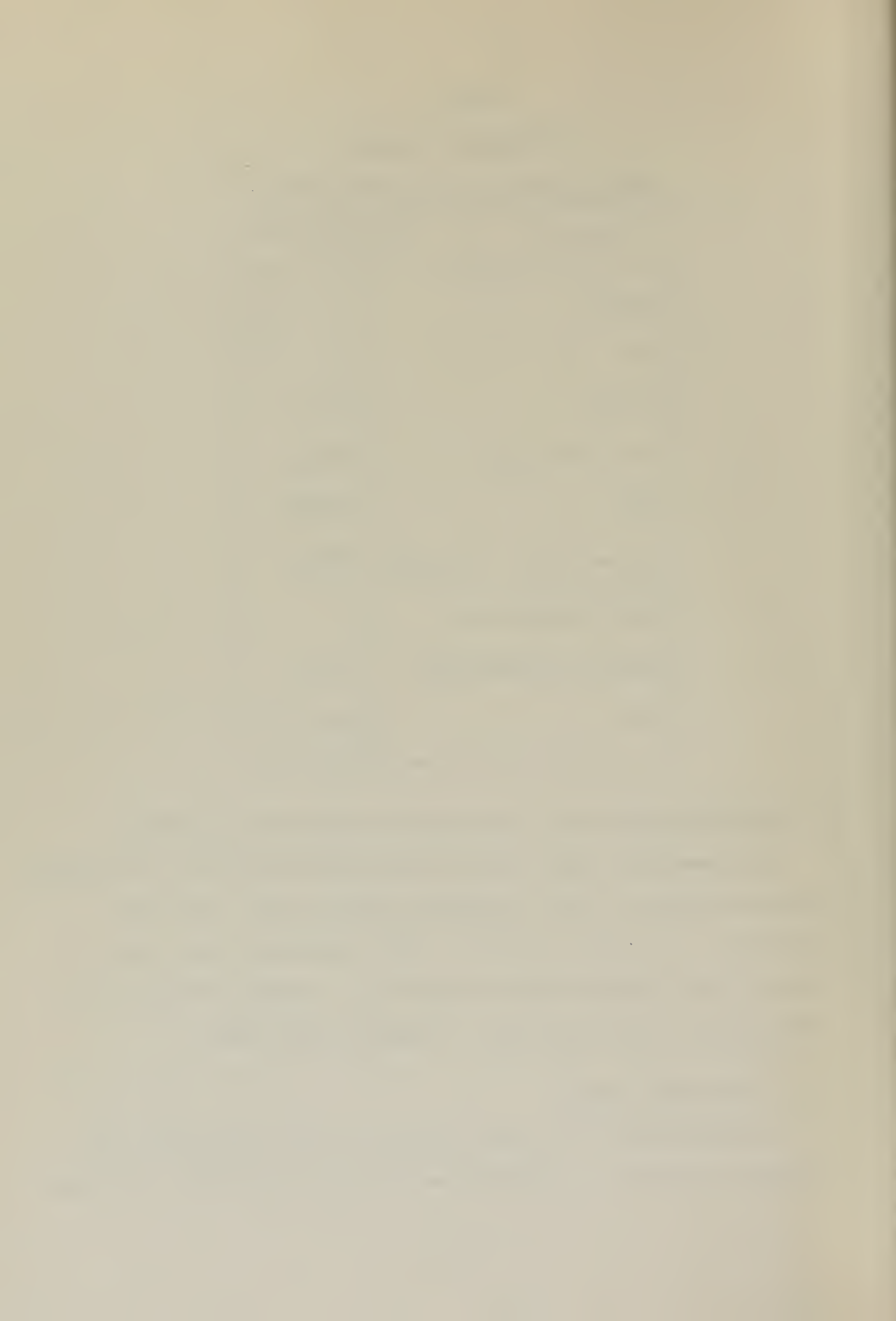
Variable	Multiplication Factor
Length	$l_c = \nabla^{1/3}$
Area	$l_c^2 = \nabla^{2/3}$
Volume	$l_c^3 = \nabla$
Linear Velocity	$\sqrt{g l_c}$
Time	$\sqrt{l_c/g}$
Angular Rate, Frequency	$\sqrt{g/l_c}$
Linear Acceleration	$g$
Angular Acceleration	$g/l_c$
Force	$\rho g \nabla = \Delta$

#### B. SEMISUBMERGED SHIP FORM USED FOR THEORETICAL ANALYSIS

The geometric form used in this discussion and in investigations conducted by Naval Undersea Center (NUC), San Diego, California, is shown in Fig. 2. The dimensions are given in terms of the characteristic length,  $l_c$ . Figure 3 will aid in interpreting the results for a specific ship size.

#### C. COORDINATE SYSTEM

A body moving in a fluid can move in all six degrees of freedom of motion -- translation along each of three orthogonal







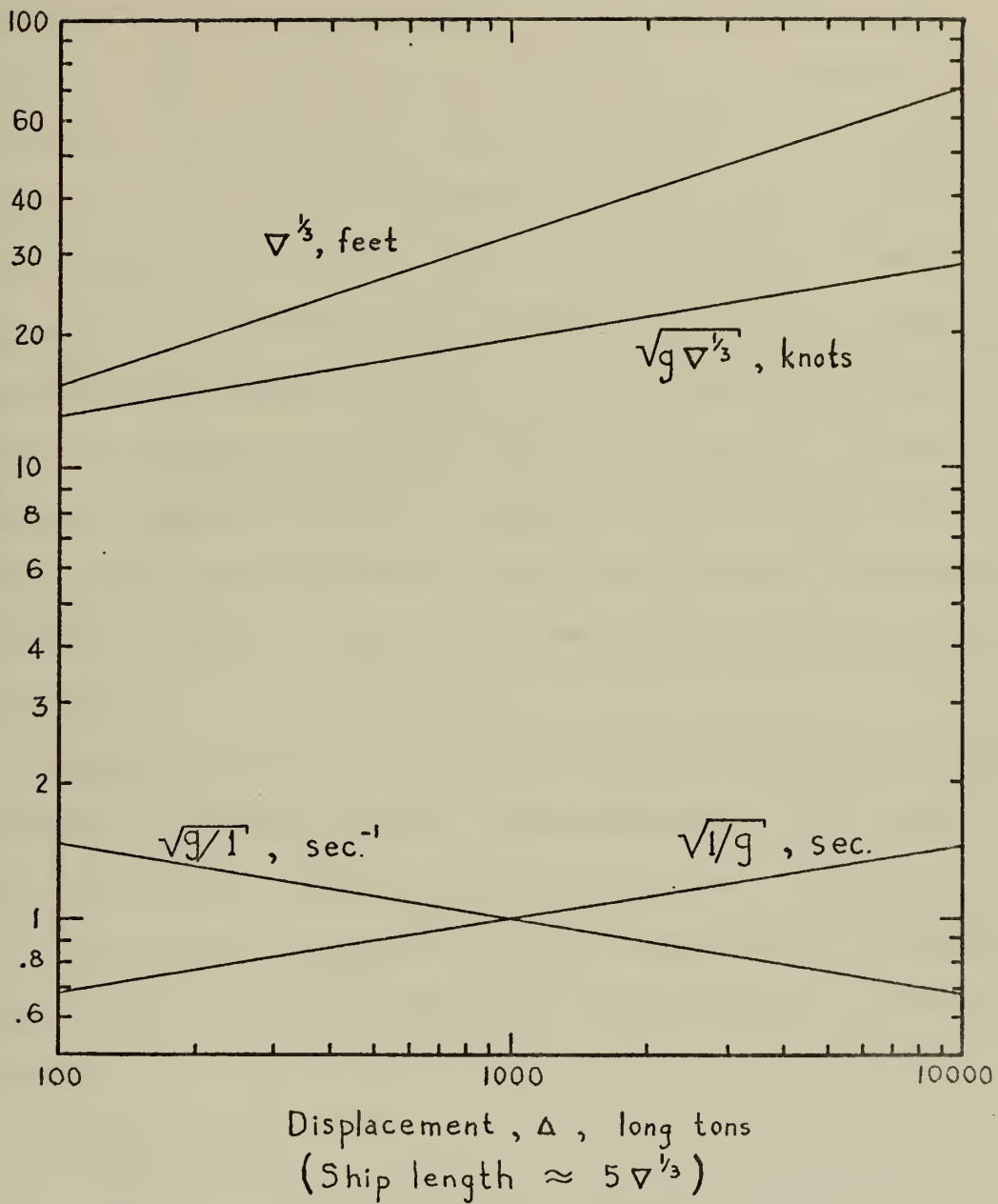


Figure 3. Basic Scaling Parameters as a Function of Ship Displacement [Ref. 3].



axes and rotation about each of the three axes. The choice of a coordinate system should result in one in which the equations of motion can be most conveniently analyzed. The ship under investigation has a plane of symmetry (as have most ships in existence), which is defined by the ship's centerline and a line perpendicular to the ship's deck. Two of the axes are chosen to lie in this plane of symmetry with the remaining axis being orthogonal to the plane. This choice simplifies the expressions for the hydrodynamic forces through symmetry and simplifies the equations of motion because the axes are parallel to the principal axes of inertia [Ref. 2]. If the axes are located such that their origin coincides with the ship's center of mass, the axes become the principal axes of inertia.

The ship's position is given in an Earth-fixed right-hand cartesian coordinate system. The attitude of the ship can be given by an Euler angle transformation from axes parallel to the Earth-fixed axis system to the ship-fixed axis system as chosen above. Figure 4 shows the relationship between the two systems.

1.  $X_s$  - Axis

The  $X_s$  - axis is the ship-fixed longitudinal axis in the plane of symmetry with the positive direction being toward the bow. It is parallel to the ship's keel.





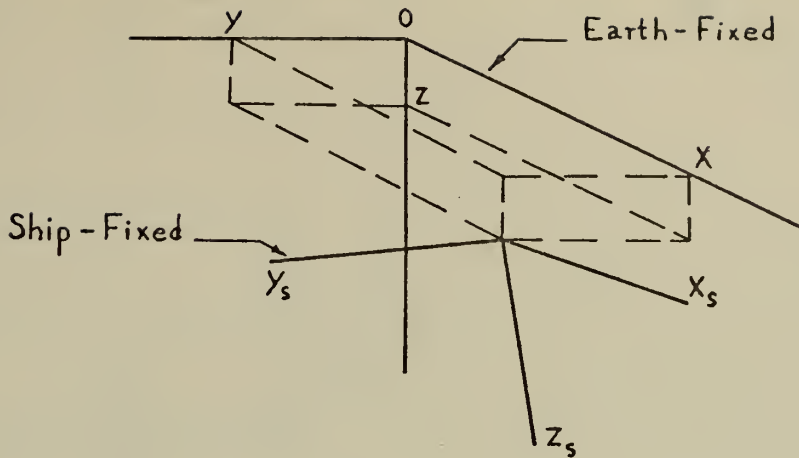


Figure 4. Coordinate System

## 2. $Y_s$ - Axis

The  $Y_s$  - axis is the ship-fixed transverse axis perpendicular to the plane of symmetry. The positive direction is measured to starboard.

## 3. $Z_s$ - Axis

The  $Z_s$  - axis is the "vertical axis" in the plane of symmetry. The positive direction is measured downward toward the keel.

## 4. Angles of Rotation

The axis system that has been chosen forms a consistent right-handed coordinate system. If  $\phi$  is the roll angle,  $\theta$  is the pitch angle and  $\psi$  is the yaw angle, then the positive rotations are as indicated in Fig. 5.

## D. LONGITUDINAL RESPONSE PROBLEM

Previous investigations of the semisubmerged ship response [Ref. 3] have indicated that the pitch and heave motions in



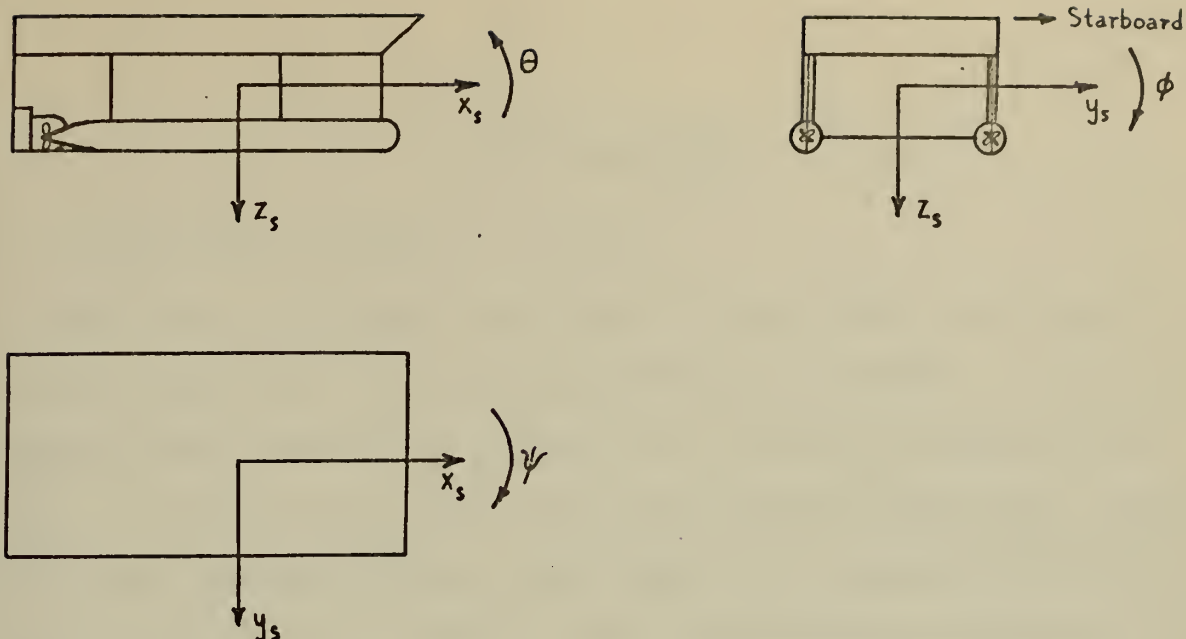


Figure 5. Angles of Rotation

regular head waves are quite small. However, the ship's natural longitudinal response to following waves having a height-to-wavelength ratio of 0.05 has been found to be greater than desired for wavelengths greater than one ship length. In particular, with a non-dimensional speed of 1.65 (high speed), the heave response to a wavelength of 10 (height of 0.5) has been found to be greater than 1.25. The values for a 2000-ton-displacement ship (refer to Fig. 2 for dimensions) would be

wavelength,  $\lambda$  = 410 ft.

wave height,  $h$  = 20.5 ft.

heave,  $z$  = 51.25 ft.

This indicates that the ship is thrown out of the water, then slammed back into the water with the upper platform submerging. This is an intolerable situation and calls for the design of a control system to reduce the ship's natural response.



### III. SIMULATION MODEL

#### A. LINEARIZED EQUATIONS OF MOTION

The force and moment equations for the ship are written in the ship-fixed axis system previously described. If it is assumed that the ship is running at a constant forward velocity,  $U$ , and that all other motion variables (velocities, angular rates and attitude angles) make only small perturbations about straight equilibrium running, then the equations of motion can be linearized and separated into two groups: (1) the lateral-direction equations, and (2) the longitudinal-direction equations [Ref. 2].

The longitudinal-direction equations of motion [Ref. 3] are written below in non-dimensional form. The vertical force is given by Eq. (3.1), the pitching moment by Eq. (3.2) and the kinematic relationships by Eqs. (3.3). The notation is defined in Table II.

$$\begin{aligned}
 \hat{w}' - \hat{U}\hat{q} = & \frac{1}{2} \hat{U}^2 [C_{z_{\hat{w}}} \hat{w} + C_{z_{\hat{q}}} \hat{q} \\
 & + C_{z_{\delta_e}} \delta_e + C_{z_{\delta_c}} \delta_c] - \hat{A}_{wL} \hat{z} \\
 & + \hat{A}_{wL} \hat{X}_{wL} \theta + \hat{Z}_{\hat{w}} \hat{w}' \\
 & + \hat{Z}_{\hat{q}} \hat{q}' + \hat{Z}_w
 \end{aligned} \tag{3.1}$$



TABLE II

## DEFINITION OF NOTATION FOR EQUATIONS OF MOTION

$C_m$	$M/(1/2 \rho U^2 \nabla)$
$\hat{Z}_w$	Non-dimensional wave forces along the $X_s$ axis
$\hat{M}_w$	Non-dimensional wave pitching moment about the $Y_s$ axis
$\hat{A}_{wL}$	Non-dimensional water plane area
$\hat{X}_{wL}$	Non-dimensional $X_s$ coordinate of the centroid of water plane area
$\hat{z}_{mp}$	Non-dimensional metacentric height in pitch
$\hat{\rho}_y$	Non-dimensional radius of gyration about the pitch axis, $Y_s$
$\theta$	Pitch angle
$\hat{z}$	Non-dimensional position of ship center of mass in Earth-fixed coordinates
$\delta_e, \delta_c$	Elevator and canard surface deflection angles
$U, w$	Velocity component along $X_s$ and $Z_s$ axes respectively
$q$	Angular rate about $Y_s$ axis
$Z$	Force along $Z_s$ axis
$M$	Moment about $Y_s$ axis
$\hat{\square}$	Non-dimensional form of $\square$
$\tau$	Non-dimensional time, $t(g/\nabla^{1/3})^{1/2}$
$\square'$	$d\square/d\tau$
$\hat{Z}_\square, \hat{M}_\square$	$\frac{\partial}{\partial \square} \hat{Z}, \frac{\partial}{\partial \square} \hat{M}$
$C_z$	$Z/(1/2 \rho U^2 \nabla^{2/3})$
$C_{z_\square}$	$\frac{\partial}{\partial \square} C_z$





$$\begin{aligned}
 \rho_{\hat{y}}^2 \hat{q}' &= 1/2 \hat{U}^2 [C_{m_{\hat{w}}} \hat{w} + C_{m_{\hat{q}}} \hat{q}' \\
 &\quad + C_{m_{\delta_e}} \delta_e + C_{m_{\delta_c}} \delta_c] - z_{mp} \theta \\
 &\quad + \hat{A}_{wL} \hat{X}_{wL} \hat{z} + \hat{M}_{\hat{w}} \hat{w}' \\
 &\quad + \hat{M}_{\hat{q}} \hat{q}' + \hat{M}_{\hat{w}}
 \end{aligned} \tag{3.2}$$

$$\begin{aligned}
 \theta' &= \hat{q} \\
 \hat{z}' &= -\hat{U}\theta + \hat{w}
 \end{aligned} \tag{3.3}$$

The equations of motion can be rewritten in a form where they are functions of pitch ( $\theta$ ), heave ( $\hat{z}$ ), their respective first and second derivatives, control surface deflections and wave forces and moments by utilizing Eqs. (3.3). These equations are shown below with the coefficients replaced by their numerical values as determined by previous investigations [Ref. 3].

$$\begin{aligned}
 \hat{z}'' &= 1/2 \hat{U} [-4.303(\hat{z}' + \hat{U}\theta) \\
 &\quad - 4.763\theta' - 1.50\hat{U} \delta_e \\
 &\quad - 0.57\hat{U} \delta_c] - 0.608\hat{z} \\
 &\quad - 0.0647\theta - 1.075(\hat{z}'' + \hat{U}\theta') \\
 &\quad - 0.364\theta'' + \hat{Z}_w
 \end{aligned} \tag{3.4}$$

$$\begin{aligned}
 1.412\theta'' &= 1/2 \hat{U} [-4.763(\hat{z} + \hat{U}\theta) \\
 &\quad - 15.08\theta' - 2.85\hat{U} \delta_e \\
 &\quad + 0.90\hat{U} \delta_c] - 1.045\theta \\
 &\quad - 0.0647\hat{z} - 0.364(\hat{z}'' + \hat{U}\theta') \\
 &\quad - 2.142\theta'' + \hat{M}_w
 \end{aligned} \tag{3.5}$$



## B. TRANSFER FUNCTIONS

Reference [3] gives the response of the ship in pitch and heave resulting from 0.1-radian control surface deflections. These responses can be determined from the transfer functions relating the responses to the control surface deflections. In order to determine if the model used in this investigation was equivalent to the one used by NUC, San Diego, the transfer functions were derived as shown below and the responses to the control surface deflections were obtained.

The linear Eqs. (3.4) and (3.5) can be Laplace transformed; the result of doing this is shown below with the assumption made that the initial conditions are zero. The numerical values of the coefficients  $a_i$  and  $b_i$ ,  $i=1,\dots,8$ , are given in Table III.

$$\begin{aligned}\hat{z}(s)s^2 &= a_1\hat{z}(s)s + a_2\hat{z}(s) + a_3\theta(s)s^2 \\ &\quad + a_4\theta(s)s + a_5\theta(s) + a_6\delta_e \\ &\quad + a_7\delta_c + a_8\hat{z}_w\end{aligned}\tag{3.6}$$

$$\begin{aligned}\theta(s)s^2 &= b_1\theta(s)s + b_2\theta(s) + b_3\hat{z}(s)s^2 \\ &\quad + b_4\hat{z}(s)s + b_5\hat{z}(s) + b_6\delta_e \\ &\quad + b_7\delta_c + b_8\hat{M}_w\end{aligned}\tag{3.7}$$

One method of determining transfer functions is to draw the signal flow graph corresponding to Eqs. (3.6) and (3.7) and then apply Mason's Gain Rule to the resulting graph [Ref. 4]. Referring to Fig. 6 and Table III for the appropriate coefficient values, it can be seen that the transfer functions will have the



TABLE III

Coefficient	Value	Coefficient	Value
$a_1$	$-1.0369 \hat{U}$	$b_1$	$-2.2240 \hat{U}$
$a_2$	$-0.2930$	$b_2$	$-0.6701 \hat{U}^2 - 0.2940$
$a_3$	$-0.1754$	$b_3$	$-0.1024$
$a_4$	$-1.6658 \hat{U}$	$b_4$	$-0.6701 \hat{U}$
$a_5$	$-1.0369 \hat{U}^2 - 0.0312$	$b_5$	$-0.0182$
$a_6$	$-0.3614 \hat{U}^2$	$b_6$	$-0.4010 \hat{U}^2$
$a_7$	$-0.1373 \hat{U}^2$	$b_7$	$+0.1266 \hat{U}^2$
$a_8$	$+0.4819$	$b_8$	$+0.2814$

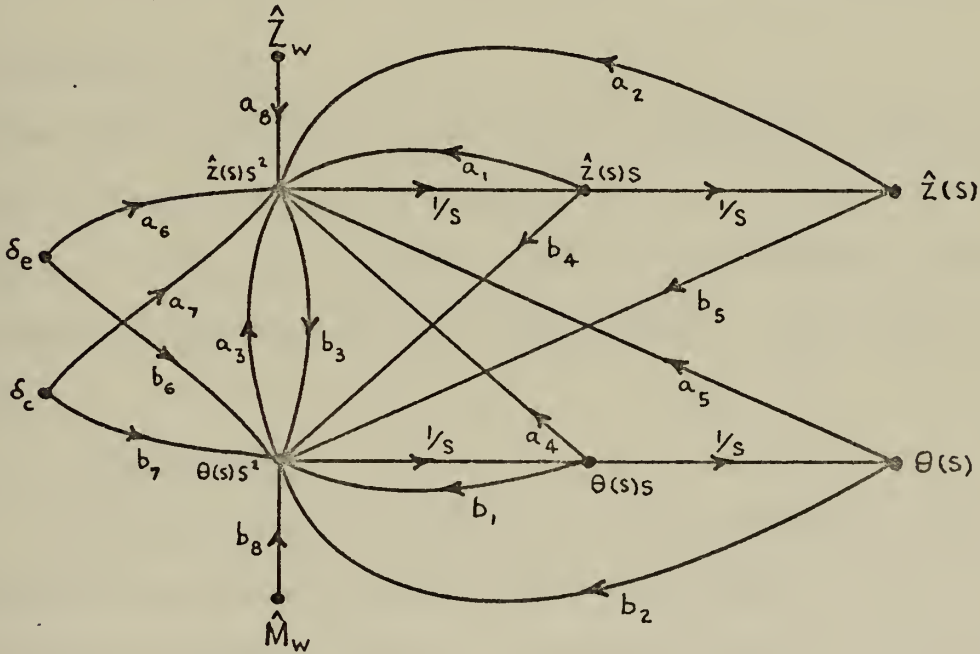


Figure 6. Signal Flow Graph.



ship's non-dimensional speed,  $U$ , as the determining parameter. The resulting transfer functions are of the form

$$\frac{X(s)}{Y(s)} = \frac{N_2 s^2 + N_1 s + N_0}{D_4 s^4 + D_3 s^3 + D_2 s^2 + D_1 s + D_0} \quad (3.8)$$

where the coefficients  $N_i$ ,  $i=0,1,2$ , and  $D_j$ ,  $j=0,1,\dots,4$  are given in Table IV.

Reference [3] investigates the ship's response for two distinct speeds,  $\hat{U}=1.0$  and  $1.65$ . Referring to Fig. 3, it can be seen that for a 2000-ton-displacement ship, these values correspond to speeds of 21.8 knots and 36 knots respectively. The transfer functions for these two speeds are given in Table V, and the responses resulting from 0.1-radian control surface deflections were found to agree with those contained in Ref. [3].

### C. COMPUTER MODEL

The time histories of the ship's responses, pitch, pitch velocity, heave and heave velocity, can be found by using a computer. A choice, however, must be made whether to use analog or digital simulation for the ship model. Both models are given below.

#### 1. Analog Model

An appropriate model for analog simulation can be easily achieved by normalizing Eq. (3.8) with respect to  $D_4$ . The resulting model is shown in Fig. 7. A penalty must be paid for the ease with which simulation has been achieved and that is that the states  $x_1$  through  $x_4$  have no physical significance. In order to determine some physical quantity (e.g.,  $\hat{z}$ ,  $\hat{z}'$ ,  $\phi$ ,  $\theta'$ ), linear combinations of the states  $x_1$  through  $x_4$  are required.





TABLE IV

COEFFICIENT VALUES FOR EQUATION (3.8).

$\frac{X(s)}{Y(s)}$	$N_2$	$N_1$	$N_0$	$D_4$	$D_3$	$D_2$	$D_1$	$D_0$
$\frac{\theta}{\delta_c}$	$b_7 + a_7 b_3$	$a_7 b_4 - a_1 b_7$	$a_7 b_5 - a_2 b_7$	$1.0 - a_3 b_3$	$-a_1 b_1 - a_3 b_4$ $-a_4 b_3$	$a_1 b_1 - a_2 - a_3 b_5$ $-b_2 - a_5 b_3 - a_4 b_4$	$a_1 b_2 + a_2 b_1$ $-a_4 b_5 - a_5 b_4$	$a_2 b_2 - a_5 b_5$
$\frac{\theta}{\delta_e}$	$b_6 + a_6 b_3$	$a_6 b_4 - a_1 b_6$	$a_6 b_5 - a_2 b_6$					
$\frac{\hat{z}}{\delta_c}$	$a_7 + a_3 b_7$	$a_4 b_7 - a_7 b_1$	$a_5 b_7 - a_7 b_2$					
$\frac{\hat{z}}{\delta_e}$	$a_6 + a_3 b_6$	$a_4 b_6 - a_6 b_1$	$a_5 b_6 - a_6 b_2$					



TABLE V  
TRANSFER FUNCTIONS  
( $\hat{U} = 1.0$  and  $1.65$ )

$\frac{X(s)}{Y(s)}$	$\hat{U} = 1.0$	$\hat{U} = 1.65$
$\frac{\theta}{\delta_c}$	$\frac{0.5348S^2 + 0.8489S + 0.1505}{\beta}$	$\frac{0.6734S^2 + 1.7639S + 0.1896}{\beta}$
$\frac{\theta}{\delta_e}$	$\frac{-1.383S^2 - 0.6597S - 0.4216}{\beta}$	$\frac{-1.7421S^2 - 1.3707S - 0.5309}{\beta}$
$\frac{\hat{z}}{\delta_c}$	$\frac{-0.6066S^2 - 1.963S - 1.017}{\beta}$	$\frac{-0.7638S^2 - 4.0785S - 3.1226}{\beta}$
$\frac{\hat{z}}{\delta_e}$	$\frac{-1.1066S^2 - 0.5168S + 0.3032}{\beta}$	$\frac{-1.3935S^2 - 1.0737S + 1.8127}{\beta}$
$\beta$	$3.733S^4 + 11.301S^3 + 8.874S^2 + 3.441S + 1.0$	$1.727S^4 + 8.624S^3 + 9.415S^2 + 2.676S + 1.0$



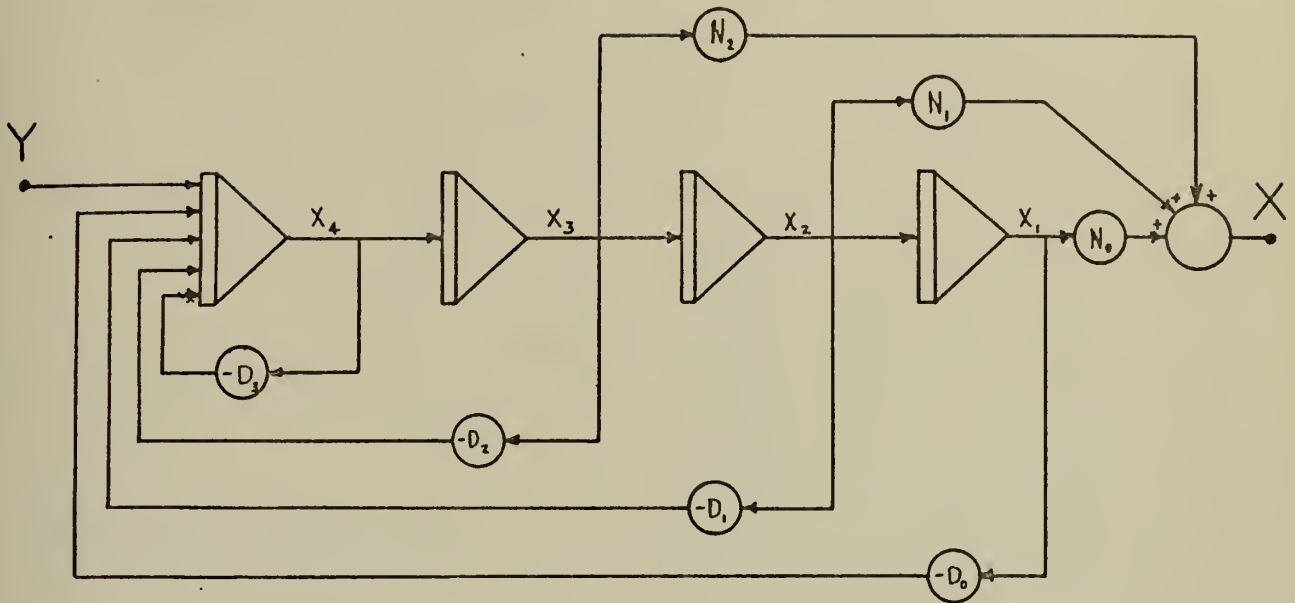


Figure 7. Analog Model

(Assumes no phase reversal through integrators)

## 2. Digital Model

The digital model could easily be solved by choosing the states as being the same as those in the analog model, again, however, the chosen states have no physical meaning.

A more desirable model is achieved by choosing the states as being heave, heave velocity, pitch and pitch velocity. These states can be obtained by algebraic manipulation of Eqs. (3.6) and (3.7). In their present form, each of these equations contains the transforms of the second derivative of both heave and pitch. This explicit interdependence, illustrated by the  $a_3$ - $b_3$  loop in Fig. 6, must be removed in order to obtain a workable model. This is accomplished by substituting Eq. (3.6) into (3.7) and Eq. (3.7) into (3.6).



The states are chosen as indicated above, resulting in a state differential equation which describes the ship. This equation has the form

$$\dot{\underline{x}}(t) = \underline{A}\underline{x}(t) + \underline{B}\underline{u}(t) + \underline{C}\underline{w}(t) \quad (3.9)$$

where the state vector is defined as

$$\underline{x}(t) \equiv \begin{bmatrix} \hat{z} \\ \dot{\hat{z}} \\ \theta \\ \dot{\theta} \end{bmatrix}$$

the control vector is

$$\underline{u}(t) \equiv \begin{bmatrix} \delta_e(t) \\ \delta_c(t) \end{bmatrix}$$

and the wave-force vector is

$$\underline{w}(t) \equiv \begin{bmatrix} \hat{z}_w \\ \hat{M}_w \end{bmatrix}$$

The coefficient matrices are

$$\underline{A} = \begin{bmatrix} 0 & 1 & 0 & 0 \\ -0.2951 & -0.9362\hat{U} & -0.9362\hat{U}^2 + 0.0207 & -1.299\hat{U} \\ 0 & 0 & 0 & 1 \\ 0.012 & -0.5742\hat{U} & -0.5742\hat{U}^2 - 0.2961 & -2.091\hat{U} \end{bmatrix}$$





$$\underline{B} = \begin{bmatrix} 0 & 0 \\ -0.2964\hat{U}^2 & -0.1624\hat{U}^2 \\ 0 & 0 \\ -0.3706\hat{U}^2 & 0.1432\hat{U}^2 \end{bmatrix}$$

and

$$\underline{C} = \begin{bmatrix} 0 & 0 \\ 0.4907 & -0.0503 \\ 0 & 0 \\ -0.0502 & 0.2865 \end{bmatrix}$$

Equation (3.9) is readily simulated on a digital computer to give the ship's time response to control surface deflections and known wave forces and moments.



#### IV. CONTROL SYSTEMS FOR THE SEMISUBMERGED SHIP

Optimal control theory [Ref. 5] was used to derive three controllers for the semisubmerged ship. The derivations of the control laws are based upon two assumptions: (1) the states in Eq. (3.9) are directly measurable, and (2) no measurement noise exists in the measurement of the states.

##### A. PERFORMANCE MEASURE

The performance measure gives a quantitative measure of the quality of response of the system under consideration. With the exception of long waves ( $\hat{\lambda} > 14$ ) where the wave crest might impact with the upper platform and it would be more advantageous to follow the contour of the wave, it is desired to maintain the ship as stable as possible in the Earth-fixed coordinate system. This requires that the state vector be maintained close to the equilibrium point (origin). The control surfaces however, should not have excessive deflections which would run them into mechanical or electrical stops, nor should they overload the actuation system and result in loss of the control system. In view of the above, the requirement for the control system becomes:

The control system must maintain the state vector,  $\underline{x}(t)$ , as close to the origin as possible without an excessive expenditure of control effort.

The performance measure then chosen is

$$J = \frac{1}{2} \int_{t_0}^{t_f} [\underline{x}^T(t) \underline{Q} \underline{x}(t) + \underline{u}^T(t) \underline{R} \underline{u}(t)] dt \quad (4.1)$$



where the final time  $t_f$  is assumed to be fixed,  $\underline{Q}$  is a real symmetric positive semi-definite weighting matrix and  $\underline{R}$  is a real symmetric positive definite weighting matrix. It is assumed that the states and controls are not bounded and that the final state,  $\underline{x}(t_f)$ , is free. No penalty has been placed on minimizing the deviation of the final state from its desired value,  $\underline{0}$ . It is desired to determine the control  $\underline{u}^*(t)$  that minimizes this performance measure.

#### B. CONTROL LAW FOR THE SHIP IN A CALM SEA

The system of equations defining the ship in a calm sea ( $\underline{w}(t)=\underline{0}$ ) is

$$\dot{\underline{x}}(t) = \underline{A}\underline{x} + \underline{B}\underline{u}(t) \quad (4.2)$$

The requirement to minimize the performance measure  $J$ , given by Eq. (4.1) leads to the well-known optimal control law [Ref. 5]

$$\begin{aligned} \underline{u}^*(t) &= -\underline{R}^{-1}\underline{B}^T \underline{K}(t) \underline{x}(t) \\ &\equiv \underline{F}(t) \underline{x}(t) \end{aligned} \quad (4.3)$$

where  $\underline{K}(t)$  is the real symmetric positive definite solution to the Riccati equation

$$\dot{\underline{K}}(t) = -\underline{K}(t)\underline{A} - \underline{A}^T \underline{K}(t) - \underline{Q} + \underline{K}(t)\underline{B}\underline{R}^{-1}\underline{B}^T \underline{K}(t) \quad (4.4)$$

which satisfies the boundary condition

$$\underline{K}(t_f) = \underline{0}$$

The optimal control law given in Eq. (4.3) is seen to be a time-varying feedback of the state vector  $\underline{x}(t)$ . The closed-loop system state equations reduce to

$$\dot{\underline{x}}(t) = [\underline{A} + \underline{B}\underline{F}(t)] \underline{x}(t) \quad (4.5)$$



when the optimal control law is used. Figure 8 shows this system in block diagram form.

### C. THE OPTIMAL CONTROL LAW FOR THE SHIP WHEN SUBJECTED TO WAVE FORCES

The Hamiltonian for the forced system is

$$\begin{aligned}
 (\underline{x}(t), \underline{u}(t), \underline{p}(t), t) = & 1/2 \underline{x}^T(t) \underline{Q} \underline{x}(t) + 1/2 \underline{u}^T(t) \underline{R} \underline{u}(t) \\
 & + \underline{p}^T(t) \underline{A} \underline{x}(t) + \underline{p}^T(t) \underline{B} \underline{u}(t) \\
 & + \underline{p}^T(t) \underline{C} \underline{w}(t)
 \end{aligned} \tag{4.6}$$

where  $\underline{p}(t)$  is a vector of Lagrange multipliers called costates. The theorem that the variation of the augmented functional

$$\begin{aligned}
 J_a = \int_{t_0}^{t_f} \{ & 1/2 [\underline{x}^T(t) \underline{Q} \underline{x}(t) + \underline{u}^T(t) \underline{R} \underline{u}(t)] \\
 & + \underline{p}^T(t) [\underline{A} \underline{x}(t) + \underline{B} \underline{u}(t) + \underline{C} \underline{w}(t) - \dot{\underline{x}}(t)] \} dt
 \end{aligned} \tag{4.7}$$

equals zero on an extremal requires that the following necessary conditions hold for the state equation, costate equation, and control [Ref. 5]:

$$\dot{\underline{x}}^*(t) = \underline{A} \underline{x}^*(t) + \underline{B} \underline{u}^*(t) + \underline{C} \underline{w}(t) \tag{4.8}$$

$$\dot{\underline{p}}^*(t) = - \frac{\partial}{\partial \underline{x}} = - \underline{Q} \underline{x}^*(t) - \underline{A}^T \underline{p}^*(t) \tag{4.9}$$

$$\underline{0} = - \frac{\partial}{\partial \underline{u}} = \underline{R} \underline{u}^*(t) + \underline{B}^T \underline{p}^*(t) \tag{4.10}$$

where the asterisk denotes an extremal.  $\underline{R}$  is a positive definite matrix, therefore Eq. (4.9) can be solved for the optimal control to give

$$\underline{u}^*(t) = - \underline{R}^{-1} \underline{B}^T \underline{p}^*(t) \tag{4.11}$$





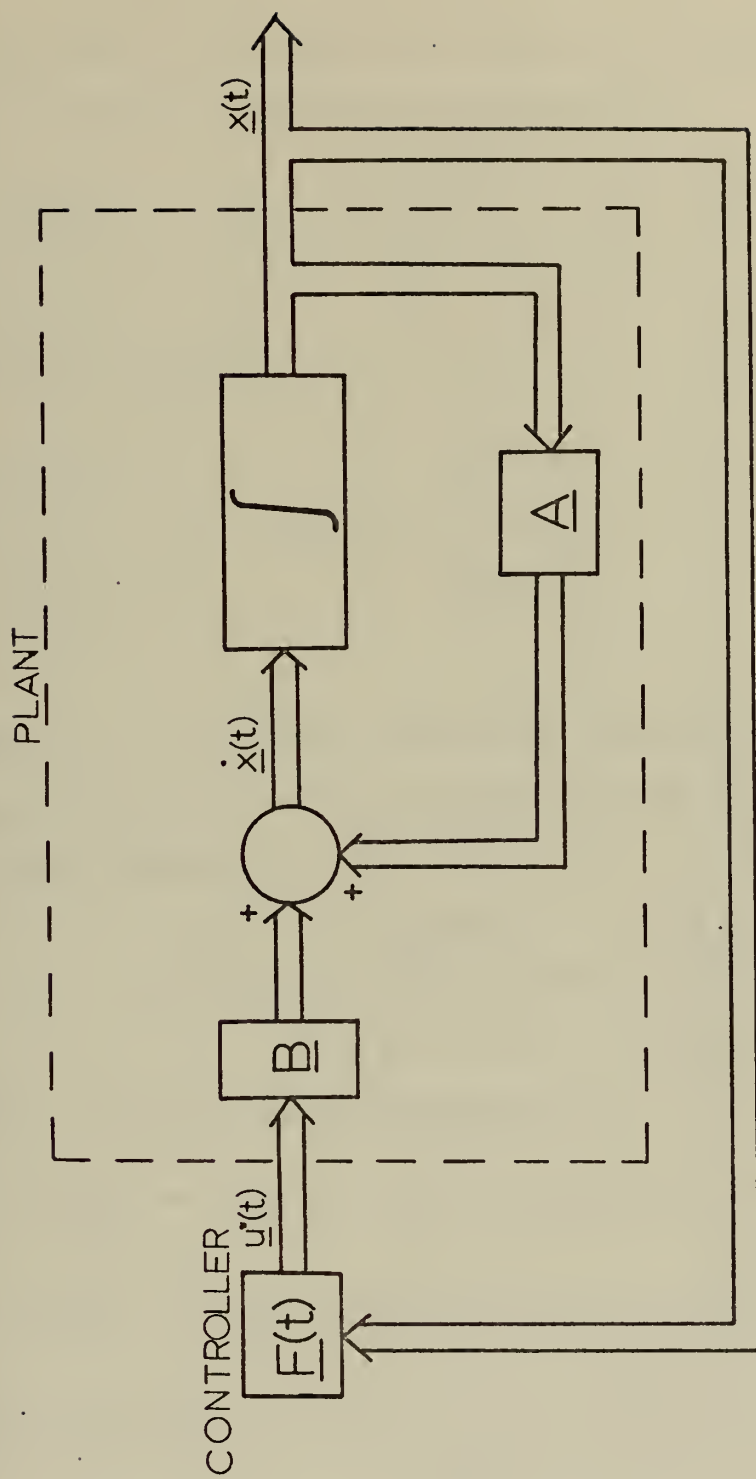


Figure 8. Linear Regulator Plant with Optimal Feedback Controller



Substitution of Eq. (4.11) into Eq. (4.8) yields

$$\dot{\underline{x}}^*(t) = \underline{A}\underline{x}^*(t) - \underline{B}\underline{R}^{-1}\underline{B}^T \underline{p}^*(t) + \underline{C}\underline{w}(t) \quad (4.12)$$

Equations (4.9) and (4.12) now form a system of  $2n$  linear nonhomogeneous differential equations

$$\begin{bmatrix} \dot{\underline{x}}^*(t) \\ \dot{\underline{p}}^*(t) \end{bmatrix} = \begin{bmatrix} \underline{A} & -\underline{B}\underline{R}^{-1}\underline{B}^T \\ -\underline{Q} & -\underline{A}^T \end{bmatrix} \begin{bmatrix} \underline{x}^*(t) \\ \underline{p}^*(t) \end{bmatrix} + \begin{bmatrix} \underline{C}\underline{w}(t) \\ \underline{0} \end{bmatrix} \quad (4.13)$$

whose solution is

$$\begin{bmatrix} \underline{x}^*(t_f) \\ \underline{p}^*(t_f) \end{bmatrix} = \underline{\phi}(t_f, t) \begin{bmatrix} \underline{x}^*(t) \\ \underline{p}^*(t) \end{bmatrix} + \int_t^{t_f} \underline{\phi}(t_f, \tau) \begin{bmatrix} \underline{C}\underline{w}(\tau) \\ \underline{0} \end{bmatrix} d\tau \quad (4.14)$$

where  $\underline{\phi}$  is the state transition matrix of Eq. (4.13). If  $\underline{\phi}$  is partitioned and the integral in Eq. (4.14) is replaced by a  $2n \times 1$  vector

$$\int_t^{t_f} \underline{\phi}(t_f, \tau) \begin{bmatrix} \underline{C}\underline{w}(\tau) \\ \underline{0} \end{bmatrix} d\tau = \begin{bmatrix} \underline{f}_1(t) \\ \underline{f}_2(t) \end{bmatrix} \quad (4.15)$$

Eq. (4.14) can be rewritten as

$$\underline{x}^*(t_f) = \underline{\phi}_{11}(t_f, t) \underline{x}^*(t) + \underline{\phi}_{12}(t_f, t) \underline{p}^*(t) + \underline{f}_1(t) \quad (4.16)$$

$$\underline{p}^*(t_f) = \underline{\phi}_{21}(t_f, t) \underline{x}^*(t) + \underline{\phi}_{22}(t_f, t) \underline{p}^*(t) + \underline{f}_2(t) \quad (4.17)$$

The boundary condition for the costates is

$$\underline{p}^*(t_f) = \underline{0}$$



Therefore, Eq. (4.17) can be solved as

$$\begin{aligned} \underline{p}^*(t) = & - \underline{\phi}_{22}^{-1}(t_f, t) \underline{\phi}_{21}(t_f, t) \underline{x}^*(t) \\ & - \underline{\phi}_{22}^{-1}(t_f, t) \underline{f}_2(t) \end{aligned} \quad (4.18)$$

Kalman [Ref. 6] has shown that the required inverse,  $\underline{\phi}_{22}^{-1}(t_f, t)$ , exists for all  $t \in [t_0, t_f]$  so that Eq. (4.18) can be rewritten as

$$\underline{p}^*(t) = \underline{K}(t) \underline{x}^*(t) + \underline{s}(t) \quad (4.19)$$

Equation (4.19) can now be substituted into Eq. (4.11) resulting in the optimal control law (Eq. (4.20)) similar to that in Ref. [7].

$$\begin{aligned} \underline{u}^*(t) &= -\underline{R}(t)^{-1} \underline{B}(t)^T \underline{K}(t) \underline{x}^*(t) - \underline{R}(t)^{-1} \underline{B}(t)^T \underline{s}(t) \\ &\equiv \underline{F}(t) \underline{x}^*(t) + \underline{v}(t) \end{aligned} \quad (4.20)$$

Equation (4.20) indicates that the optimal control law contains a linear function of the system states, and also a command signal,  $\underline{v}(t)$ , that not only depends upon the system parameters, but also upon future values of the wave forcing function,  $\underline{w}(t)$ . This indicates that the optimal control law must be anticipatory in effect.

The matrix  $\underline{K}(t)$  and the vector  $\underline{s}(t)$  can be obtained by differentiating Eq. (4.19)

$$\dot{\underline{p}}^*(t) = \dot{\underline{K}}(t) \underline{x}^*(t) + \underline{K}(t) \dot{\underline{x}}^*(t) + \dot{\underline{s}}(t) \quad (4.21)$$

and substituting Eqs. (4.8), (4.11) and (4.19) into Eq. (4.21).



$$\begin{aligned}
\dot{\underline{p}}^*(t) &= \dot{\underline{K}}(t) \underline{x}^*(t) + \underline{K}(t) [\underline{A} \underline{x}^*(t) + \underline{B} \underline{u}^*(t) + \underline{C} \underline{w}(t)] + \dot{\underline{s}}(t) \\
&= \dot{\underline{K}}(t) \underline{x}^*(t) + \underline{K}(t) [\underline{A} \underline{x}^*(t) - \underline{B} \underline{R}^{-1} \underline{B}^T \underline{p}^*(t) + \underline{C} \underline{w}(t)] + \dot{\underline{s}}(t) \\
&= \dot{\underline{K}}(t) \underline{x}^*(t) + \underline{K}(t) [\underline{A} \underline{x}^*(t) - \underline{B} \underline{R}^{-1} \underline{B}^T (\underline{K}(t) \underline{x}^*(t) + \underline{s}(t)) \\
&\quad + \underline{C} \underline{w}(t)] + \dot{\underline{s}}(t)
\end{aligned} \tag{4.22}$$

However, substitution of Eq. (4.19) into the costate Eq. (4.9) also results in

$$\dot{\underline{p}}^*(t) = -\underline{Q} \underline{x}^*(t) - \underline{A}^T (\underline{K}(t) \underline{x}^*(t) + \underline{s}(t)) \tag{4.23}$$

Equations (4.22) and (4.23) can be equated which, after collecting terms, yields

$$\begin{aligned}
&[\dot{\underline{K}}(t) + \underline{K}(t) \underline{A} - \underline{K}(t) \underline{B} \underline{R}^{-1} \underline{B}^T \underline{K}(t) + \underline{A}^T \underline{K}(t) + \underline{Q}] \underline{x}^*(t) \\
&+ [\dot{\underline{s}}(t) + \underline{A}^T \underline{s}(t) - \underline{K}(t) \underline{B} \underline{R}^{-1} \underline{B}^T \underline{s}(t) + \underline{K}(t) \underline{C} \underline{w}(t)] = \underline{0}
\end{aligned} \tag{4.24}$$

which must be satisfied for all  $\underline{x}(t)$  and  $\underline{w}(t)$ . This results in the matrix differential equation for  $\underline{K}(t)$ ,

$$\dot{\underline{K}}(t) = -\underline{K}(t) \underline{A} - \underline{A}^T \underline{K}(t) - \underline{Q} + \underline{K}(t) \underline{B} \underline{R}^{-1} \underline{B}^T \underline{K}(t) \tag{4.4}$$

which is the same as that given earlier for the calm sea condition, and an additional vector differential equation,

$$\dot{\underline{s}}(t) = -[\underline{A}^T - \underline{K}(t) \underline{B} \underline{R}^{-1} \underline{B}^T] \underline{s}(t) - \underline{K}(t) \underline{C} \underline{w}(t) \tag{4.25}$$

The boundary conditions to be satisfied are

$$\underline{K}(t_f) = \underline{0}$$

$$\underline{s}(t_f) = \underline{0}$$





Equations (4.4) and (4.25) can now be integrated backward in time from  $t_f$  to  $t_0$  and the resulting solutions can be stored and substituted into Eq. (4.20) to give the optimal control law

$$\begin{aligned}\underline{u}'(t) &= -\underline{R}^{-1}\underline{B}^T\underline{K}(t)\underline{x}^*(t) - \underline{R}^{-1}\underline{B}^T\underline{s}(t) \\ &\equiv \underline{F}(t)\underline{x}^*(t) + \underline{v}(t)\end{aligned}\quad (4.20)$$

The controlled system, shown in Fig. 9, is now defined by the matrix differential equation

$$\dot{\underline{x}}(t) = [\underline{A} + \underline{B}\underline{F}(t)]\underline{x}(t) + \underline{B}\underline{v}(t) + \underline{C}\underline{w}(t) \quad (4.26)$$

#### D. A SUBOPTIMAL CONTROL LAW FOR THE SHIP WHEN SUBJECTED TO WAVE FORCES

The optimal control law given by Eq. (4.20) requires that the command signal  $\underline{v}(t)$  be determined either by (1) integrating Eq. (4.25) backwards in time assuming the forcing signal  $\underline{w}(t)$  is known, or (2) storing previously computed values of  $\underline{v}(t)$  in a look-up table and selecting the one which corresponds to the appropriate time history of  $\underline{w}(t)$ . Either of the above methods would require the use of either an existing onboard computer or a computer dedicated specifically to the control system for computation and storage. The suboptimal control system derived below was investigated to determine if this added complexity could be reduced or altogether avoided.

Referring to the system equation given by Eq. (4.26), the objective is to have the state vector,  $\underline{x}(t)$ , approach  $\underline{0}$ . This requires that  $\dot{\underline{x}}(t)$  also approach  $\underline{0}$ . This can only occur if when  $\underline{x}(t) \approx \underline{0}$ ,

$$\underline{B}\underline{v}(t) = -\underline{C}\underline{w}(t) \quad (4.27)$$



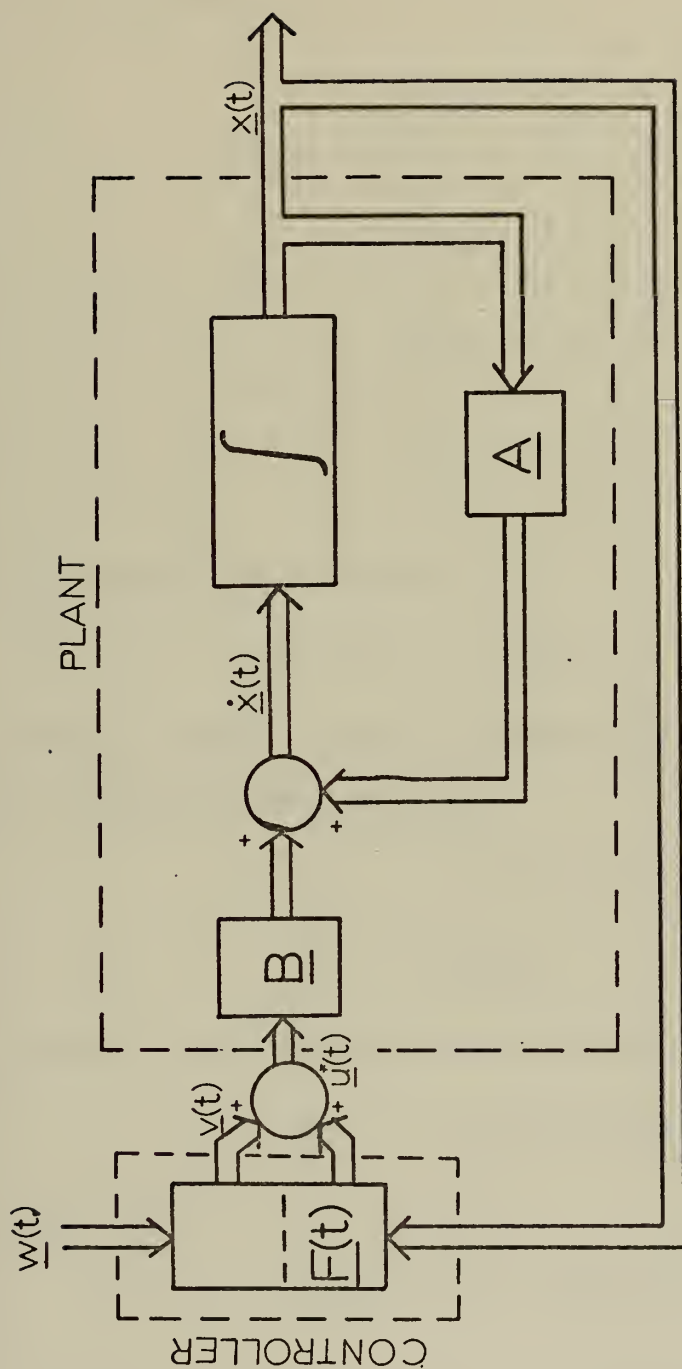


Figure 9. Linear Regulator Plant with Optimal Feedback Controller for External Disturbances ( $\underline{w}(t)$ ).



In general, Eq. (4.27) cannot be solved for  $\underline{v}(t)$  since  $\underline{B}^{-1}$  does not exist; however here the first and third rows of both  $\underline{B}$  and  $\underline{C}$  are zero which allows two new matrices,  $\underline{B}'$  and  $\underline{C}'$ , to be defined as

$$\begin{aligned}\underline{B}' &= \begin{bmatrix} b_{21} & b_{22} \\ b_{41} & b_{42} \end{bmatrix} \\ \underline{C}' &= \begin{bmatrix} c_{21} & c_{22} \\ c_{41} & c_{42} \end{bmatrix}\end{aligned}\tag{4.28}$$

It can be shown (see Appendix A) that

$$\underline{B}'\underline{v}(t) = -\underline{C}'\underline{w}(t)\tag{4.29}$$

and since  $\underline{B}'$  and  $\underline{C}'$  are (2x2) matrices and  $\underline{B}'^{-1}$  exists, Eq. (4.29) can be solved to yield

$$\begin{aligned}\underline{v}(t) &= -\underline{B}'^{-1}\underline{C}'\underline{w}(t) \\ &\equiv \underline{G}\underline{w}(t)\end{aligned}\tag{4.30}$$

The control law can now be written as

$$\underline{u}(t) = \underline{F}(t)\underline{x}(t) + \underline{G}\underline{w}(t)\tag{4.31}$$

and Eq. (3.9) becomes

$$\dot{\underline{x}}(t) = [\underline{A} + \underline{B}\underline{F}(t)]\underline{x}(t) + [\underline{B}\underline{G} + \underline{C}]\underline{w}(t)\tag{4.32}$$

It can be easily shown that as defined, the matrix equality

$$\underline{B}\underline{G} = -\underline{C}\tag{4.33}$$



holds (see Appendix B) so that if  $\underline{w}(t)$  is exactly known, Eq. (4.32) reduces to Eq. (4.5), the system equation for calm seas.

$$\dot{\underline{x}}(t) = [\underline{A} + \underline{B}\underline{F}(t)]\underline{x}(t) \quad (4.5)$$

Therefore, if the suboptimal control law given by Eq. (4.31) is used, the computer capability required by the optimal control law is avoided.

Reference [7] shows that the eigenvalues of the matrix  $[\underline{A} + \underline{B}\underline{F}(t)]$  have negative real parts so that after initial transients, the system states will approach zero. Figure 10 shows the block diagram for this system.

#### E. CONSTANT STATE FEEDBACK

The control laws given by Eqs. (4.3), (4.20) and (4.31) contain the time-varying feedback matrix  $\underline{K}(t)$ . This matrix was determined, as previously stated, by integrating Eq. (4.4) backwards in time. Although  $\underline{K}(t)$  can be computed and stored prior to utilization of the above control laws (since the solution of Eq. (4.4) does not depend upon the system states), the complexity of the control system would be increased over one which incorporated constant rather than time-varying feedback of the system states.

Kalman [Ref. 6] has shown that if (1) the plant is completely controllable, (2) there is no cost penalty for final state vector deviations from the desired final state, and (3)  $\underline{A}$ ,  $\underline{B}$ ,  $\underline{R}$  and  $\underline{Q}$  are constant matrices, then  $\underline{K}(t)$  approaches  $\underline{K}$  (a constant matrix) as  $t_f$  approaches infinity. To determine whether the





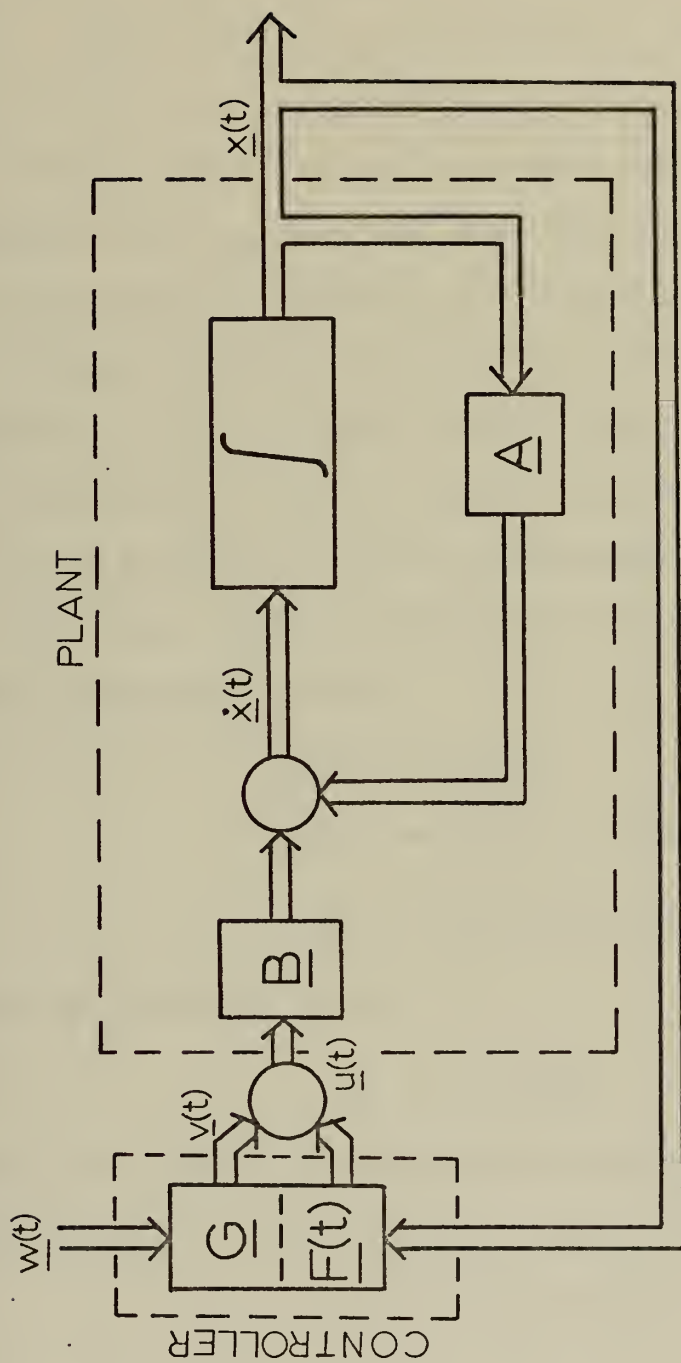


Figure 10. Linear Regulator Plant with Suboptimal Feedback Controller for External Disturbances ( $w(t)$ )



plant is completely controllable, the rank of the matrix

$$\underline{E} = [\underline{B} \quad \underline{A}\underline{B} \quad \underline{A}^2\underline{B} \quad \dots \quad \underline{A}^{n-1}\underline{B}] \quad (4.34)$$

must be evaluated. The plant is completely controllable if and only if  $\underline{E}$  has a rank of  $n$  (in this particular case  $n$  is four). Equation (4.34) was evaluated and found to have a rank of four, so this system is controllable as anticipated.

The ship meets all of the above requirements with the exception that  $t_f$  does not approach infinity (although it may be quite large). However, the solution to Eq. (4.4) using the NPS IBM-360/67 computer (Figs. 11 through 15) shows that the feedback gain matrix does reach steady-state constant values in a very short time ( $\approx 3.1$  sec. for a 2000-ton-displacement ship) and hence  $\underline{K}(t)$  can be approximated by the constant matrix  $\underline{K}$  to give the following control laws which are used in the remaining investigation:

$$\underline{u}(t) = \underline{F}\underline{x}(t) \quad (4.35)$$

$$\underline{u}^*(t) = \underline{F}\underline{x}(t) + \underline{v}(t) \quad (4.36)$$

$$\underline{u}(t) = \underline{F}\underline{x}(t) + \underline{G}\underline{w}(t) \quad (4.37)$$

$\underline{F}$  can be obtained from

$$\underline{F} = -\underline{R}^{-1}\underline{B}^T\underline{K} \quad (4.38)$$

where  $\underline{K}$  is the steady-state solution to Eq. (4.4) and hence also satisfies the nonlinear algebraic equation

$$\underline{0} = -\underline{K}\underline{A} - \underline{A}^T\underline{K} - \underline{Q} + \underline{K}\underline{B}\underline{R}^{-1}\underline{B}^T\underline{K} \quad (4.39)$$



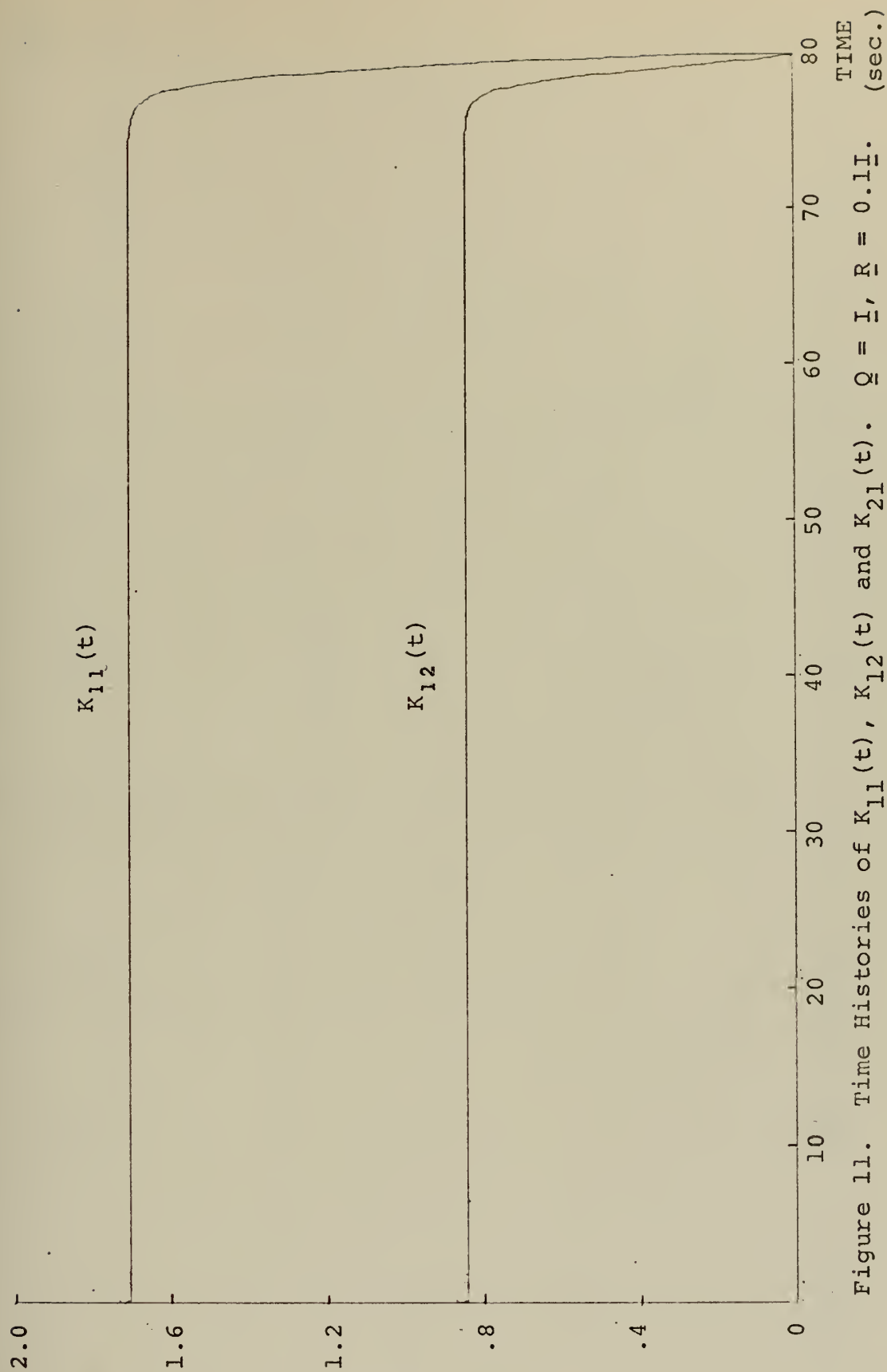


Figure 11. Time Histories of  $K_{11}(t)$ ,  $K_{12}(t)$  and  $K_{21}(t)$ .  $\bar{Q} = \bar{I}$ ,  $\bar{R} = 0.1\bar{I}$ . (sec.)



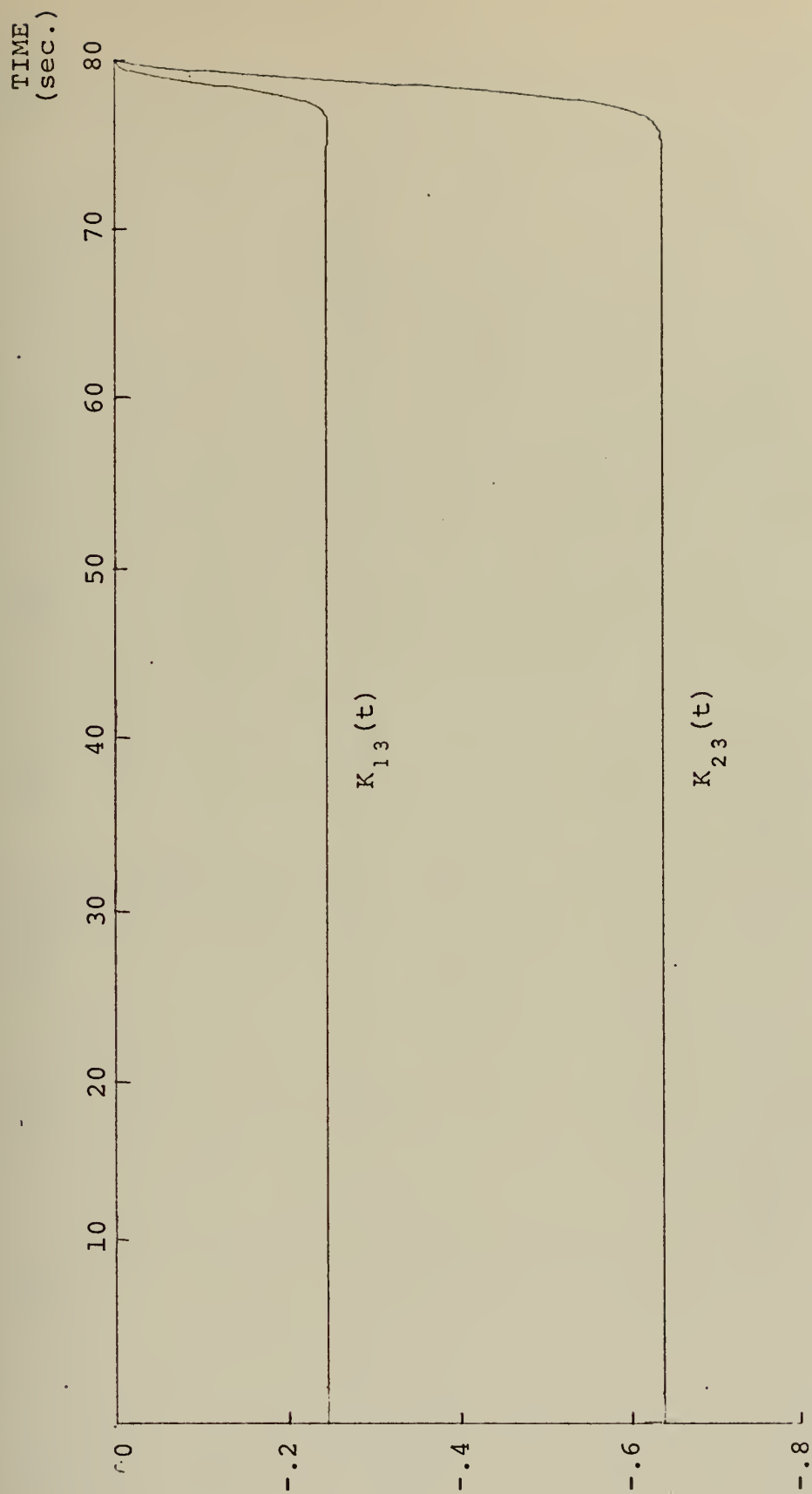


Figure 12. Time Histories of  $K_{13}(t)$ ,  $K_{23}(t)$ ,  $K_{31}(t)$  and  $K_{32}(t)$ .  $\underline{Q} = \underline{I}$ ,  $\underline{R} = 0.1\underline{I}$ .





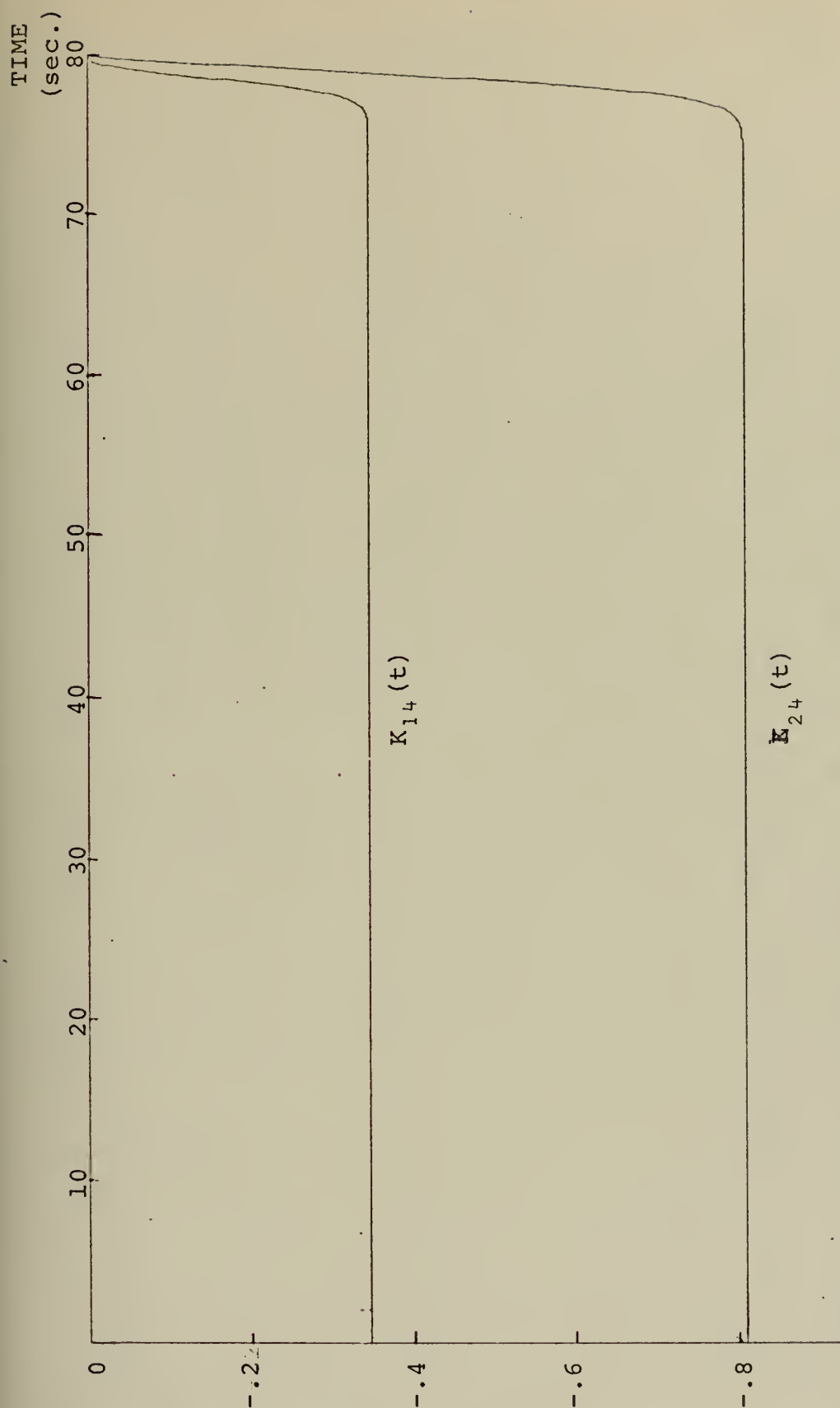


Figure 13. Time Histories of  $K_{14}(t)$ ,  $K_{24}(t)$ ,  $K_{41}(t)$  and  $K_{42}(t)$ .  $\bar{Q} = \bar{I}$ ,  $\bar{R} = 0.1\bar{I}$ .



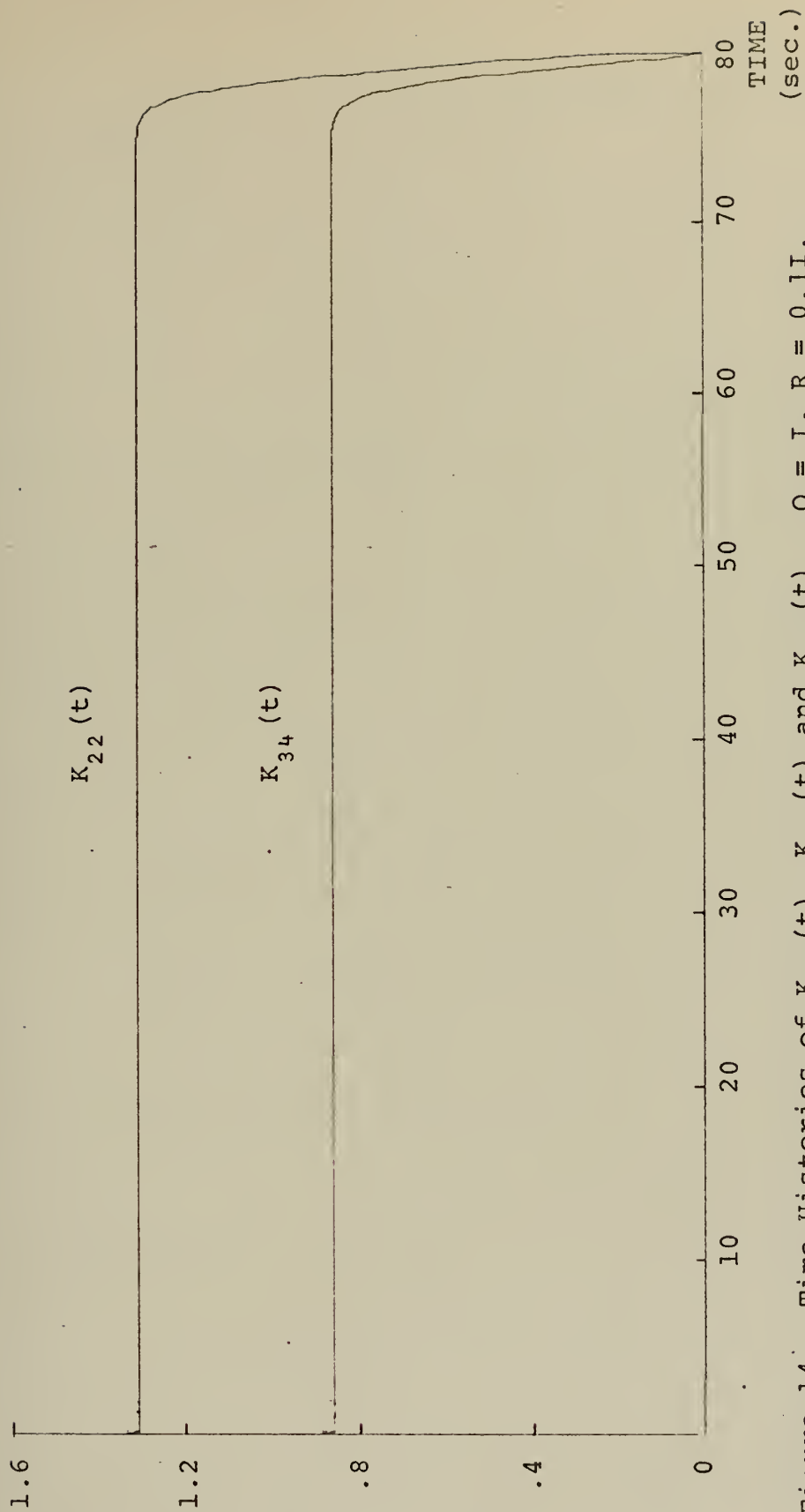


Figure 14. Time Histories of  $K_{22}(t)$ ,  $K_{34}(t)$  and  $K_{43}(t)$ .  $\bar{Q} = \bar{I}$ ,  $\bar{R} = 0.1\bar{I}$ .



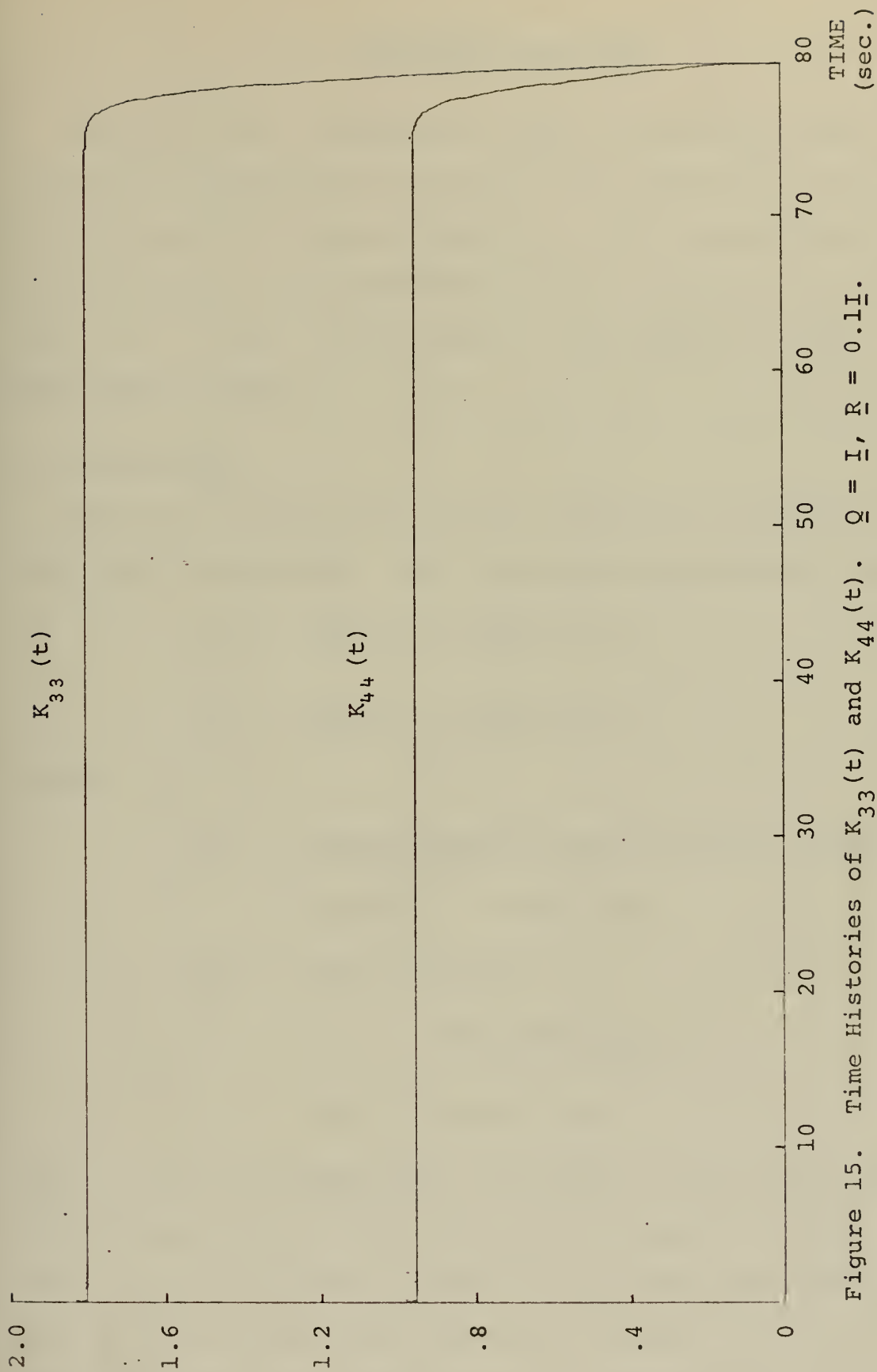


Figure 15. Time Histories of  $K_{33}(t)$  and  $K_{44}(t)$ .  $\bar{Q} = \bar{I}$ ,  $\bar{R} = 0.1\bar{I}$ .



## V. SIMULATION PROCEDURE

The NPS-360/67 computer was used to solve the ship's time response incorporating the control laws determined previously for various wave forcing functions. The computer program is given following the appendices, and a flowchart is shown in Fig. 16. In order to solve Eqs. (4.25) and (4.32),  $\underline{w}(t)$  and  $v(t)$  must be known.

### A. WAVE MODEL

The wave forces were estimated using the properties of deep water Airey waves. The resulting equations are [Ref. 3]

$$\hat{z}_w = A \cos(-\hat{\sigma}' \tau) + B \sin(-\hat{\sigma}' \tau) \quad (5.1)$$

$$\hat{M}_w = C \cos(-\hat{\sigma}' \tau) + D \sin(-\hat{\sigma}' \tau) \quad (5.2)$$

where

$$\begin{aligned} \hat{\sigma}' &= \text{non-dimensional wave encounter frequency} \\ &= (2\pi/\hat{\lambda})^{1/2} - (2\pi\hat{U}/\hat{\lambda}) \cos \psi \end{aligned} \quad (5.3)$$

$$\begin{aligned} \psi &= \text{wave direction} \\ &= \begin{array}{ll} 0^\circ & (\text{following sea}) \\ 180^\circ & (\text{ahead sea}) \end{array} \end{aligned} \quad (5.4)$$

and  $\hat{\lambda}$  is the non-dimensional wavelength of the ocean wave. The coefficients A, B, C and D are graphed versus  $\hat{\lambda}$  in Ref. [3]. A least squares polynomial curve fitting subroutine, LSQPL2, was used to fit a sixth-order polynomial to each of the graphs. Each polynomial is a function of  $\hat{\lambda}$ . The resulting polynomials





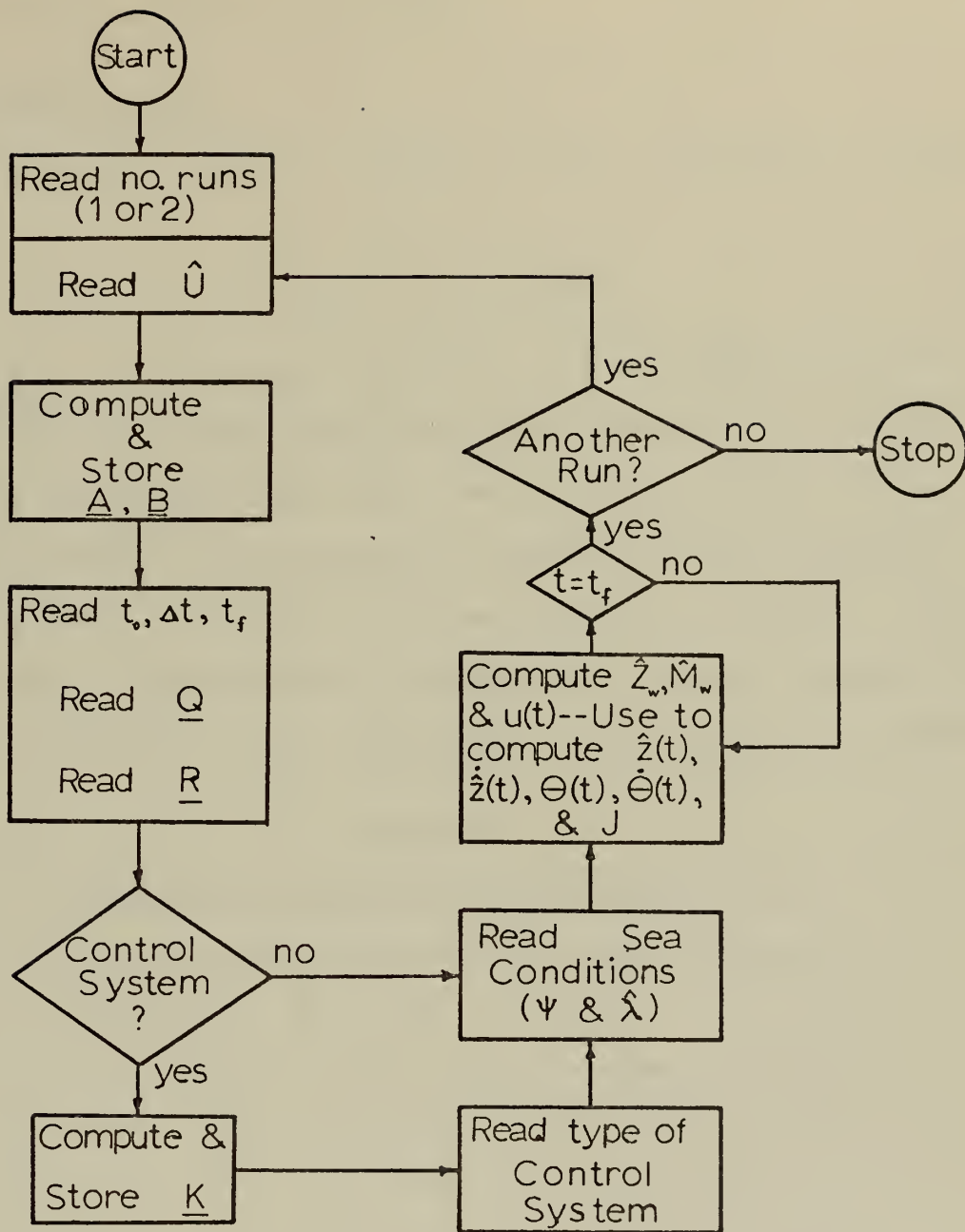


Figure 16. Computer Flowchart.



are used in the computer program to simulate the wave forces and moments acting on the ship.

## B. COMMAND SIGNAL

The optimal control law (Eq. (4.36)) requires the command signal

$$\underline{v}(t) = -\underline{R}^{-1}\underline{B}^T \underline{s}(t) \quad (5.5)$$

where  $\underline{s}(t)$  is the solution to Eq. (4.25). Equation (5.5) was solved for the three cases shown in Table VI. All three cases are for following seas ( $\psi=0^\circ$ ) which, as previously stated, is a sea condition which gives an undesirable ship response. The results for case three are shown in Figs. 17 and 18. It is seen that as expected for a sinusoidal forcing function, the command signal is also sinusoidal in form with the exception

TABLE VI  
PARAMETERS USED IN SOLVING EQUATION (5.5)

Case No.	$\underline{Q}$	$\underline{R}$	$\hat{U}$	$\hat{\lambda}$	$\psi$
1	$\underline{I}$	$\underline{I}$	1.0	10.0	$0^\circ$
2	$\underline{I}$	$0.5\underline{I}$	1.0	10.0	$0^\circ$
3	$\underline{I}$	$0.1\underline{I}$	1.0	10.0	$0^\circ$

$\underline{I}$  = Identity Matrix

being where  $t$  approaches  $t_f$  and the boundary condition

$$\underline{v}(t_f) = \underline{0}$$

must be met.



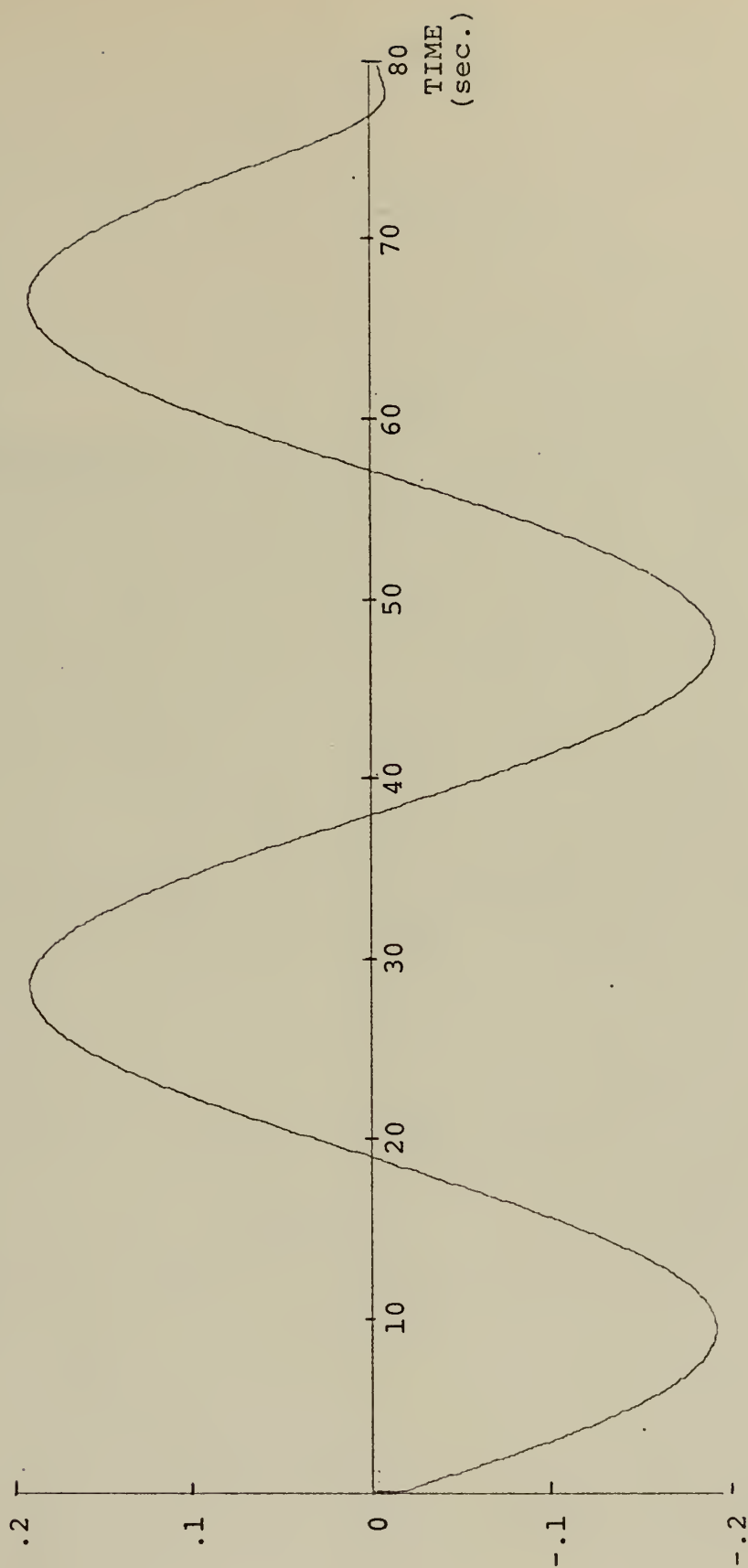


Figure 17. Time History of Command Signal  $V_1(t)$ .  
 $\bar{Q} = \bar{I}$ ,  $\bar{R} = 0.1\bar{I}$ ,  $\hat{U} = 1.0$ ,  $\psi = 0^\circ$ ,  $\hat{\lambda} = 10$ .



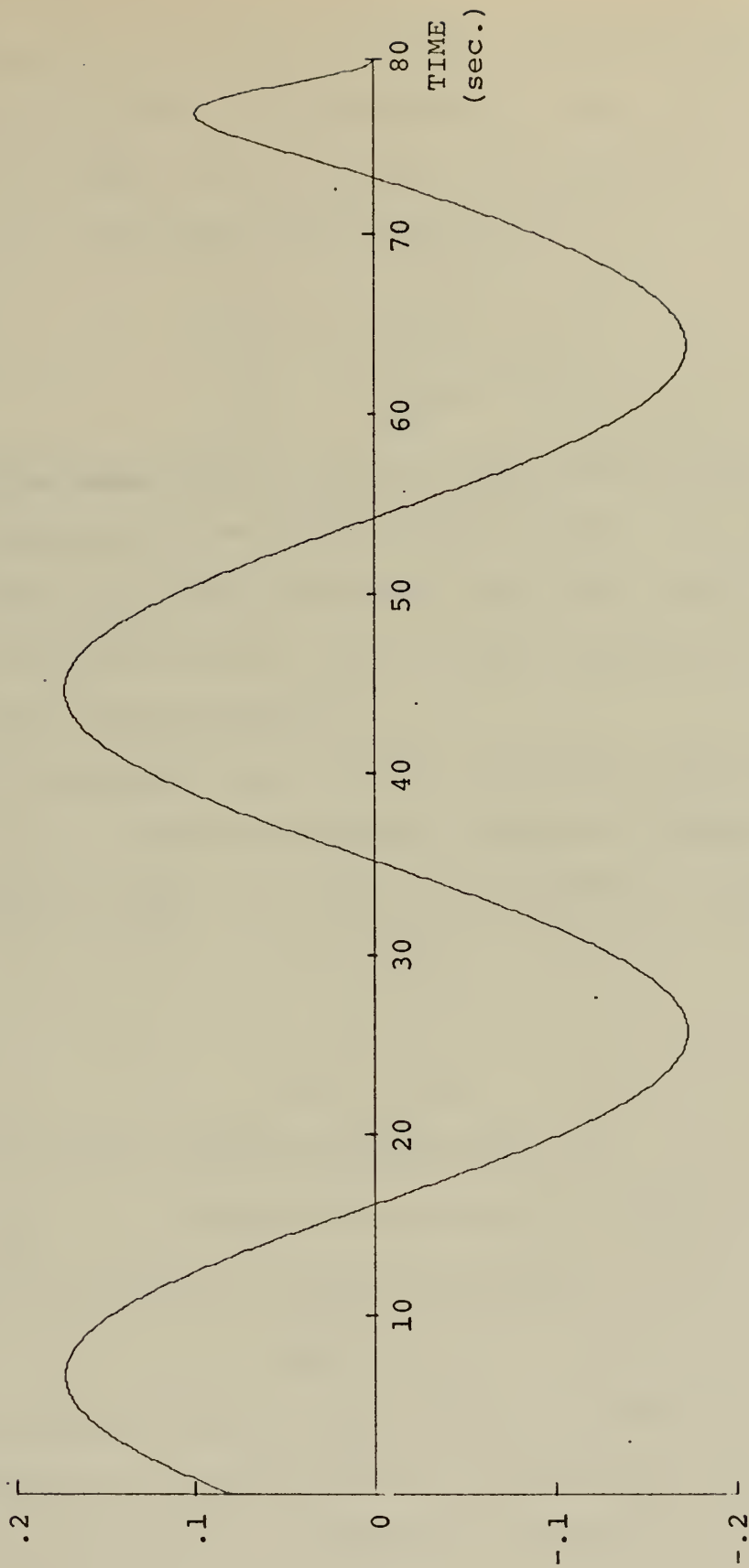


Figure 18. Time History of Command Signal  $V_2(t)$ .  
 $\underline{Q} = \underline{I}$ ,  $\underline{R} = 0.1\underline{I}$ ,  $\hat{U} = 1.0$ ,  $\psi = 0^\circ$ ,  $\hat{\lambda} = 10$ .





Since Eq. (4.25 must be solved forward in time and Eq. (5.5) can only be solved backward in time, it becomes necessary to have a model for  $\underline{y}(t)$  to use in solving Eq. (4.25). The model that was chosen was of the form

$$\begin{aligned} \underline{v}_1(t) &= M_1 \sin(-\hat{\sigma}\tau + \gamma_1) \\ \underline{v}_2(t) &= M_2 \sin(-\hat{\sigma}\tau + \gamma_2) \end{aligned} \quad (5.6)$$

where the magnitudes,  $M_1$  and  $M_2$ , and phase angles,  $\gamma_1$  and  $\gamma_2$ , were determined from the solutions to Eq. (5.5) and the final time deviations from sinusoidal form were ignored. The models for the three cases in Table VI are incorporated in the computer program as subroutine EST.

An alternative approach for obtaining the command signal is to use a frequency approach instead of integrating Eq. (4.25) backward in time. If a new time variable,  $\tau$ , is defined as

$$\tau = t_f - t$$

then

$$d\tau = -dt$$

and Eq. (4.25) can be rewritten as

$$\dot{\underline{s}}(\tau) = [\underline{A}^T - \underline{KBR}^{-1}\underline{B}^T]\underline{s}(\tau) + \underline{KCw}(\tau) \quad (5.7)$$

which satisfies the initial condition

$$\underline{s}(0) = \underline{0}$$

As previously stated,  $[\underline{A} - \underline{BR}^{-1}\underline{B}^T\underline{K}]$  is stable and since the transpose of a stable matrix is also stable, Eq. (5.7) is a stable equation in  $\tau$  (backwards in time  $t$ ).



The Laplace transform of  $s(\tau)$ , after invoking the boundary condition, is given by

$$\underline{S}(s) = [\underline{sI} - \underline{A}^T + \underline{KBR}^{-1} \underline{B}^T]^{-1} \underline{KCW}(s) \quad (5.8)$$

If  $w(\tau)$  is a periodic function with a discrete Fourier spectrum  $\underline{W}(f)$ , then the spectrum  $\underline{S}(f)$  is given by

$$\underline{S}(f) = [j2\pi f \underline{I} - \underline{A}^T + \underline{KBR}^{-1} \underline{B}^T]^{-1} \underline{KCW}(f) \quad (5.9)$$

and  $\underline{s}(\tau)$  can be obtained by taking the inverse Fourier transform of Eq. (5.9). This approach will hold for any general function  $\underline{w}(\tau)$  since the initial condition of Eq. (5.7) is zero.



## VI. RESULTS

The three controllers derived in the previous chapter will be called (1) the "constant-gain controller" -- given by Eq. (4.35), (2) the "optimal controller" -- given by Eq. (4.36) and (3) the "suboptimal controller" -- given by Eq. (4.37). Although the constant-gain controller was derived for the calm sea condition, its use was also investigated for the condition where  $\underline{w}(t) \neq \underline{0}$ . Figures 19 and 20 show the ship's heave and pitch response to a following sea of wavelength 10 when the ship's speed is 1.65 and no control system is used.

### A. CASES INVESTIGATED

The following assumptions were made in the first five cases listed below.

- (1) The control surface deflections were instantaneous.
- (2) The wave forces and moments,  $\underline{w}(t)$ , were non-zero and exactly known.
- (3) The state vector weighting matrix,  $\underline{Q}$ , was equal to the identity matrix,  $\underline{I}$ .
- (4) Contact of the underwater hulls and control surfaces with the air-water interface was ignored.
- (5) Initial conditions which were considered severe
$$\begin{aligned}\hat{z}(t_0) &= -0.5 \\ \dot{\hat{z}}(t_0) &= 0.0 \\ \theta(t_0) &= 0.5 \text{ radians} \\ \dot{\theta}(t_0) &= 0.0 \text{ radians/sec.}\end{aligned}$$

were used (refer to Fig. 2).



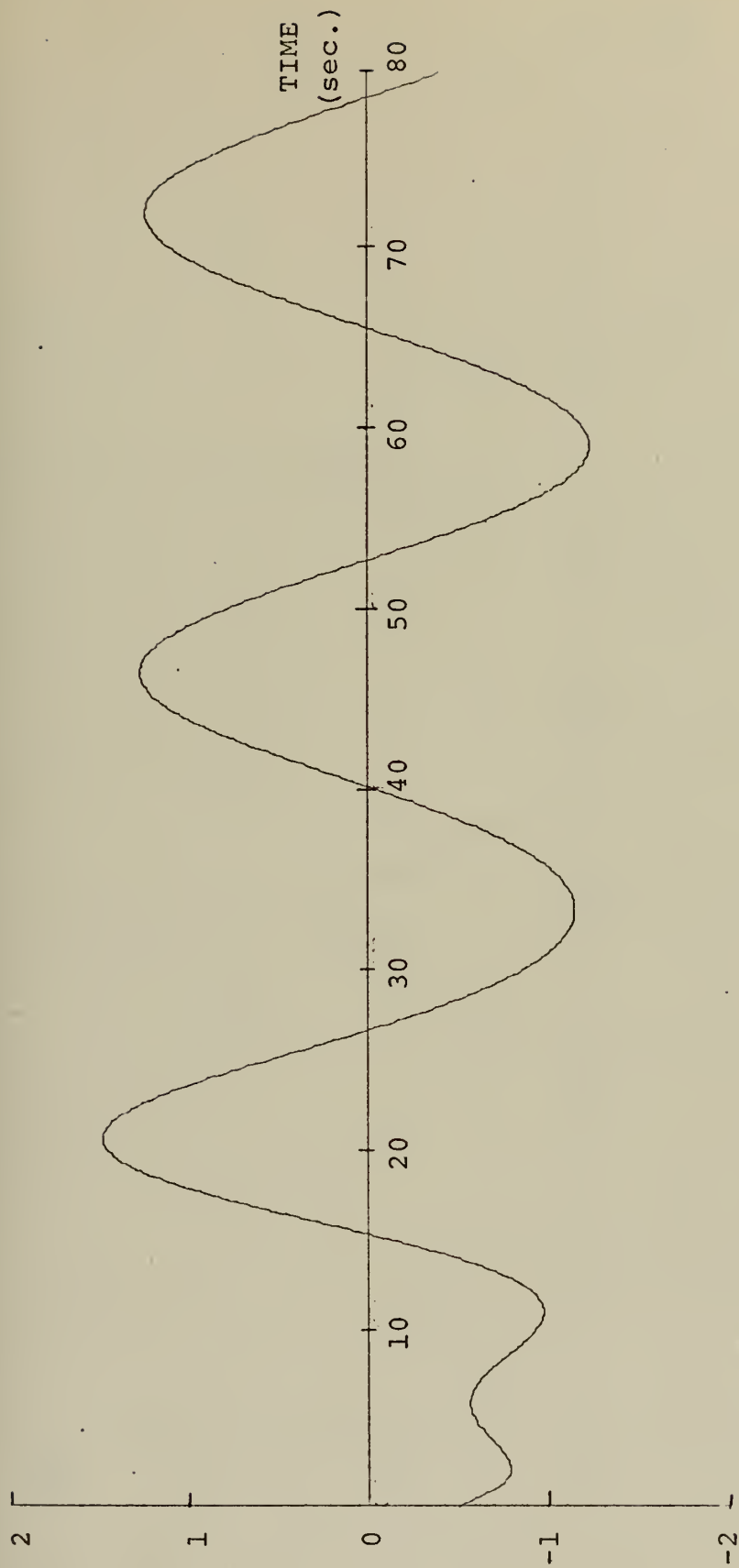


Figure 19. Heave Response with No Control System  
 $\hat{U} = 1.65, \psi = 0^\circ, \hat{\lambda} = 10$





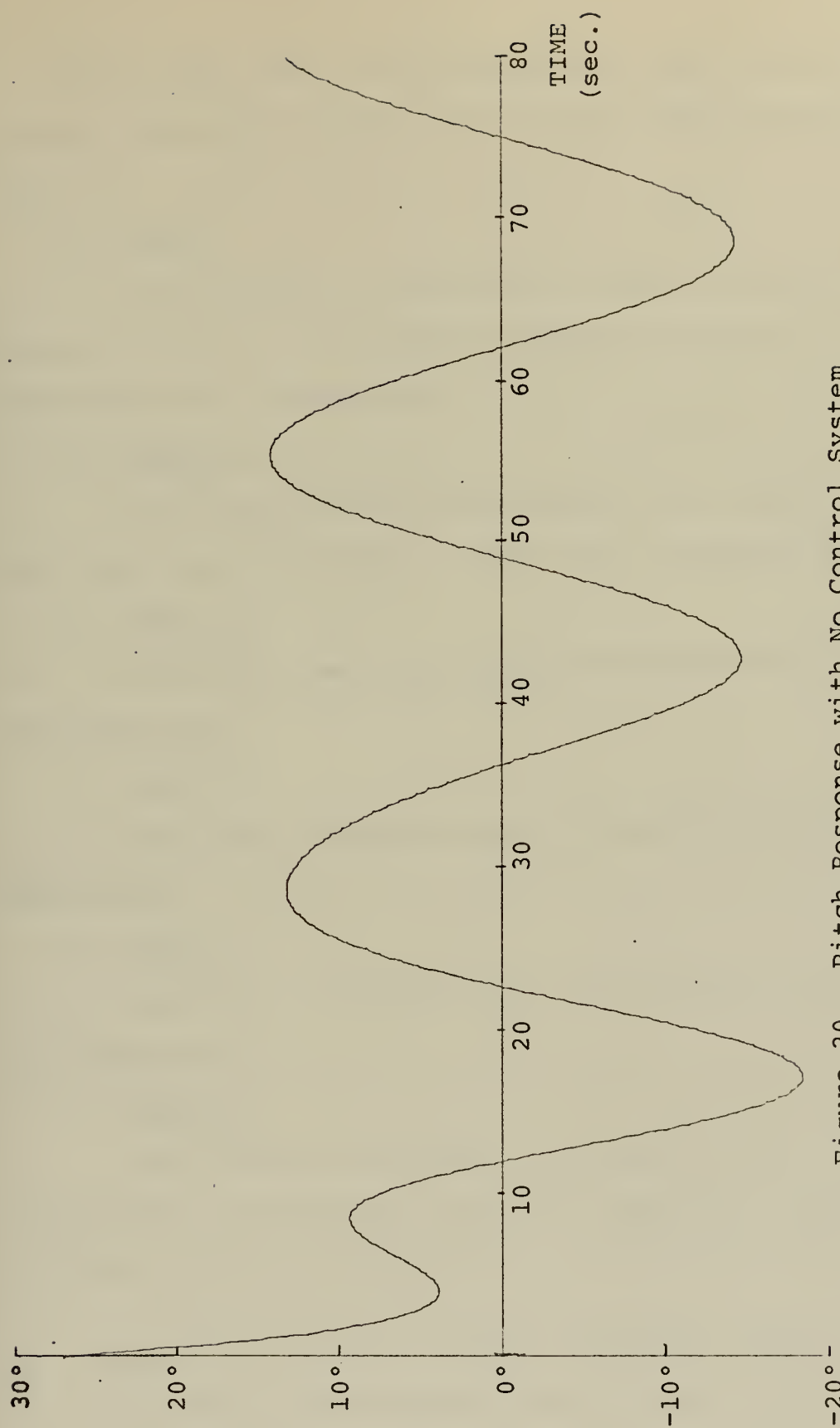


Figure 20. Pitch Response with No Control System  
 $\hat{U} = 1.65$ ,  $\psi = 0^\circ$ ,  $\hat{\lambda} = 10$



In the sixth case it was assumed that  $\underline{w}(t)$  was not known exactly; the other assumptions indicated above remained in force.

1. Case I

The reduction of the control weighting matrix  $\underline{R}$  and the resultant effect on the ship's response and control surface deflections was investigated.

2. Case II

The control surface deflections were constrained to  $\pm 30^\circ$  limits and the effect on the ship's response was determined.

3. Case III

The ship's response using the Constant-Gain Controller was determined.

4. Case IV

The ship's response using the Optimal Controller was determined.

5. Case V

The ship's response using the Suboptimal Controller was determined.

6. Case VI

The effect of imperfect estimates of  $\underline{w}(t)$  on the ship's response was investigated using the Suboptimal Controller. The estimate of  $\underline{w}(t)$  was perturbed by  $\pm 15$  percent of its true value.

B. THE EFFECT OF VARYING CONTROL WEIGHTING MATRIX (CASE I)

The values of the weighting matrix  $\underline{R}$  in Eq. (4.1) determine how much emphasis is placed upon the expenditure of control



effort as compared to maintaining the state vector, weighted by  $\underline{Q}$ , close to the origin. It is seen that as the values of  $\underline{R}$  are made smaller compared to those of  $\underline{Q}$ , more emphasis will be placed upon maintaining  $\underline{x}(t)$  close to the origin.

The ship's response in heave and pitch is shown in Figs. 21 and 22 for a following sea with a wavelength of 10 and a ship speed of 1.0. The Optimal Controller was used with two different  $\underline{R}$  matrices

$$\underline{R} = \begin{bmatrix} 1.0 & 0 \\ 0 & 1.0 \end{bmatrix}$$

and

$$\underline{R} = \begin{bmatrix} 0.5 & 0 \\ 0 & 0.5 \end{bmatrix}$$

The figures show, as expected, that heave and pitch are reduced as  $\underline{R}$  is reduced. The corresponding increase in control effort is shown in Figs. 23 and 24 for the Elevator and Canard respectively.

#### C. CONSTRAINED CONTROL SURFACE DEFLECTIONS (CASE II)

A large canard deflection (see Fig. 24) was required to reduce the state vector to its steady-state value when  $\underline{R}$  was reduced. The ship's response to the same conditions as in Case I above with  $\underline{R} = 0.5\underline{I}$  is shown in Figs. 25 and 26 where the control surface deflections were arbitrarily limited to  $\pm 30^\circ$ . The difference in state trajectories between the unconstrained and constrained control surface deflections is almost negligible; additional verification is provided by the



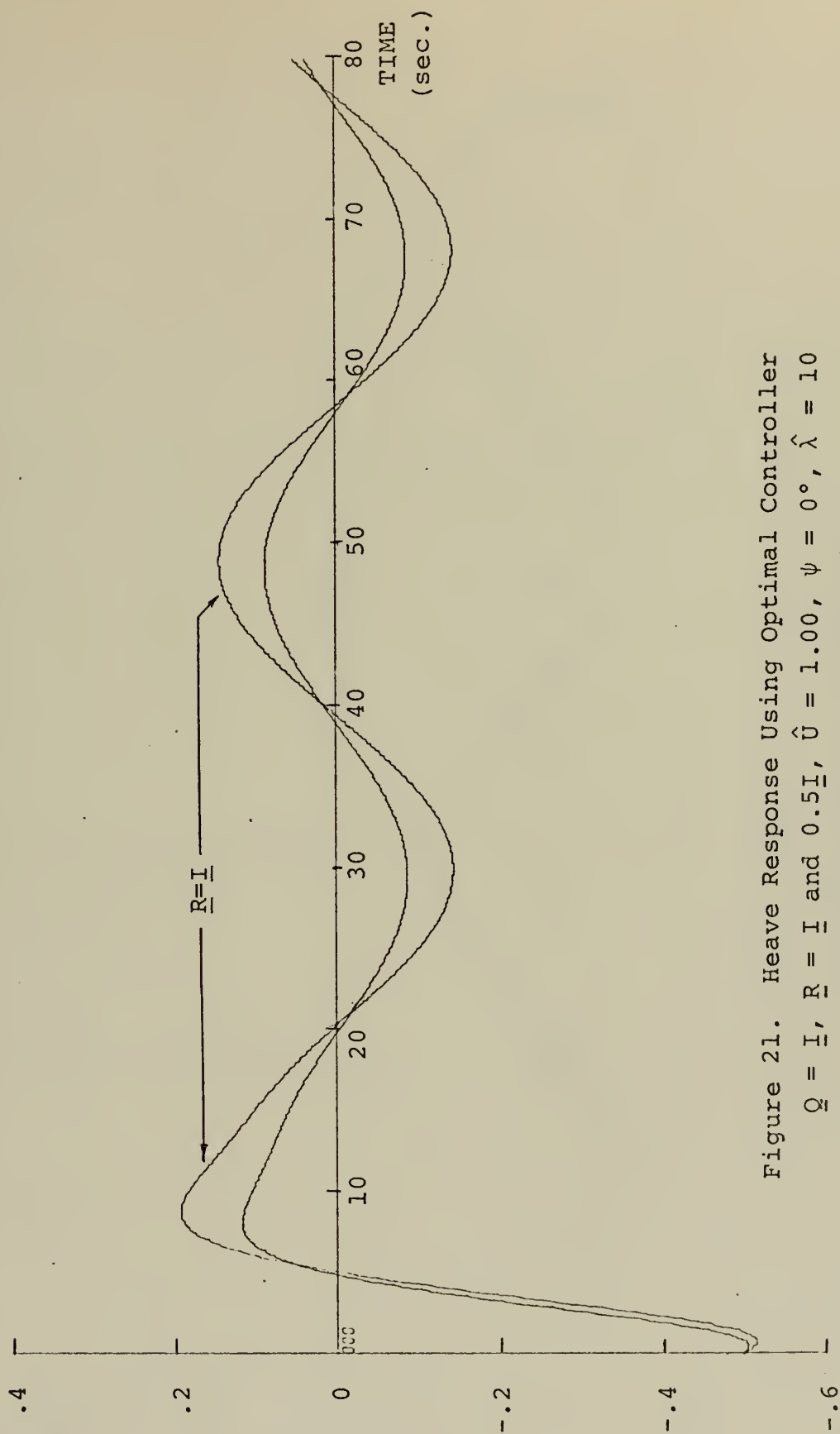


Figure 21. Heave Response Using Optimal Controller  
 $\bar{Q} = \bar{I}$ ,  $\bar{R} = \bar{I}$  and  $0.5\bar{I}$ ,  $\hat{U} = 1.00$ ,  $\psi = 0^\circ$ ,  $\hat{\lambda} = 10$   
 Control Surfaces Unconstrained





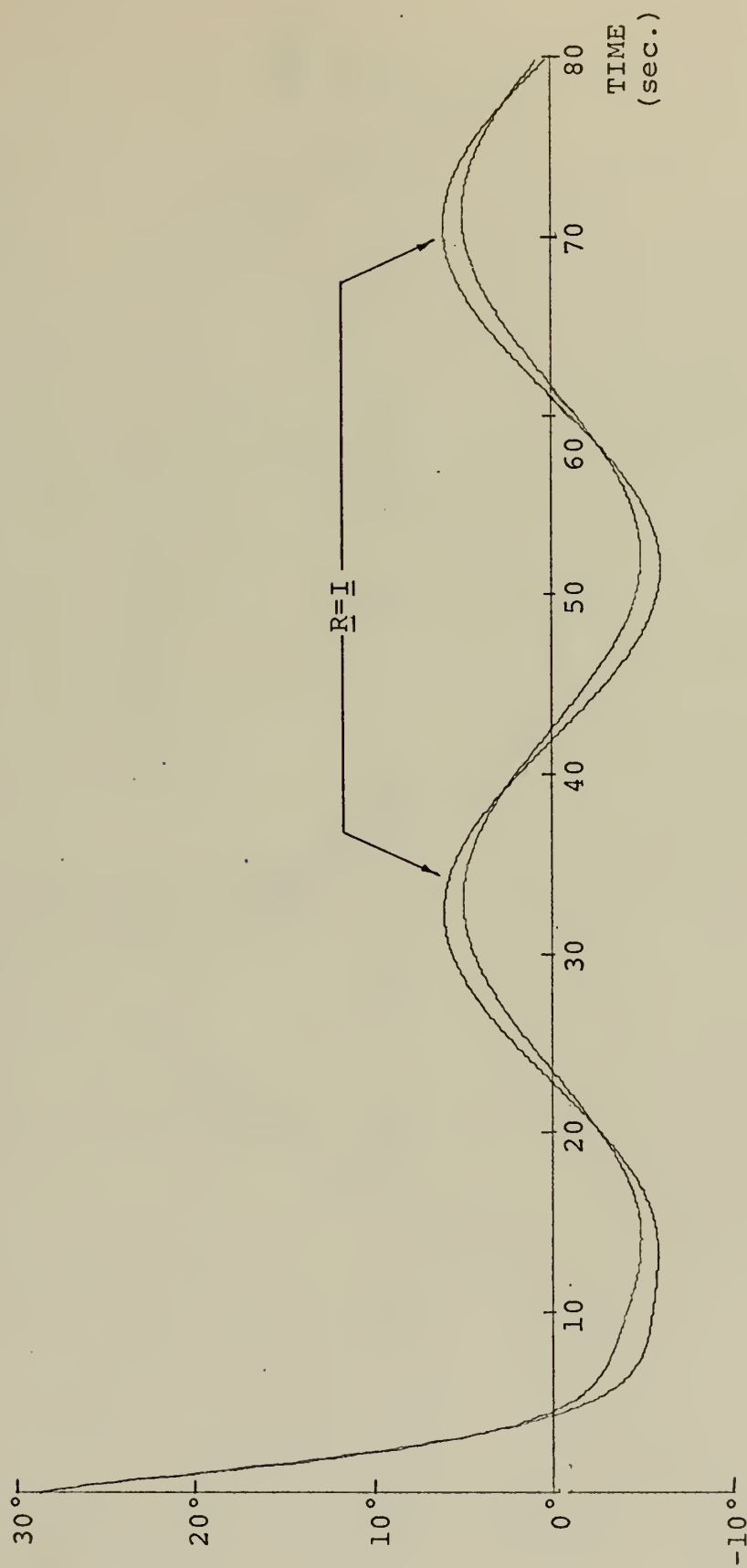


Figure 22. Pitch Response Using Optimal Controller  
 $\bar{Q} = \bar{I}$ ,  $\bar{R} = \bar{I}$  and  $0.5\bar{I}$ ,  $\hat{U} = 1.00$ ,  $\psi = 0^\circ$ ,  $\hat{\lambda} = 10$   
 Control Surfaces Unconstrained



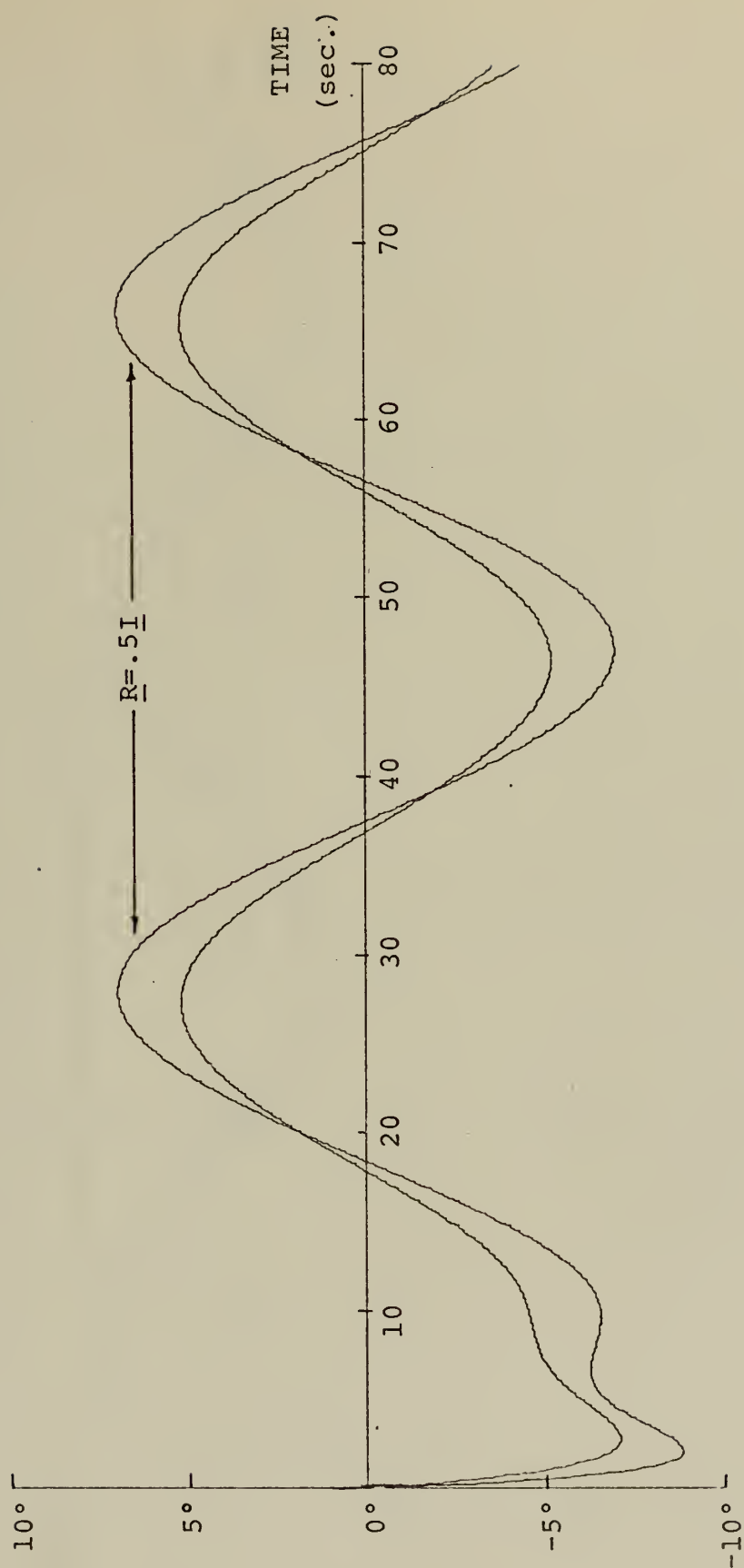


Figure 23. Elevator Response Using Optimal Controller  
 $\bar{Q} = \bar{I}$ ,  $\bar{R} = \bar{I}$  and  $0.5\bar{I}$ ,  $\hat{U} = 1.00$ ,  $\psi = 0^\circ$ ,  $\hat{\lambda} = 10$   
 Control Surfaces Unconstrained



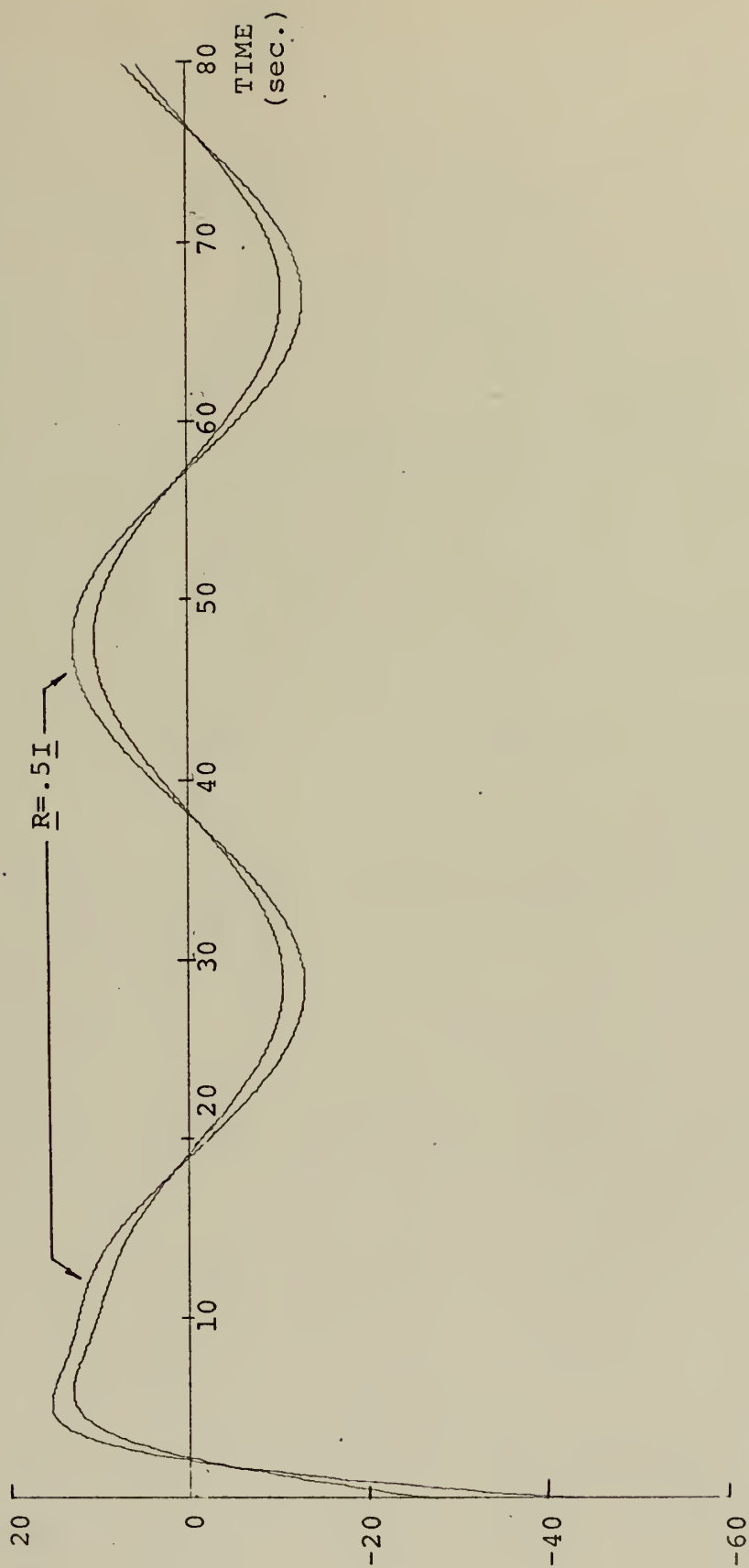


Figure 24. Canard Response Using Optimal Controller  
 $\bar{Q} = \bar{I}$ ,  $\bar{R} = \bar{I}$  and  $0.5\bar{I}$ ,  $\hat{U} = 1.00$ ,  $\psi = 0^\circ$ ,  $\hat{\lambda} = 10$   
 Control Surfaces Unconstrained



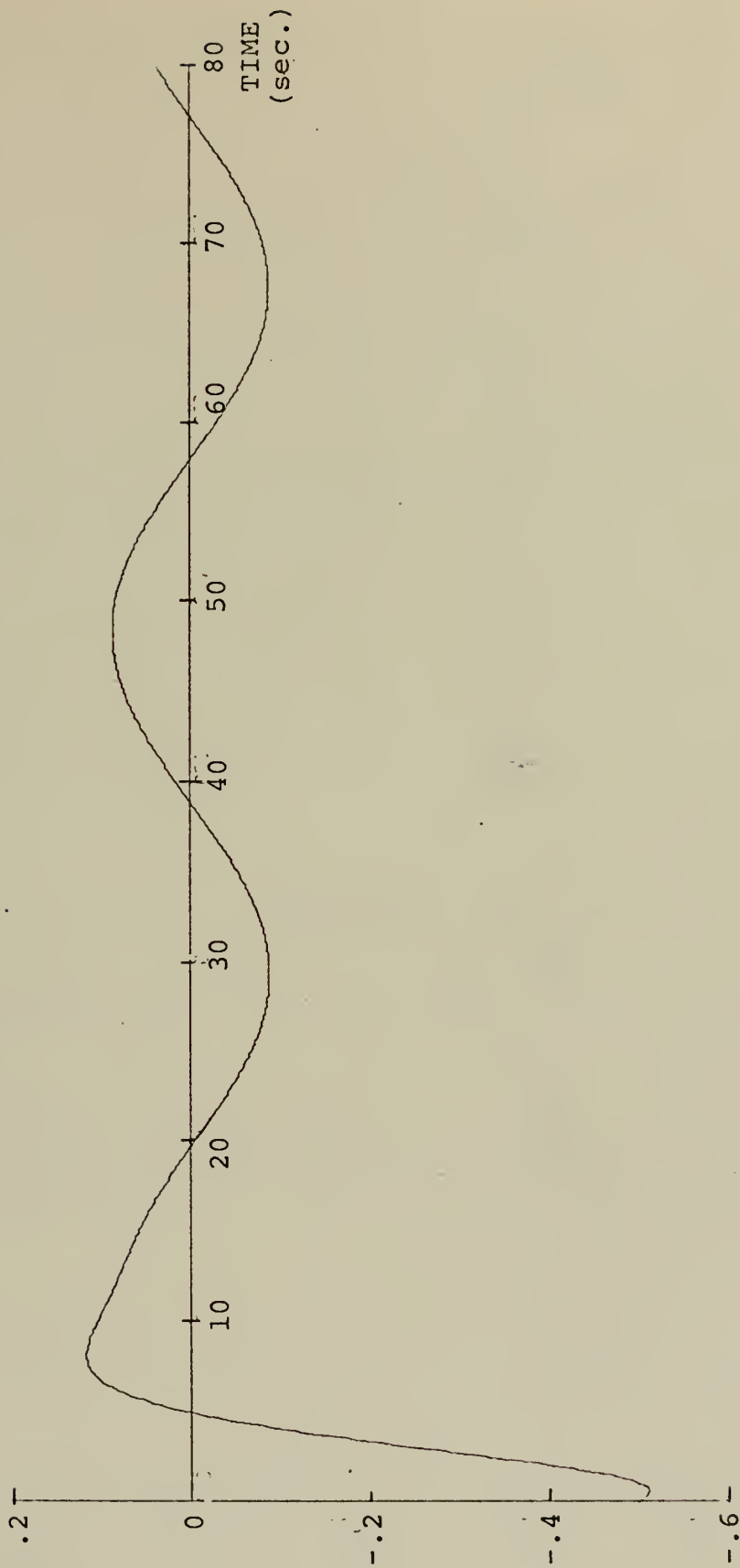


Figure 25. Heave Response Using Optimal Controller  
 $\underline{Q} = \underline{I}$ ,  $\underline{R} = 0.5\underline{I}$ ,  $\hat{U} = 1.00$ ,  $\psi = 0^\circ$ ,  $\hat{\lambda} = 10$   
 Control Surfaces Constrained to  $\pm 30^\circ$





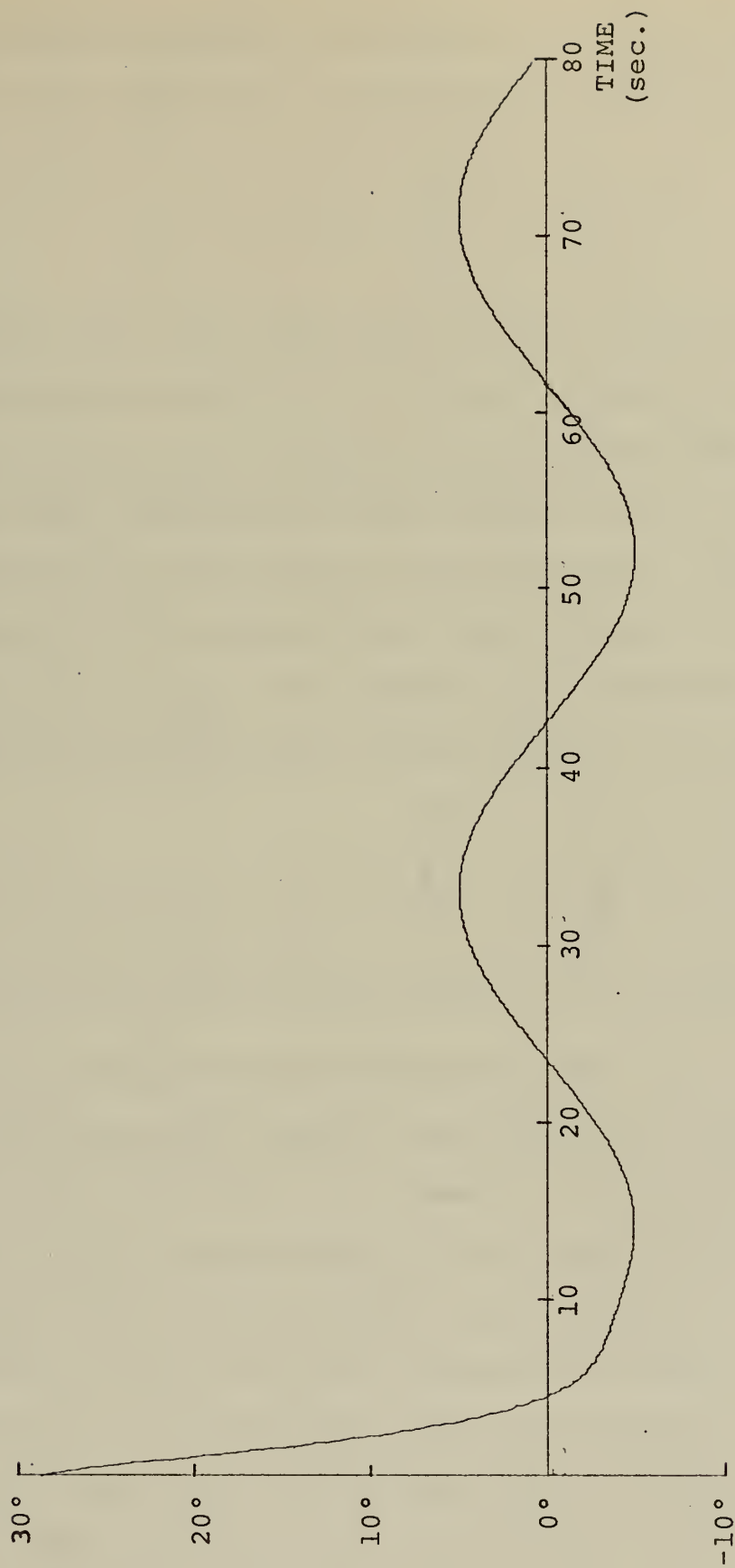


Figure 26. Pitch Response Using Optimal Controller

$$\underline{Q} = \underline{I}, \underline{R} = 0.5\underline{I}, \hat{U} = 1.00, \psi = 0^\circ, \hat{\lambda} = 10$$

Control Surfaces Constrained to  $\pm 30^\circ$



performance measure (see Table VII). It was found that an additional reduction in the control weighting matrix to

$$\underline{R} = \begin{bmatrix} 0.1 & 0 \\ 0 & 0.1 \end{bmatrix}$$

brought the state vector much closer to the origin but with unconstrained control deflections, produced unrealistic deflection angles in the initial control period. The control surfaces were then constrained to the previous limits and the resultant differences in the state trajectories were negligible since the period of constraint was small compared to the total control interval  $[t_0, t_f]$ . As a result, all remaining cases have constrained control surface deflections ( $\pm 30^\circ$ ) and

$$\underline{R} = \begin{bmatrix} 0.1 & 0 \\ 0 & 0.1 \end{bmatrix}$$

to bring the state vector closer to the origin.

#### D. THE CONSTANT-GAIN CONTROLLER (CASE III)

As previously stated, this controller was not derived for the case where  $\underline{w}(t) \neq 0$ . However, since it is based upon feedback of the system states, it will tend to reduce any disturbance of the state vector from its equilibrium point. Figures 27 through 29 show the ship's response and control surface deflections for a following sea with a wavelength of 10 when the ship's speed is 1.65. As expected, the state vector's deviation from equilibrium has been reduced (refer to Figs. 19 and 20 for comparison) and the Constant-Gain Controller can be used without any knowledge of  $\underline{w}(t)$ .



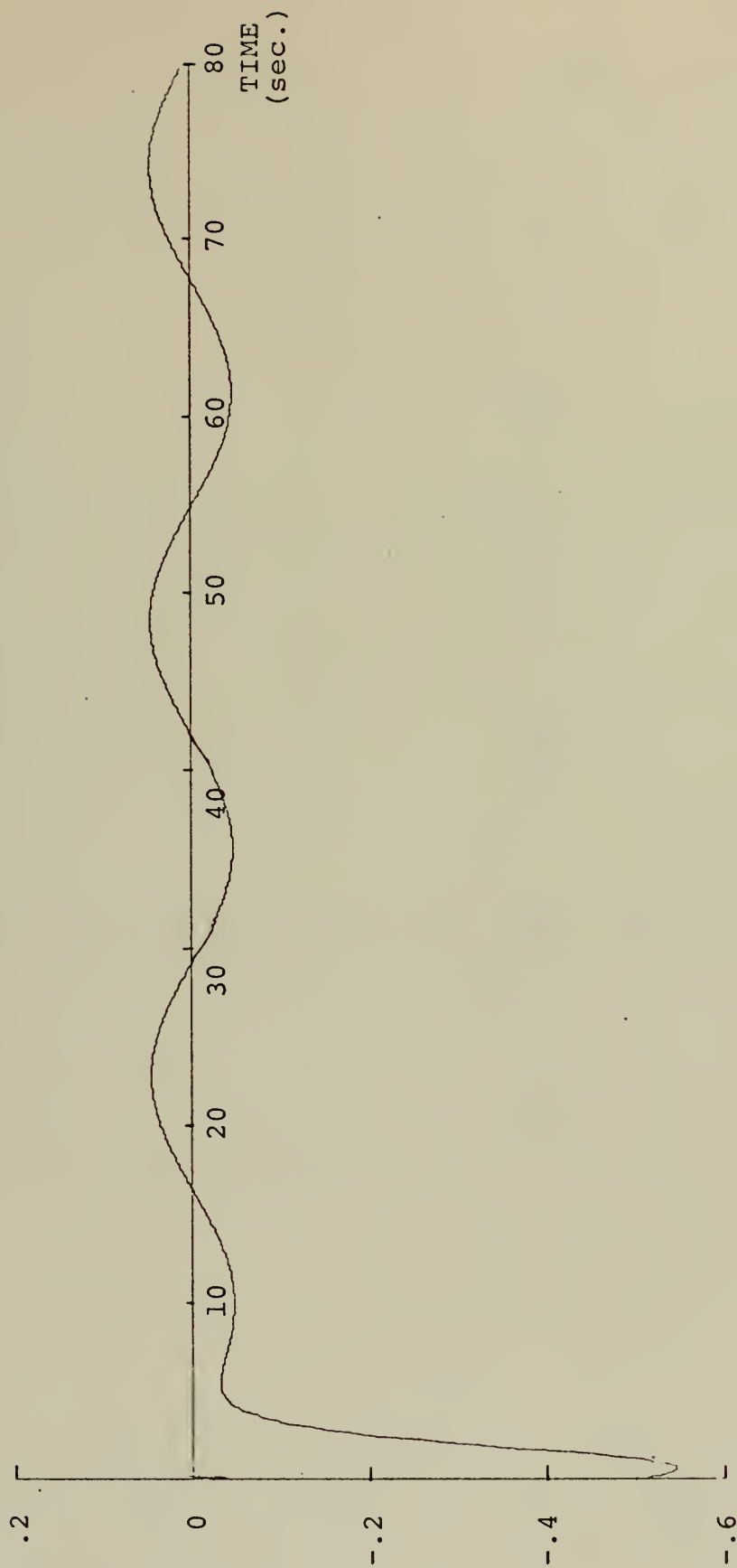


Figure 27. Heave Response Using Constant-Gain Controller

$$\underline{Q} = \underline{I}, \underline{R} = 0.1\underline{I}, \hat{U} = 1.65, \psi = 0^\circ, \hat{\lambda} = 10$$

Control Surfaces Constrained to  $\pm 30^\circ$



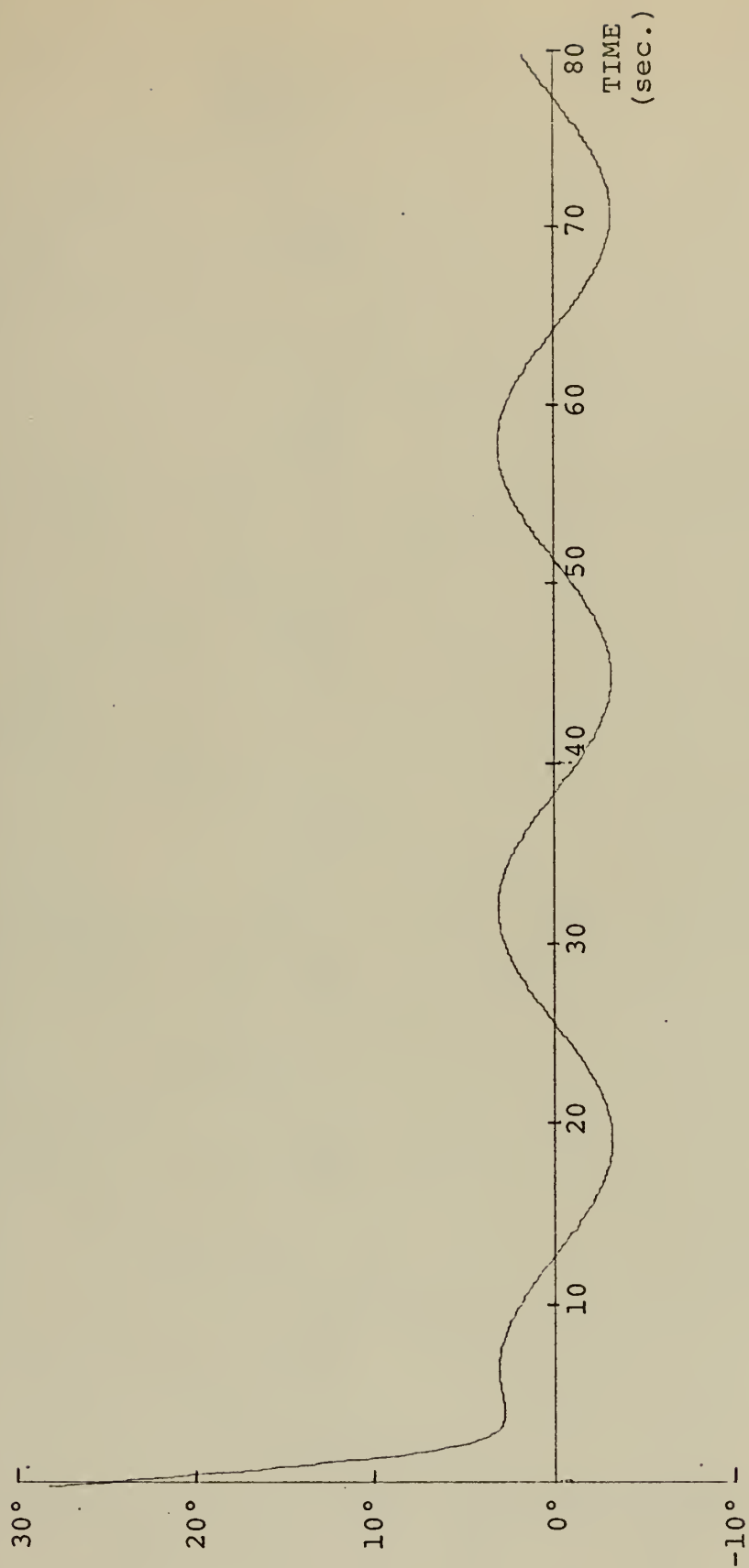


Figure 28. Pitch Response Using Constant-Gain Controller

$$\bar{Q} = \bar{I}, \bar{R} = 0.1\bar{I}, \hat{U} = 1.65, \psi = 0^\circ, \hat{\lambda} = 10$$

Control Surfaces Constrained to  $\pm 30^\circ$





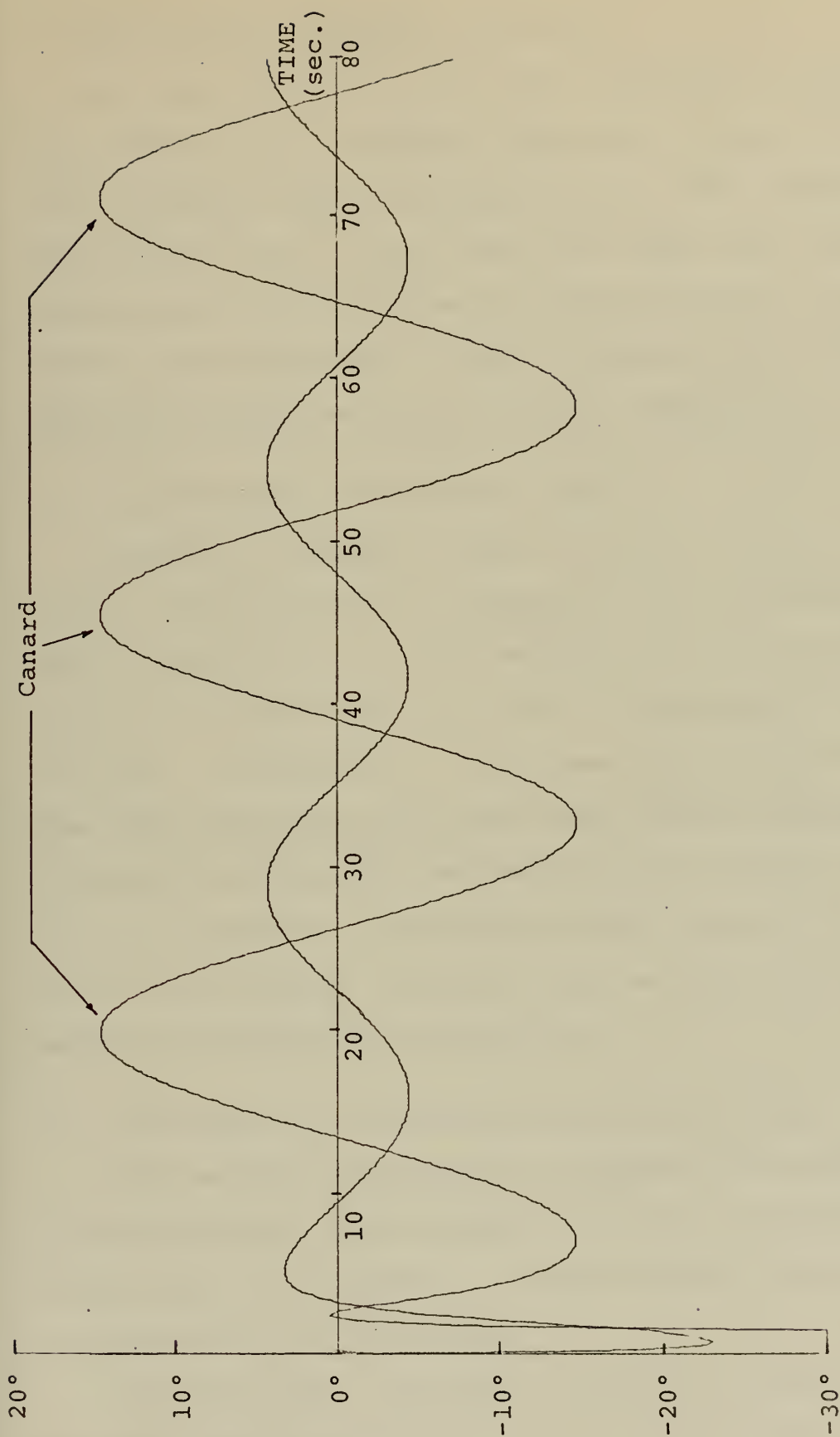


Figure 29. Elevator and Canard Response Using Constant-Gain Controller

$$\bar{Q} = \bar{I}, \bar{R} = 0.1\bar{I}, \hat{U} = 1.65, \psi = 0^\circ, \hat{\lambda} = 10$$

Control Surfaces Constrained to  $\pm 30^\circ$



#### E. THE OPTIMAL CONTROLLER (CASE IV)

The ship's response using this controller is shown in Figs. 30 and 31. The ship's speed was 1.00 and the seas were following with a wavelength of 10. The control surface deflections (Fig. 32) are seen to be less than those of the Constant-Gain Controller as are the deviations of the state vector from equilibrium. This is expected since the Optimal Controller minimizes the performance measure  $J$ .

#### F. THE SUBOPTIMAL CONTROLLER (CASE V)

Figures 33 through 35 show the ship's response and control surface deflections for a following sea of wavelength 10 and a ship's speed of 1.65. The response and control surface deflections for an ahead sea ( $\psi = 180^\circ$ ) of wavelength 10 are shown in Figs. 36 through 38. It is seen that, as previously stated, the state approaches zero after the initial transients. Although the states are maintained at the origin after the initial transients, the control effort required is greater than that of the Optimal Controller and, as expected, the performance measure is greater (see Table VII).

#### G. THE EFFECT OF INACCURATE ESTIMATION OF WAVE FORCE (CASE VI)

The response of the ship to imperfect estimates of  $\underline{w}(t)$  was investigated for the case where only the estimates of the amplitudes were imperfect. It was assumed that the wavelength and phase were known exactly.

The Suboptimal Controller was used to control the ship when the amplitude of  $\underline{w}(t)$  was not exactly known. The ship was



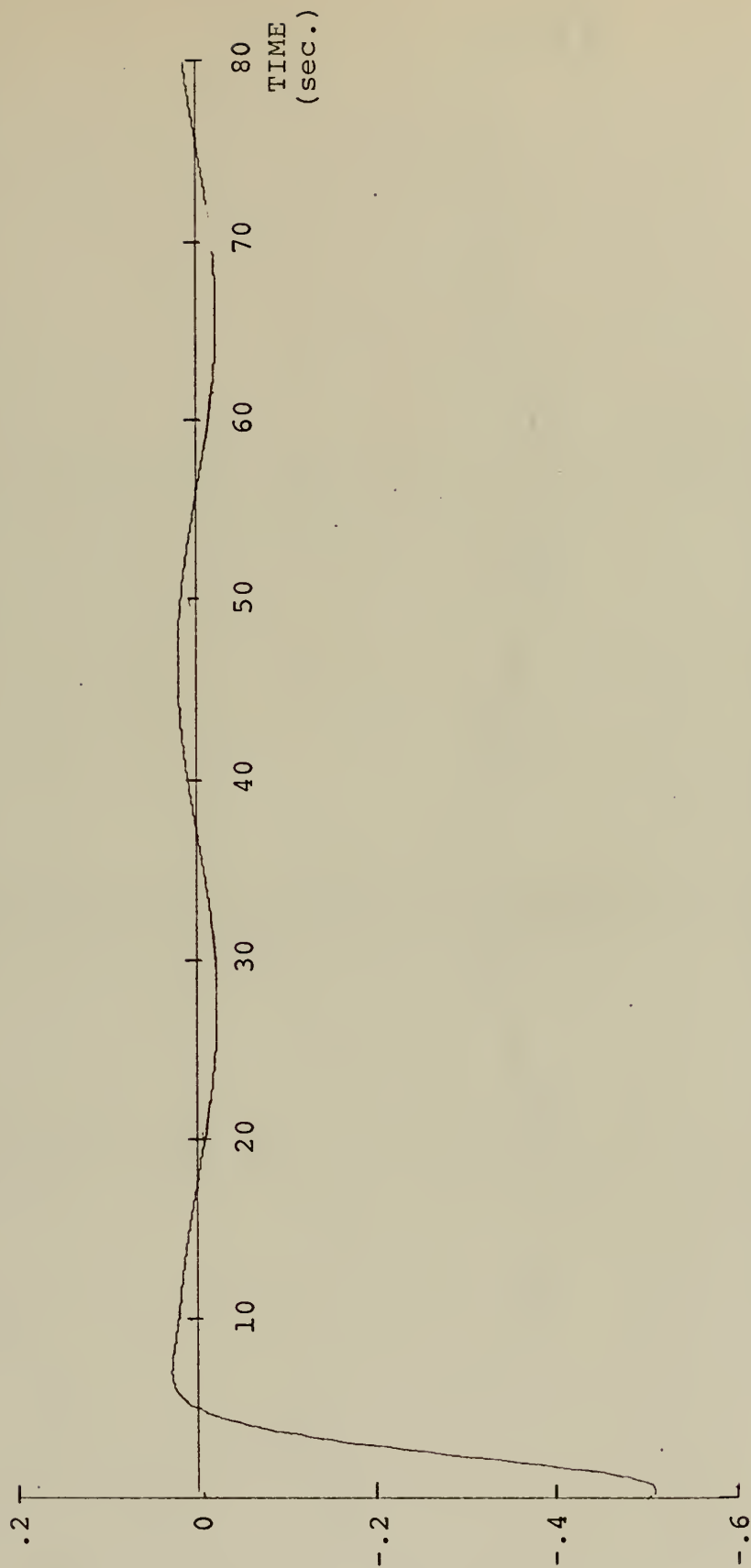


Figure 30. Heave Response Using Optimal Controller

$$\bar{Q} = \bar{I}, \bar{R} = 0.1\bar{I}, \hat{U} = 1.00, \psi = 0^\circ, \hat{\lambda} = 10$$

Control Surfaces Constrained to  $\pm 30^\circ$



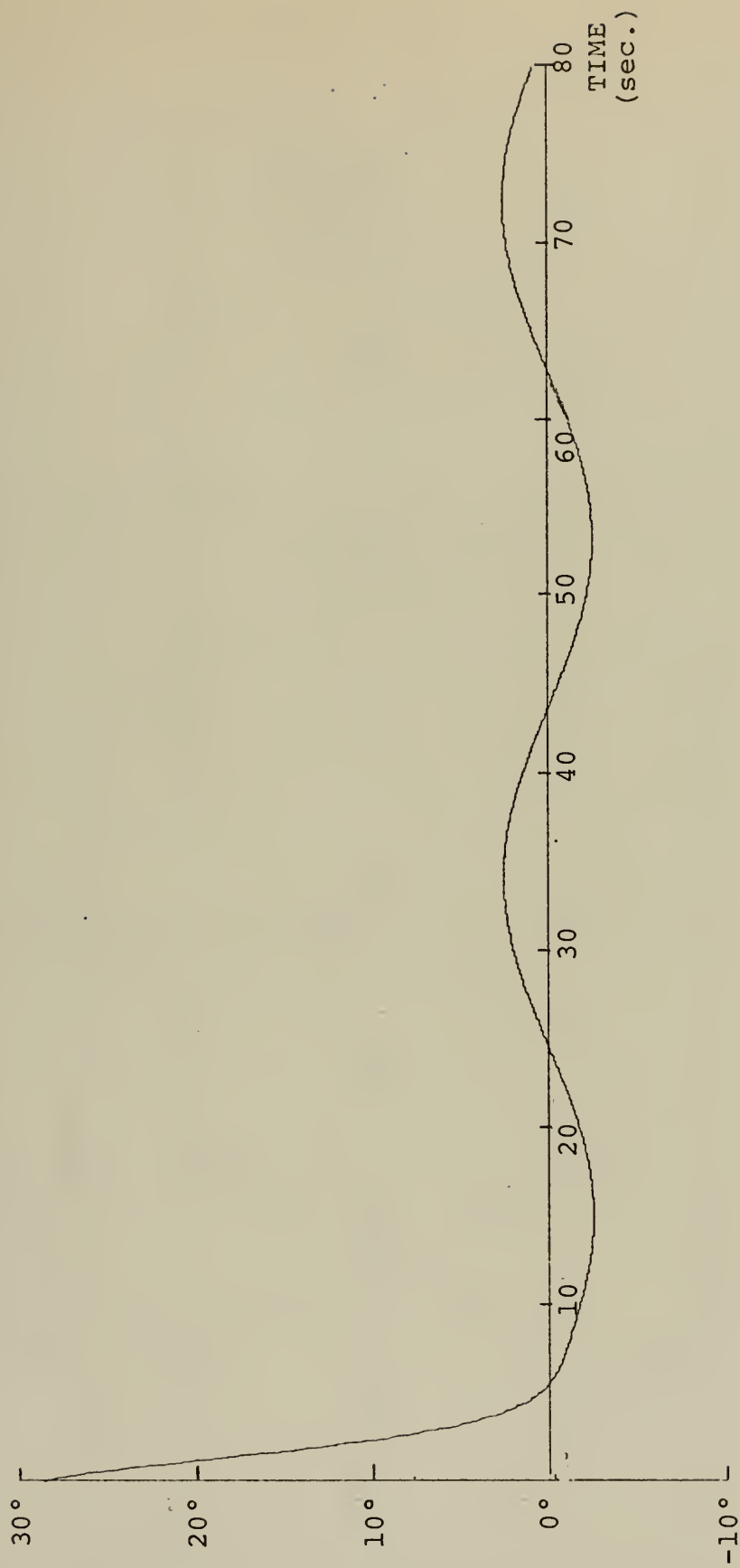


Figure 31. Pitch Response Using Optimal Controller

$$\underline{\hat{Q}} = \underline{I}, \underline{R} = 0.1\underline{I}, \underline{\hat{U}} = 1.00, \psi = 0^\circ, \hat{\lambda} = 10$$

Control Surfaces Constrained to  $\pm 30^\circ$





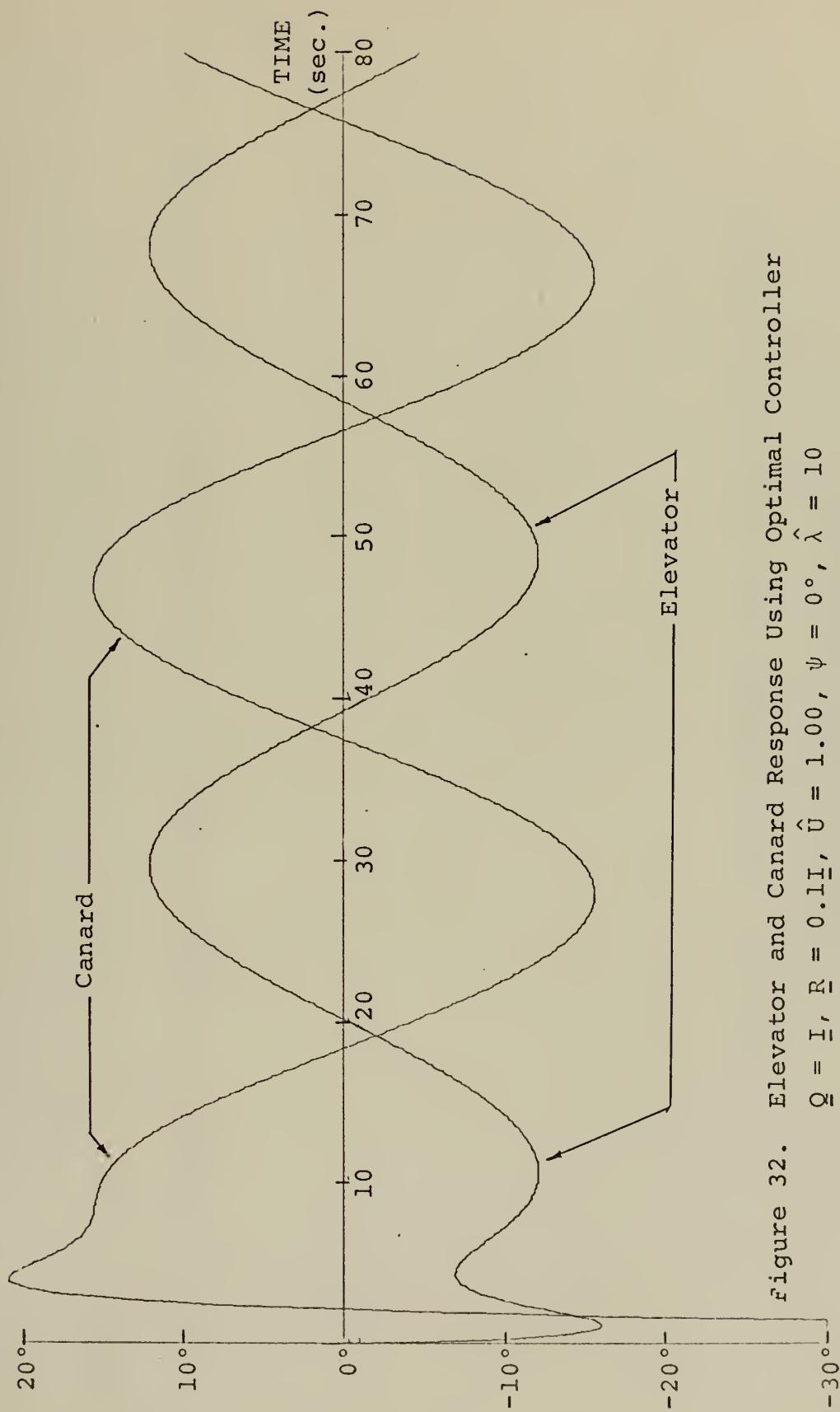


Figure 32. Elevator and Canard Response Using Optimal Controller

$$\underline{Q} = \underline{I}, \underline{R} = 0.1\underline{I}, \hat{U} = 1.00, \psi = 0^\circ, \hat{\lambda} = 10$$

Control Surfaces Constrained to  $\pm 30^\circ$



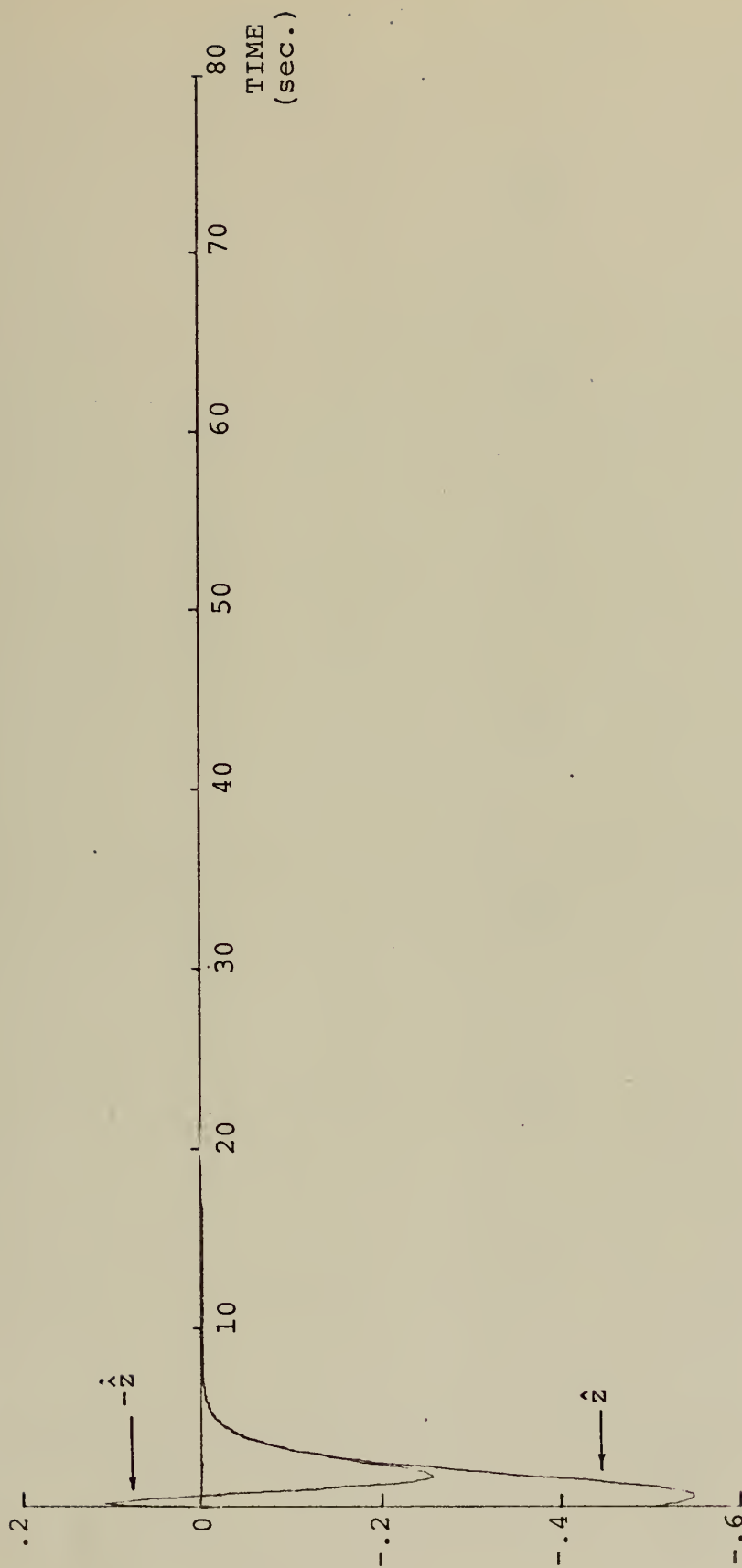


Figure 33. Heave Response Using Suboptimal Controller

$\bar{Q} = \bar{I}$ ,  $R = 0.1\bar{I}$ ,  $\hat{U} = 1.65$ ,  $\psi = 0^\circ$ ,  $\hat{\lambda} = 10$   
Control Surfaces Constrained to  $\pm 30^\circ$



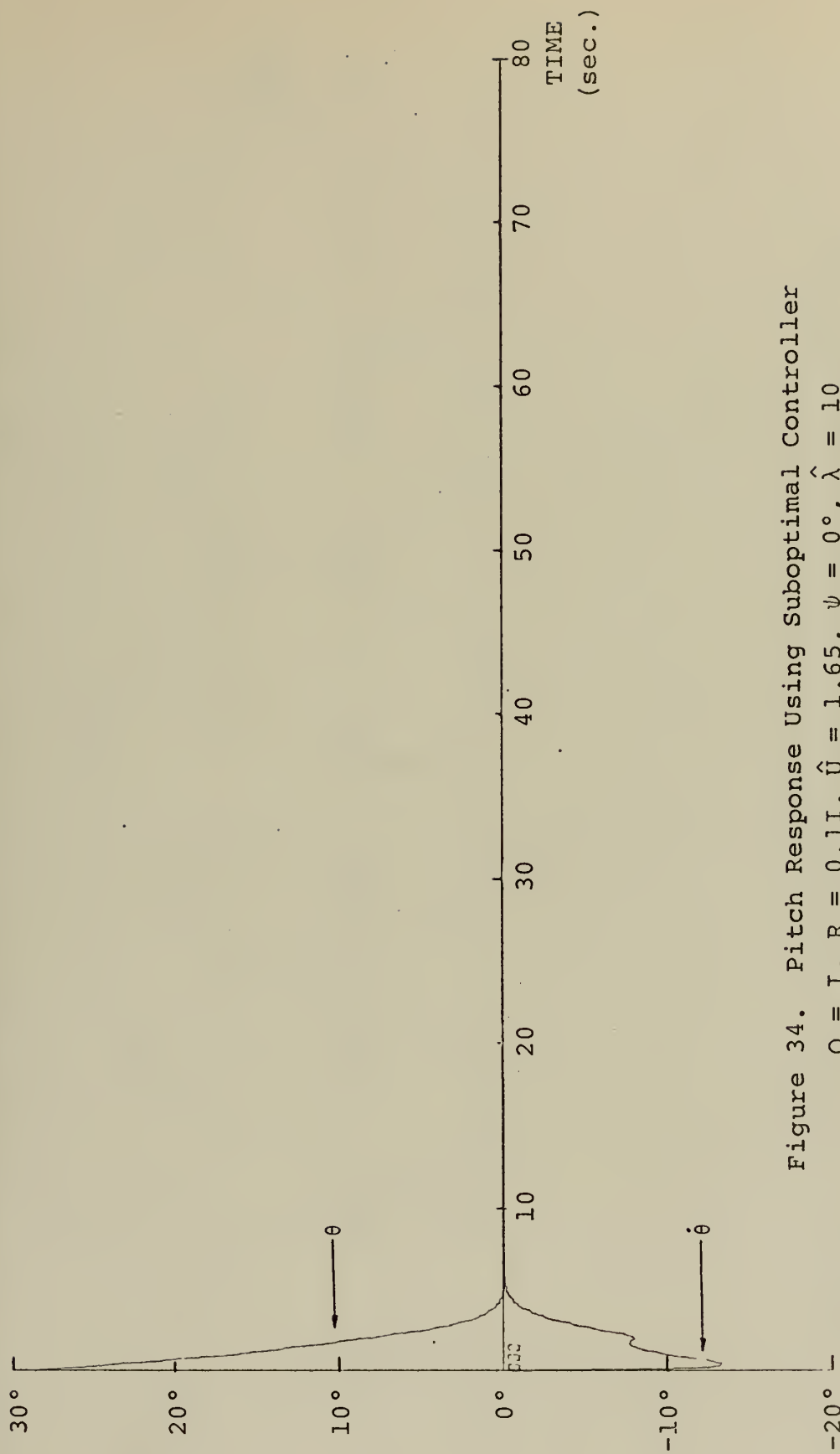


Figure 34. Pitch Response Using Suboptimal Controller

$$\bar{Q} = \underline{I}, \bar{R} = 0.1\underline{I}, \hat{U} = 1.65, \psi = 0^\circ, \hat{\lambda} = 10$$

Control Surfaces Constrained to  $\pm 30^\circ$



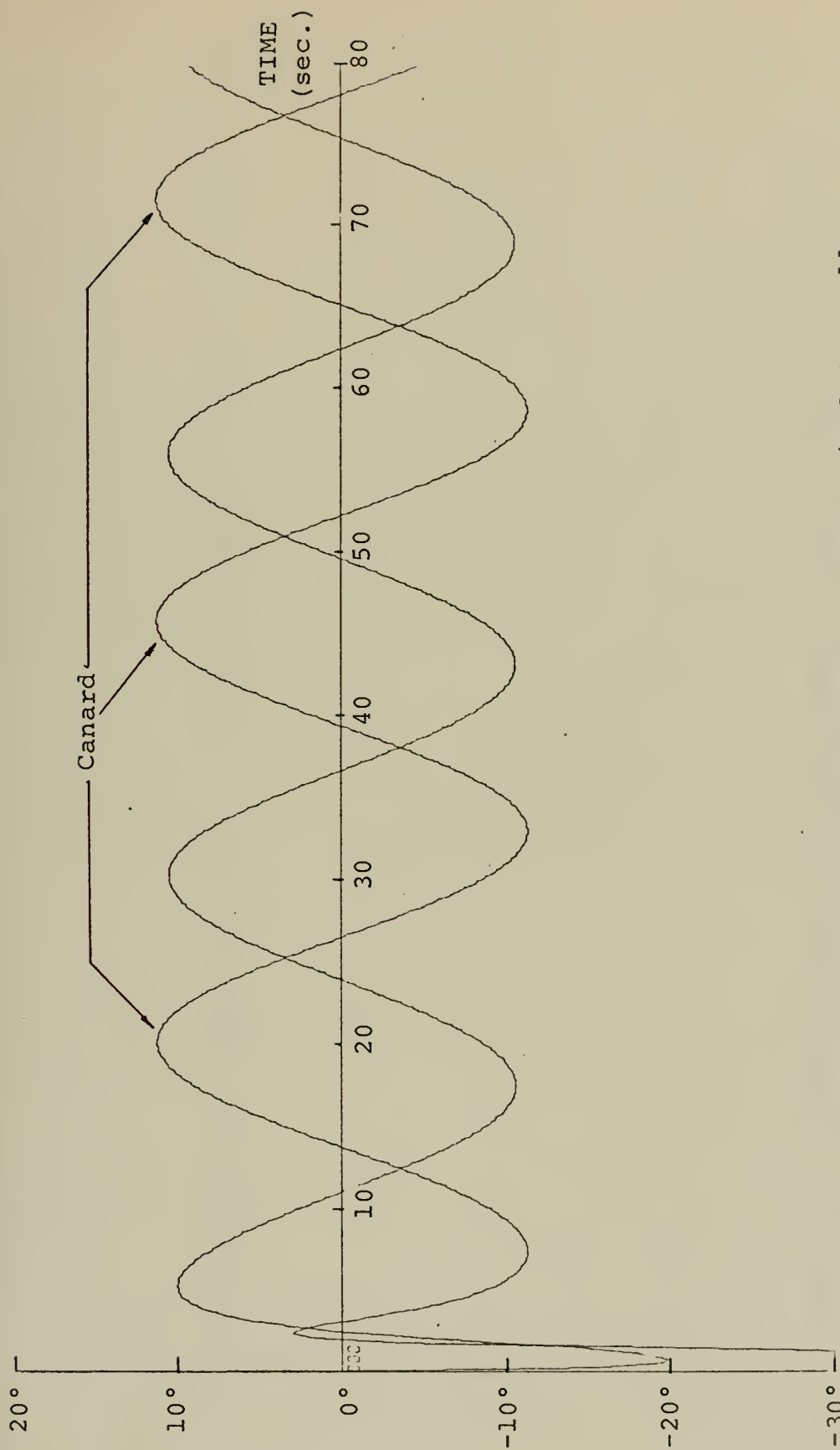


Figure 35. Elevator and Canard Response Using Suboptimal Controller

$$\bar{Q} = \underline{I}, \bar{R} = 0.1\underline{I}, \hat{U} = 1.65, \psi = 0^\circ, \hat{\lambda} = 10$$

Control Surfaces Constrained to  $\pm 30^\circ$





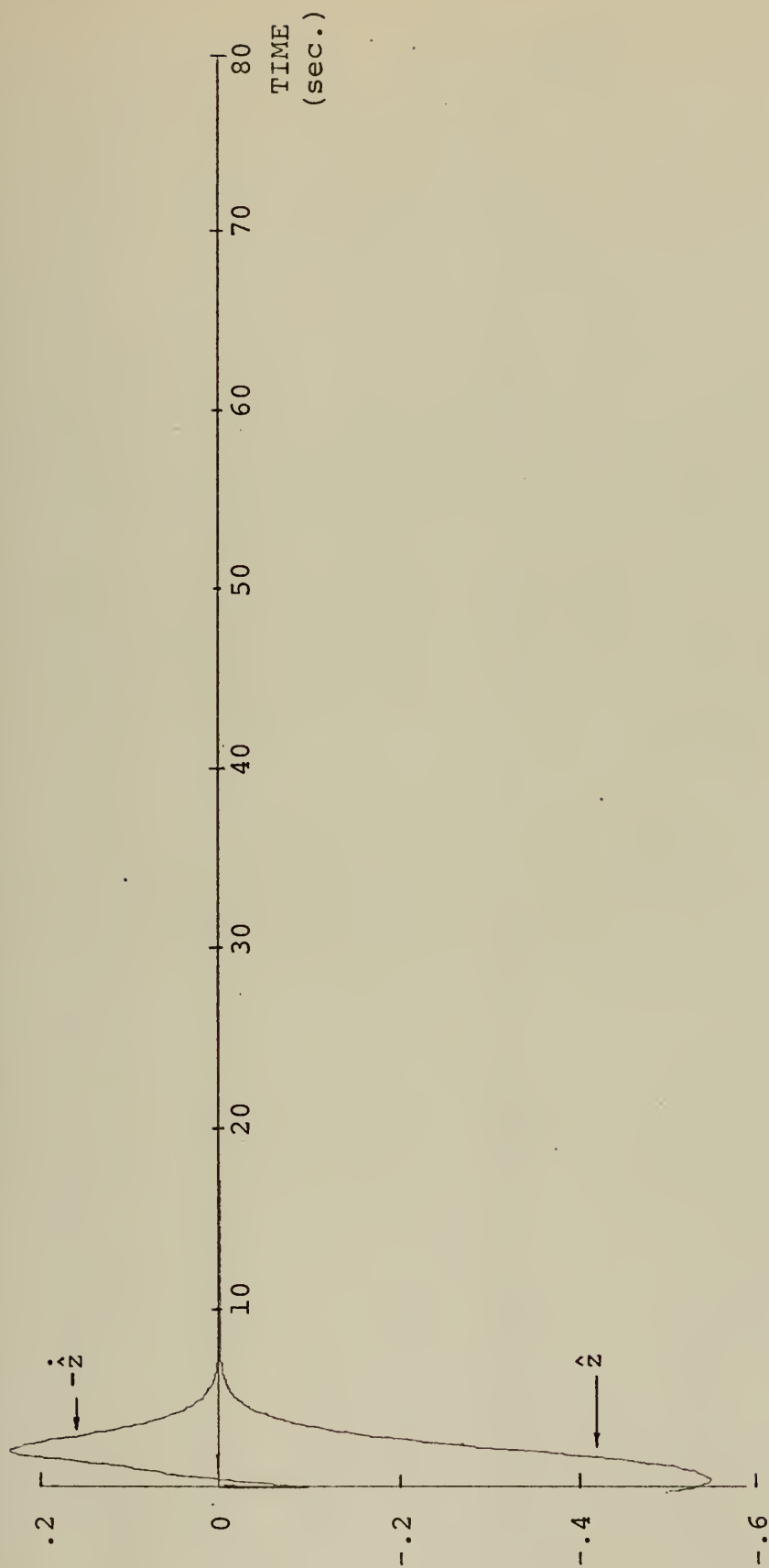


Figure 36. Heave and Heave Velocity Response Using Suboptimal Controller

$$\underline{Q} = \underline{I}, \underline{R} = 0.1\underline{I}, \hat{U} = 1.65, \psi = 180^\circ, \hat{\lambda} = 10$$

Control Surfaces Constrained to  $\pm 30^\circ$



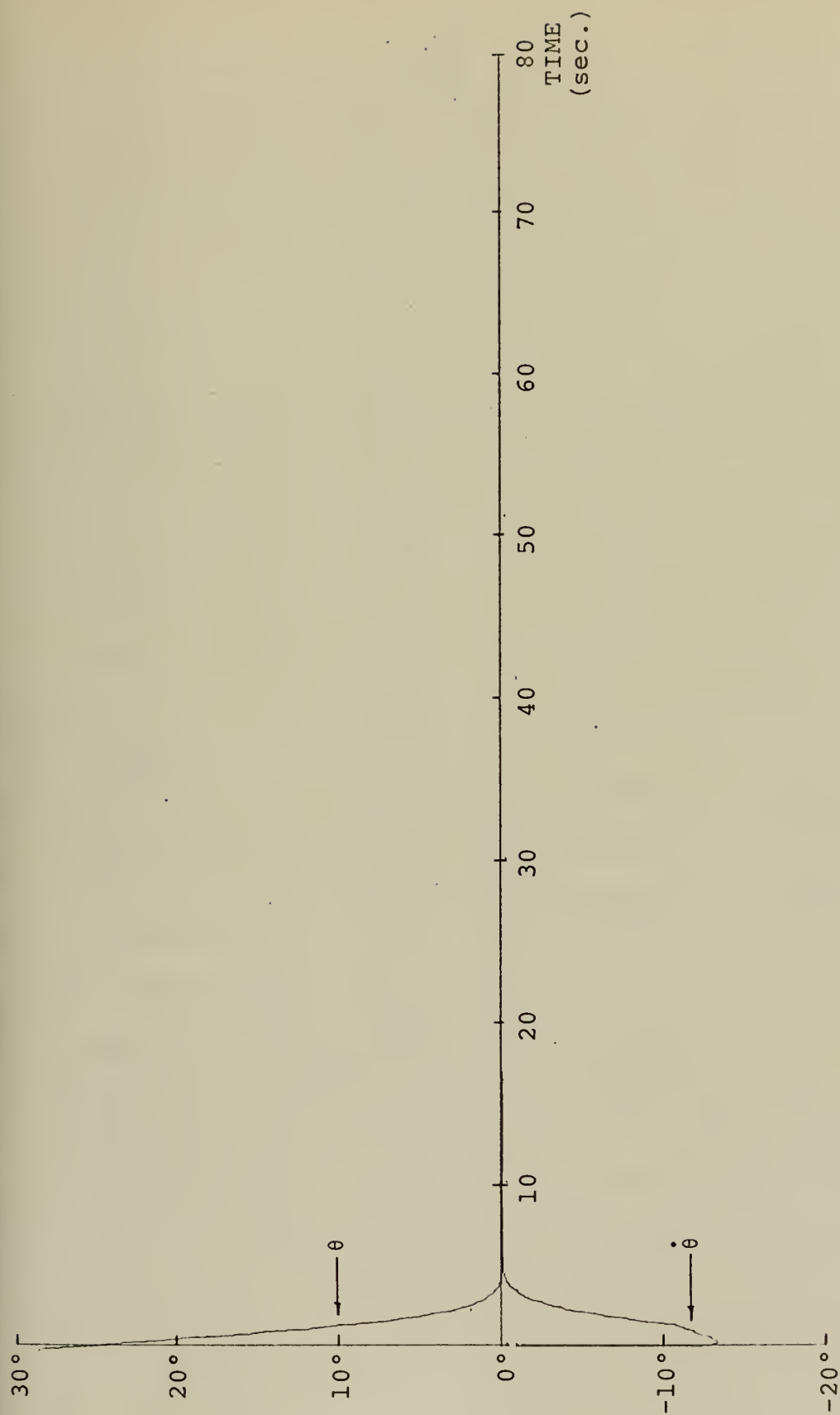


Figure 37. Pitch and Pitch Velocity Response Using Suboptimal Controller

$$\underline{Q} = \underline{I}, \underline{R} = 0.1\underline{I}, \hat{U} = 1.65, \psi = 180^\circ, \hat{\lambda} = 10$$

Control Surfaces Constrained to  $\pm 30^\circ$



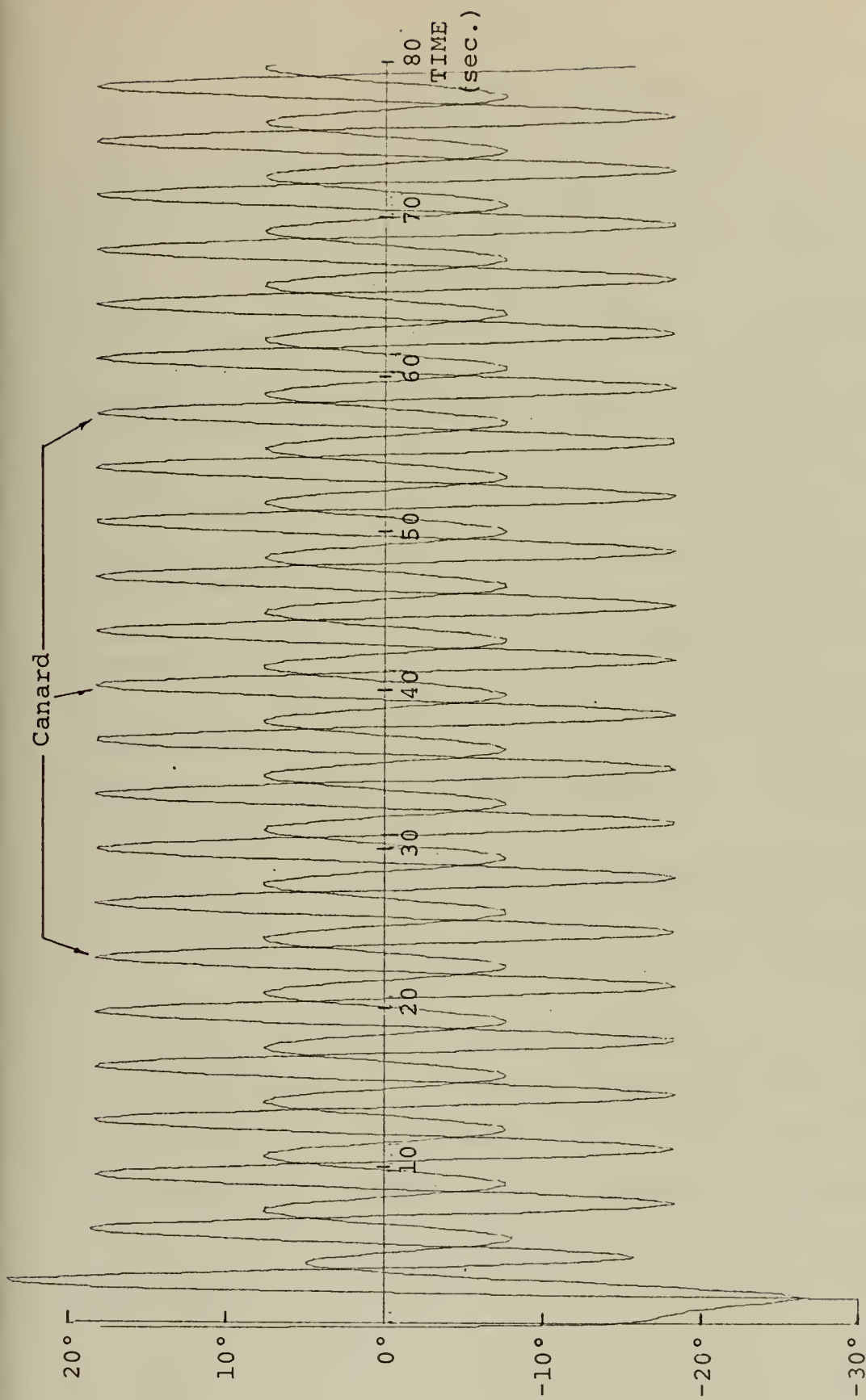


Figure 38. Elevator and Canard Response Using Suboptimal Controller

$$\underline{Q} = \underline{I}, \underline{R} = 0.1\underline{I}, \hat{U} = 1.65, \psi = 180^\circ, \hat{\lambda} = 10$$

Control Surfaces Constrained to  $\pm 30^\circ$



TABLE VII

## PERFORMANCE MEASURES

 $t_0 = 0 \text{ sec.}, t_f = 80 \text{ sec.}$ 

Controller	$\underline{Q}$	$\underline{R}$	$\hat{U}$	$\psi$	$\hat{\lambda}$	$\underline{w}(t)$	J
None	$\underline{I}$	$0.1\underline{I}$	1.65	$0^\circ$	10	--	$9.328477 \times 10^4$
Optimal (unconstrained)	$\underline{I}$	$\underline{I}$	1.00	$0^\circ$	10	Known	$8.5290623 \times 10^2$
Optimal (unconstrained)	$\underline{I}$	$0.5\underline{I}$	1.00	$0^\circ$	10	Known	$6.5330823 \times 10^2$
Optimal (constrained)	$\underline{I}$	$0.5\underline{I}$	1.00	$0^\circ$	10	Known	$6.5468393 \times 10^2$
Constant-Gain (constrained)	$\underline{I}$	$0.1\underline{I}$	1.65	$0^\circ$	10	Known	$3.5693990 \times 10^2$
Optimal (constrained)	$\underline{I}$	$0.1\underline{I}$	1.00	$0^\circ$	10	Known	$3.9204965 \times 10^2$
Suboptimal (constrained)	$\underline{I}$	$0.1\underline{I}$	1.65	$0^\circ$	10	Known	$3.2483721 \times 10^2$
Suboptimal (constrained)	$\underline{I}$	$0.1\underline{I}$	1.65	$180^\circ$	10	Known	$3.9344051 \times 10^2$
Suboptimal (constrained)	$\underline{I}$	$0.1\underline{I}$	1.65	$0^\circ$	10	Underestimated by 15 percent	$3.3556745 \times 10^2$

running in a following sea of wavelength 10 at a speed of 1.65. The ship's response in heave and pitch are shown in Figs. 39 and 40 where the amplitude of  $\underline{w}(t)$  was overestimated and underestimated by 15 percent. It is seen that the estimate error has very little effect on the performance of the Suboptimal Controller.





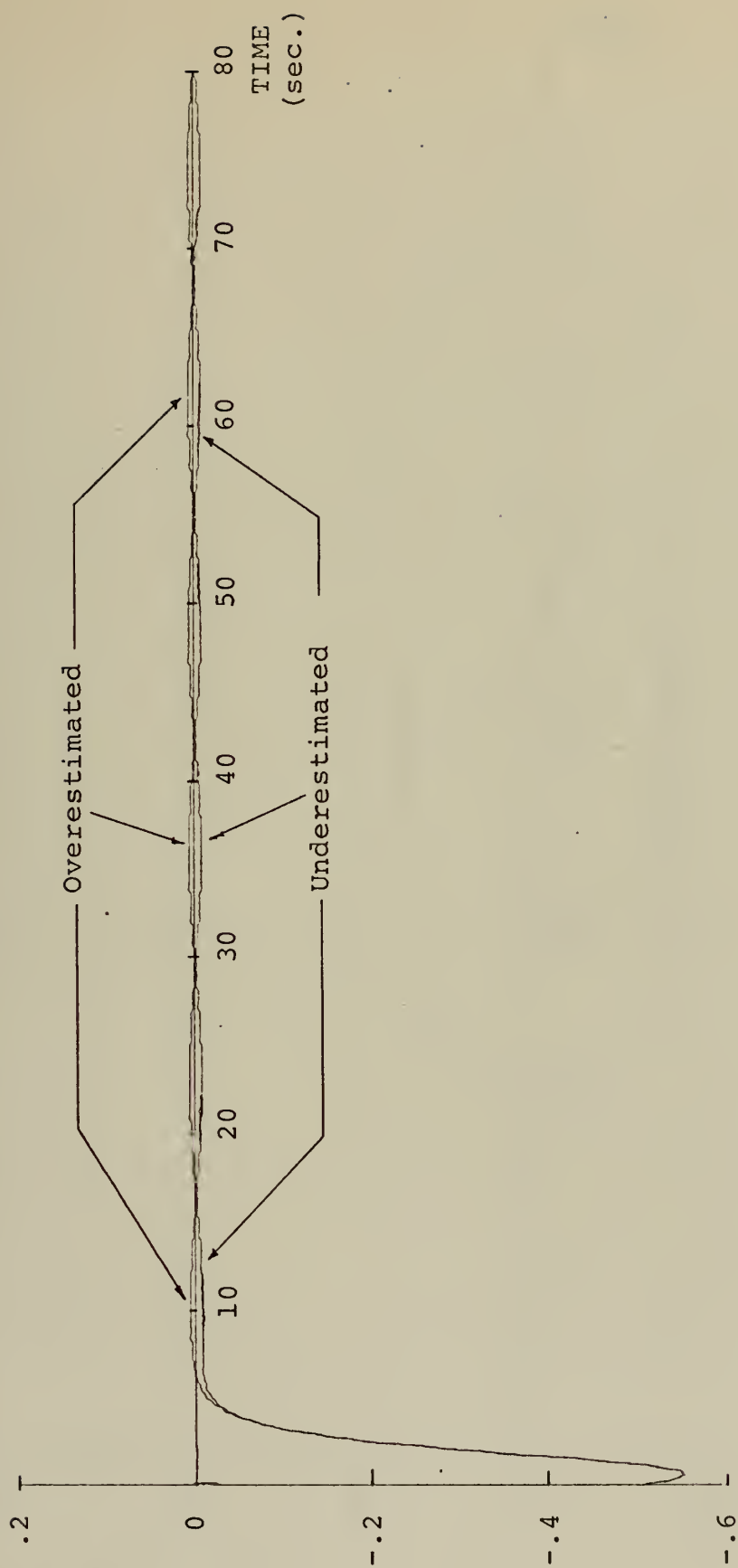


Figure 39. Heave Response Using Suboptimal Controller

$\bar{Q} = \underline{I}$ ,  $\bar{R} = 0.1\underline{I}$ ,  $\hat{U} = 1.65$ ,  $\psi = 0^\circ$ ,  $\hat{\lambda} = 10$ ,  $\bar{w}(t)$  overestimated and underestimated by 15 percent, Control Surfaces Constrained to  $\pm 30^\circ$



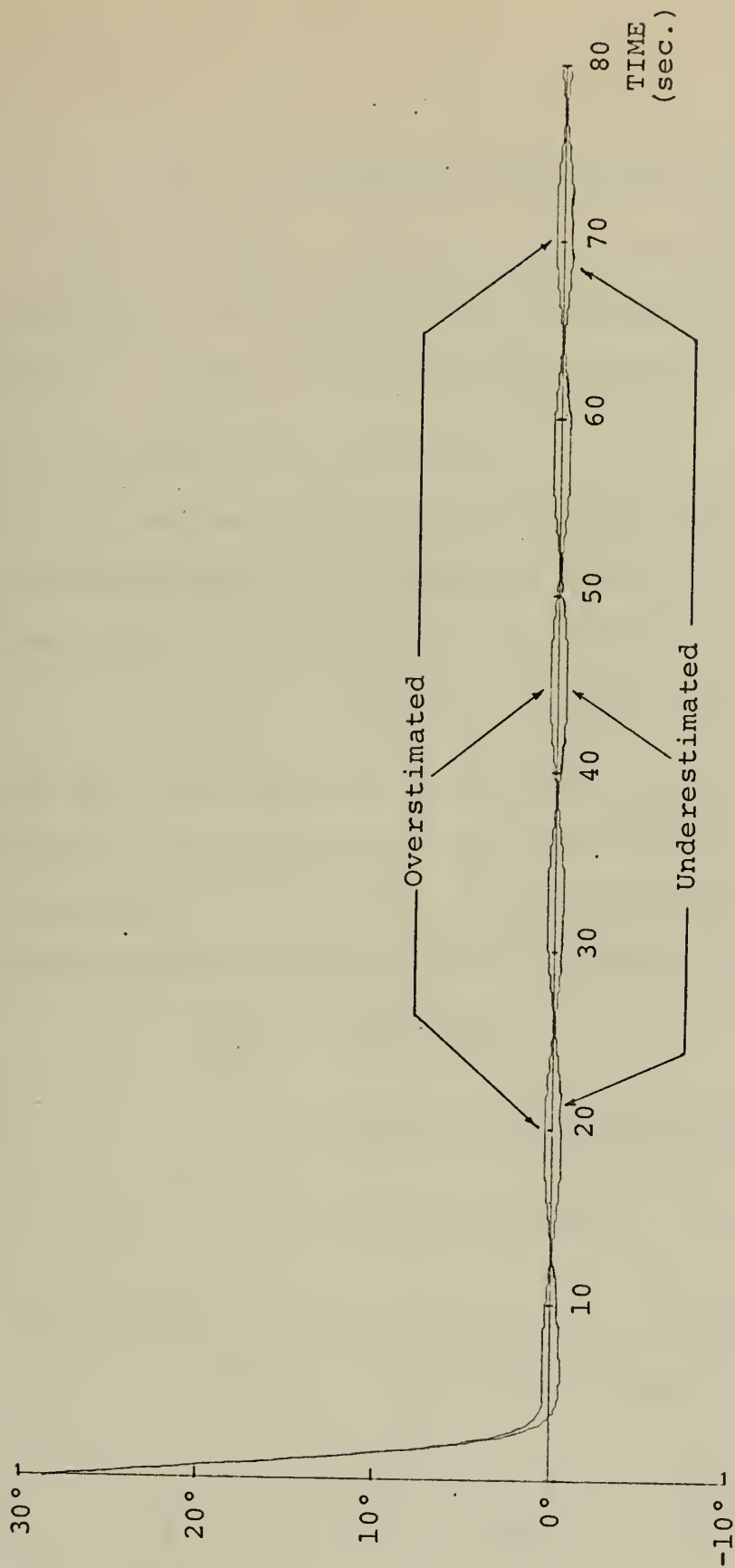


Figure 40. Pitch Response Using Suboptimal Controller

$\underline{Q} = \underline{I}$ ,  $\underline{R} = 0.1\underline{I}$ ,  $\hat{U} = 1.65$ ,  $\psi = 0^\circ$ ,  $\hat{\lambda} = 10$ ,  $\underline{w}(t)$  overestimated and underestimated by 15 percent, Control Surfaces Constrained to  $\pm 30^\circ$



## VII. PRELIMINARY WORK ON WAVE ESTIMATORS

The estimators stated below are possible candidates which can provide an estimate of  $\underline{w}(t)$  required for the operation of both the Optimal and Suboptimal Controllers.

### A. AN INPUT-SIGNAL OBSERVER

The estimator depicted in Fig. 41 consists of a model of the plant being run in parallel with the actual plant. The state equation of the model is given by

$$\dot{\underline{e}}(t) = \underline{A}\underline{e}(t) + \underline{B}\underline{u}(t) + \underline{G}[\underline{x}(t) - \underline{e}(t)] \quad (7.1)$$

and the state equation of the plant is given by Eq. (3.9). In writing this equation, it has been assumed that all states of the system are measured. If the difference between the plant and model states  $(\underline{x}(t) - \underline{e}(t))$  is called  $\underline{g}(t)$ , then

$$\begin{aligned} \dot{\underline{g}}(t) &= \dot{\underline{x}}(t) - \dot{\underline{e}}(t) \\ &= \underline{A}[\underline{x}(t) - \underline{e}(t)] - \underline{G}[\underline{x}(t) - \underline{e}(t)] + \underline{C}\underline{w}(t) \\ &= [\underline{A} - \underline{G}]\underline{g}(t) + \underline{C}\underline{w}(t) \end{aligned} \quad (7.2)$$

The solution to Eq. (7.2) is

$$\underline{g}(t) = e^{[\underline{A} - \underline{G}]t} \underline{g}(0) + \int_0^t e^{[\underline{A} - \underline{G}](t-\tau)} \underline{C}\underline{w}(\tau) d\tau \quad (7.3)$$

so that if the eigenvalues of  $\underline{G}$  are chosen such that  $e^{(\underline{A} - \underline{G})t}$  dies out quickly as  $t$  increases, then  $\underline{g}(t)$  can be closely approximated by

$$\underline{g}(t) \approx \int_0^t \underline{\phi}(t-\tau) \underline{C}\underline{w}(\tau) d\tau \quad (7.4)$$



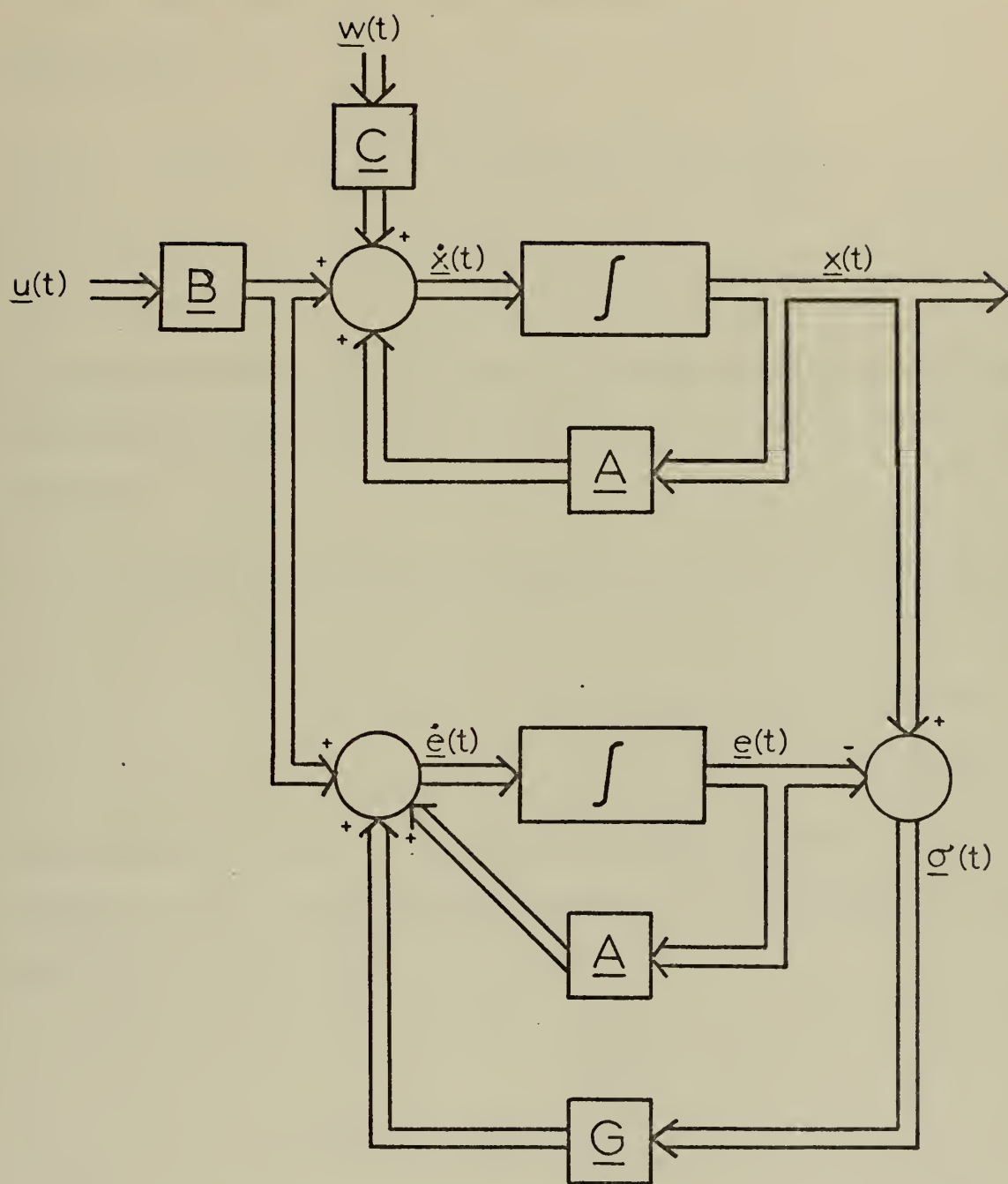


Figure 41. Input-Signal Observer





where  $\phi$  is the state transition matrix of Eq. (7.2). Referring to Eqs. (5.1) and (5.2), it is seen that Eq. (7.4) can be rewritten as

$$\underline{\sigma}(t) = \int_0^t \phi(t-\tau) \begin{bmatrix} 0 \\ \alpha_1 \cos \omega \tau + \alpha_2 \sin \omega \tau \\ 0 \\ \beta_1 \cos \omega \tau + \beta_2 \sin \omega \tau \end{bmatrix} d\tau \quad (7.5)$$

The coefficients  $\alpha_1$ ,  $\alpha_2$ ,  $\beta_1$  and  $\beta_2$  are constants and can be taken outside the integral; thus, Eq. (7.5) can be rewritten in the form

$$\begin{aligned} \sigma_i(t) = & \alpha_1 \int_0^t \phi_{i2}(t-\tau) \cos \omega \tau d\tau + \alpha_2 \int_0^t \phi_{i2}(t-\tau) \sin \omega \tau d\tau \\ & + \beta_1 \int_0^t \phi_{i4}(t-\tau) \cos \omega \tau d\tau + \beta_2 \int_0^t \phi_{i4}(t-\tau) \sin \omega \tau d\tau \\ & (i=1, \dots, 4) \end{aligned} \quad (7.6)$$

The integrals in Eq. (7.6) can be precomputed for a time interval  $(0, t_1)$  and stored in a matrix  $D(t_1)$  so that Eq. (7.6) can be put in the form

$$\underline{\sigma}(t_1) = \underline{D}(t_1) \begin{bmatrix} \alpha_1 \\ \alpha_2 \\ \beta_1 \\ \beta_2 \end{bmatrix} \quad (7.7)$$

If the state differences are now sampled and stored at times  $t_i$ ,  $i=1, \dots, k$ , then an estimate of the coefficients  $\alpha_1$ ,  $\alpha_2$ ,  $\beta_1$  and  $\beta_2$  can be obtained by determining the minimum-mean-square solution of



$$\begin{bmatrix} \underline{\sigma}(t_1) \\ \underline{\sigma}(t_2) \\ \vdots \\ \underline{\sigma}(t_k) \end{bmatrix} = \begin{bmatrix} \underline{D}(t_1) \\ \underline{D}(t_2) \\ \vdots \\ \underline{D}(t_k) \end{bmatrix} \begin{bmatrix} \alpha_1 \\ \alpha_2 \\ \beta_1 \\ \beta_2 \end{bmatrix} \equiv \underline{D} \begin{bmatrix} \alpha_1 \\ \alpha_2 \\ \beta_1 \\ \beta_2 \end{bmatrix} \quad (7.8)$$

given by

$$\begin{bmatrix} \alpha_1 \\ \alpha_2 \\ \beta_1 \\ \beta_2 \end{bmatrix} = \underline{D}^{\#} \begin{bmatrix} \underline{\sigma}(t_1) \\ \underline{\sigma}(t_2) \\ \vdots \\ \underline{\sigma}(t_k) \end{bmatrix} \quad (7.9)$$

where  $\underline{D}^{\#}$  is the pseudo-inverse of  $\underline{D}$ .

#### B. FAST-FOURIER TRANSFORM ESTIMATION

An alternative approach is to Laplace transform Eq. (7.2) to give

$$\begin{aligned} \underline{\sigma}(s) &= s[s\underline{I}-\underline{A}+\underline{G}]^{-1} \underline{\sigma}(0) \\ &\quad + [s\underline{I}-\underline{A}+\underline{G}]^{-1} \underline{C}\underline{W}(s) \end{aligned} \quad (7.10)$$

If  $\underline{w}(t)$  is a periodic function, then the spectrum  $\underline{\sum}(f)$  will be

$$\underline{\sum}(f) = [j2\pi f\underline{I}-\underline{A}+\underline{G}]^{-1} \underline{C}\underline{W}(f) \quad (7.11)$$

and an estimate of  $\underline{W}(f)$  can be determined by

$$\underline{C}\underline{W}(f) = [j2\pi f\underline{I}-\underline{A}+\underline{G}]\underline{\sum}(f) \quad (7.12)$$

where  $\underline{\sum}(f)$  can be determined by taking the Fast-Fourier Transform (FFT) of the error between the predicted and actual responses.



### C. STATE OBSERVER MODEL

A third possibility is to expand the state equation given by Eq. (3.9) by defining four additional states. The matrix product

$$\underline{C}_w(t) = \begin{bmatrix} 0 \\ \alpha_1 \cos \omega t + \alpha_2 \sin \omega t \\ 0 \\ \alpha_1 \cos \omega t + \beta_2 \sin \omega t \end{bmatrix} \quad (7.13)$$

can be rewritten as

$$\underline{C}_w(t) = \begin{bmatrix} 0 & 0 & 0 & 0 & \alpha_1 \\ \cos \omega t & \sin \omega t & 0 & 0 & \alpha_2 \\ 0 & 0 & 0 & 0 & \beta_1 \\ 0 & 0 & \cos \omega t & \sin \omega t & \beta_2 \end{bmatrix} \quad (7.14)$$

The augmented state vector is now defined as

$$\underline{x}(t) = \begin{bmatrix} \hat{z}(t) \\ \dot{\hat{z}}(t) \\ \theta(t) \\ \dot{\theta}(t) \\ \alpha_1 \\ \alpha_2 \\ \beta_1 \\ \beta_2 \end{bmatrix} \quad (7.15)$$

so that the state equation becomes



$$\dot{\underline{x}}(t) = \begin{bmatrix} \underline{A} & 0 & 0 & 0 & 0 \\ & \cos \omega t & \sin \omega t & 0 & 0 \\ & 0 & 0 & 0 & 0 \\ & 0 & 0 & \cos \omega t & \sin \omega t \\ \hline 0 & & & & 0 \end{bmatrix} \underline{x}(t) + \begin{bmatrix} \underline{B} \\ \hline 0 \end{bmatrix} \underline{u}(t) \quad (7.16)$$

$$= \underline{A}'(t)\underline{x}(t) + \underline{B}'\underline{u}(t)$$

The actual physical states ( $x_1(t)$  through  $x_4(t)$ ) are measured.

The observation matrix for the augmented system is

$$\underline{H} = [\underline{I} \quad \underline{0}] \quad (7.17)$$

If an observer, similar to Fig. 41 but with eight states and an observation matrix  $\underline{H}$ , is now run in parallel with the actual plant so that the observer's state equation is

$$\dot{\underline{e}}(t) = \underline{A}'(t)\underline{e}(t) + \underline{B}'\underline{u}(t) + \underline{G}(t) [\underline{H}\underline{e}(t) - \underline{H}\underline{x}(t)] \quad (7.18)$$

then the difference between the observer and actual state equations can be written as

$$\dot{\underline{\sigma}}(t) = [\underline{A}'(t) + \underline{G}(t)\underline{H}]\underline{\sigma}(t) \quad (7.19)$$

By choosing  $\underline{G}(t)$  so that  $[\underline{A}'(t) + \underline{G}(t)\underline{H}]$  is stable, then the states of the observer,  $\underline{e}(t)$ , will approach the states  $\underline{x}(t)$  and the error  $\underline{\sigma}(t)$  will approach zero. The states  $e_5(t)$  through  $e_8(t)$  will then be estimates of  $\alpha_1$ ,  $\alpha_2$ ,  $\beta_1$  and  $\beta_2$  respectively.

Utilizing the above method, an example can be given for the first-order case where

$$\dot{x}(t) = -ax(t) + a \cos \omega t \quad a > 0$$





The states are augmented by defining  $x_2$  so that

$$\dot{x}_1(t) = -ax_1 + (\cos t)x_2$$

$$\dot{x}_2(t) = 0$$

or

$$\dot{\underline{x}}(t) = \underline{A}(t)\underline{x}(t)$$

The observer state equation is

$$\dot{\underline{e}}(t) = \underline{A}(t)\underline{e}(t) + \underline{G}(t)\underline{H}[\underline{e}(t) - \underline{x}(t)]$$

where the observation matrix is

$$\underline{H} = [1 \quad 0]$$

The matrix

$$[\underline{A}(t) + \underline{G}(t)\underline{H}] = \begin{bmatrix} -a+g_1 & \cos \omega t \\ g_2 & 0 \end{bmatrix}$$

must now be tested for stability which can be accomplished by defining a Lyapunov function [Ref. 8]

$$V(t) \equiv 1/2 (\sigma_1^2(t) + \sigma_2^2(t)) \quad (7.20)$$

and its time derivative

$$\dot{V}(t) = \sigma_1(t)\dot{\sigma}_1(t) + \sigma_2(t)\dot{\sigma}_2(t) \quad (7.21)$$

For this example,

$$\begin{aligned} \dot{V}(t) &= (-a+g_1)\sigma_1^2(t) + (\cos \omega t)\sigma_1(t)\sigma_2(t) + g_2\sigma_1(t)\sigma_2(t) \\ &= (-a+g_1)\sigma_1^2(t) + (\cos \omega t + g_2)\sigma_1(t)\sigma_2(t) \end{aligned}$$

where if the values of  $g_1$  and  $g_2$  are chosen such that

$$g_1 < a$$

$$g_2 = -\cos \omega t$$



then Eq. (7.20) is positive definite and  $\dot{v}(t) < 0$ . The system is therefore stable and the estimator states will approach the plant states as  $t$  approaches infinity.

If this approach is used, additional work will be required to ensure that  $\underline{G}(t)$  can be selected so that  $[\underline{A}'(t) + \underline{G}(t)\underline{H}]$  is stable for the ship.



## VIII. CONCLUSIONS

### A. THE CONTROLLER

The easiest controller to implement is the Constant-Gain Controller since, as previously stated, it in no way depends upon any knowledge (past, present or future) of the wave forces and moments. This controller would also be the least expensive since the other two controllers are essentially the Constant-Gain Controller with additional computed control signals. On the other hand, both the Optimal Controller and the Suboptimal Controller would be more expensive and complex than the Constant-Gain Controller but would maintain the state vector closer to the origin.

The complexity of realizing the command signal depends on the nature of the wave forces and how they are estimated. If  $\underline{w}(t)$  is sinusoidal in form and is estimated directly in the time domain,  $\underline{y}(t)$  can be obtained directly for the Suboptimal Controller whereas the Optimal Controller requires either on-line or precomputed solutions of Eq. (4.25). In this case, the Suboptimal Controller is considered to be less complex and the "best" controller. If, however,  $\underline{w}(t)$  is some general periodic function requiring the FFT estimator or if the frequency domain approach is used for the single sinusoidal  $\underline{w}(t)$ , then the difference in complexity between the Optimal and Suboptimal Controllers is negligible and the choice of the "best" controller will depend upon how close it is desired to maintain



the state vector to the origin. In either case, the estimator output could be set to zero (if the estimates were bad) and both controllers would reduce to the Constant-Gain Controller, resulting in still satisfactory performance.

## B. RECOMMENDATIONS FOR FURTHER STUDY

The assumptions used in this investigation concerning sea conditions, control surface deflections and measurements result in the recommendations given below.

### 1. Sea Conditions

The constant height-to-wavelength ratio and single-frequency wave used in this investigation is not indicative of the true sea condition which is a spectrum of different height-to-wavelength ratios and frequencies [Ref. 2]. A more realistic model for sea conditions should be derived and the ship's response to this model investigated.

### 2. Control Dynamics

The ship's response should be investigated for the case where the dynamics of the control surface actuation system are included. This investigation assumed an instantaneous control surface deflection capability.

### 3. Measurement Noise

The ideal case of zero measurement noise was assumed throughout this investigation. Further investigation is recommended to include realistic measurement noise.

### 4. Wave Estimator

A wave estimator should be investigated for inclusion in the ship model and the response determined using the estimator and measurement noises as noted above.





## 5. Weighting Matrices

Further investigation is recommended in the determination of the values of the weighting matrices  $\underline{Q}$  and  $\underline{R}$ . The possibility of exceeding control surface or structural rates and the accompanying effects on personnel was not included in this investigation. If further investigation proves this to be a problem area, then new values for the state and control weights will have to be determined.

## 6. Wave Contouring

The inclusion of a realistic sea condition model will change the point where upper-body contact with the wave occurs, previously stated as being wavelengths greater than 14. This point of contact should be determined and a controller that would allow the ship to follow the wave contour instead of driving through the wave should be utilized for this case. This would result in a linear tracking problem instead of the linear regulator approach used in this investigation.



## APPENDIX A

Here it is shown that the matrix equality

$$\underline{B}'\underline{v}(t) = -\underline{C}'\underline{w}(t) \quad (4.29)$$

holds, where

$$\underline{B}' = \begin{bmatrix} b_{21} & b_{22} \\ b_{41} & b_{42} \end{bmatrix}$$

$$\underline{C}' = \begin{bmatrix} c_{21} & c_{22} \\ c_{41} & c_{42} \end{bmatrix}$$

and from which the command signal,  $\underline{v}(t)$ , can be obtained as

$$\underline{v}(t) = -\underline{B}'^{-1}\underline{C}'\underline{w}(t) \quad (4.30)$$

The matrix product

$$\begin{aligned} \underline{B}'\underline{v}(t) &= \begin{bmatrix} b_{21} & b_{22} \\ b_{41} & b_{42} \end{bmatrix} \begin{bmatrix} v_1(t) \\ v_2(t) \end{bmatrix} \\ &= \begin{bmatrix} b_{21}v_1(t) + b_{22}v_2(t) \\ b_{41}v_1(t) + b_{42}v_2(t) \end{bmatrix} \end{aligned}$$

and



$$\begin{aligned}
 -\underline{C}'\underline{w}(t) &= - \begin{bmatrix} C_{21} & C_{22} \\ C_{41} & C_{42} \end{bmatrix} \begin{bmatrix} w_1(t) \\ w_2(t) \end{bmatrix} \\
 &= - \begin{bmatrix} C_{21}w_1(t) + C_{22}w_2(t) \\ C_{41}w_1(t) + C_{42}w_2(t) \end{bmatrix}
 \end{aligned}$$

Therefore, since it is given by Eq. (4.27) that

$$b_{21}v_1(t) + b_{22}v_2(t) = -(C_{21}w_1(t) + C_{22}w_2(t))$$

and

$$b_{41}v_1(t) + b_{42}v_2(t) = -(C_{41}w_1(t) + C_{42}w_2(t))$$

which can be written as

$$\begin{bmatrix} b_{21}v_1(t) + b_{22}v_2(t) \\ b_{41}v_1(t) + b_{42}v_2(t) \end{bmatrix} = - \begin{bmatrix} C_{21}w_1(t) + C_{22}w_2(t) \\ C_{41}w_1(t) + C_{42}w_2(t) \end{bmatrix}$$

or,

$$\underline{B}'\underline{v}(t) = -\underline{C}'\underline{w}(t)$$



# APPENDIX B

Here it is shown that the matrix equality

$$\underline{B}\underline{G} = -\underline{C} \quad (4.33)$$

holds, which reduces the system equation to

$$\dot{\underline{x}} = [\underline{A} + \underline{B}\underline{F}(t)]\underline{x}(t), \quad (4.5)$$

a stable system whose state approaches zero as  $t$  approaches infinity, when the suboptimal controller is used.

$$\begin{aligned} \underline{B}\underline{G} &= \underline{B}(-\underline{B}'^{-1}\underline{C}') \\ &= -\underline{B}\underline{B}'^{-1}\underline{C}' \end{aligned}$$

$$= - \begin{bmatrix} 0 & 0 \\ b_{21} & b_{22} \\ 0 & 0 \\ b_{41} & b_{42} \end{bmatrix} \frac{\begin{bmatrix} b_{42} & -b_{22} \\ -b_{41} & b_{21} \end{bmatrix}}{(b_{21}b_{42} - b_{22}b_{41})} \begin{bmatrix} c_{21} & c_{22} \\ c_{41} & c_{42} \end{bmatrix}$$

$$= - \begin{bmatrix} 0 & 0 \\ 1 & 0 \\ 0 & 0 \\ 0 & 1 \end{bmatrix} \begin{bmatrix} c_{21} & c_{22} \\ c_{41} & c_{42} \end{bmatrix}$$

$$= - \begin{bmatrix} 0 & 0 \\ c_{21} & c_{22} \\ 0 & 0 \\ c_{41} & c_{42} \end{bmatrix}$$

$$= -\underline{C}$$





# SEMISUBMERGED SHIP PROGRAM

THIS PROGRAM SIMULATES A SEMISUBMERGED SHIP AND COMPUTES THE LONGITUDINAL RESPONSE FOR EITHER AHEAD OR FOLLOWING SEAS.

THE USER HAS THE CHOICE OF THREE CONTROL SYSTEMS--

SUBOPTIMAL  
CONSTANT-GAIN  
OPTIMAL

OR EITHER NONE AT ALL.

A MAXIMUM OF TWO (2) RUNS CAN BE MADE EACH TIME TO ALLOW A COMPARISON TO BE MADE IF ANY OF THE PARAMETERS ON THE DATA CARDS LISTED BELOW ARE CHANGED.

DATA CARDS--

1. NUMBER OF RUNS (1 OR 2)
2. SHIP'S NON-DIMENSIONAL SPEED (UHAT)
3. TIME PARAMETERS --INITIAL TIME (TI), TIME INCREMENT (DT),  
FINAL TIME (TF)
4. Q MATRIX--ROW #1
5. Q MATRIX--ROW #2
6. Q MATRIX--ROW #3
7. Q MATRIX--ROW #4
8. R MATRIX--ROW #1
9. R MATRIX--ROW #2
10. CONTROL OR NO CONTROL--  

>0	=>	YES
=0	=>	NO

\*\*IF NO CONTROL SYSTEM IS USED, DATA CARDS 11 & 12 ARE NOT USED\*\*

11. TYPE OF CONTROL SYSTEM--



```

-1 => SUBOPTIMAL
0  => CONSTANT-GAIN
+1 => OPTIMAL

```

12. UNSATURATED OR SATURATED CONTROLS--

```

-1 => UNSATURATED
+1 => SATURATED

```

13. SHIP'S NON-DIMENSIONAL INITIAL CONDITIONS--

```

HEAVE      VELOCITY
HEAVE      VELOCITY
PITCH      VELOCITY
PITCH      VELOCITY

```

14. SEA CONDITION--

```

-1 => FOLLOWING SEA
0  => CALM SEA
+1 => AHEAD SEA

```

15. NON-DIMENSIONAL OCEAN WAVELENGTH

IF TWO (2) RUNS ARE CALLED FOR IN DATA CARD #1, THEN DATA CARDS 16--29  
WILL HAVE THE SAME FORMAT AS CARDS 2--15.

```

// EXEC FORTCLGP, REGION.GO=166K
// FORT.SYSIN DD *
IMPLICIT REAL*8 (A-H,O-Z)
COMMON A(4,4), B(4,2), F(2,4), P(4,4), Q(4,4), RIBT(2,4), TEST, TEMPI(10),
* R(2,2), G(2,2), DEG, U(2,1), JU, JX, JT, MHATW, ZHATW, WEFQR, A1, B1, D1, E1,
* A2, B2, D2, E2, KNTRL, KSAT, NKNTRL, NK, I1, JJ, LL
* DIMENSION PRMT(5), Y(14), AUX(16,14), BT(2,4), BP(2,2),
* BPI(2,2), CP(2,2), GM(2,2), RI(2,2),
* EXTERNAL FCT, JUTP
PI=3.1415927D0
DEG=180.D0/PI

```

```

***

```

READ NUMBER OF RUNS TO BE MADE

```

READ(5,1452) NCURV

```

```

NK=NCURV

```

```

11

```

```

JU=0.D0

```

```

JX=0.D0

```

```

JT=0.D0

```

READ SHIP'S NON-DIMENSIONAL SPEED

```

***

```

```

SH000660
SH000670
SH000680
SH000690
SH000700
SH000710
SH000720
SH000730
SH000740
SH000750

```

```

SH000750
SH000770
SH000800
SH000810
SH000820

```



```

READ(5,1000) UHAT
WRITE(6,1010) UHAT

```

```

SH000830
SH000840

```

```

COMPUTE THE A MATRIX

```

```

A(1,1)=0.D0
A(1,2)=1.D0
A(1,3)=0.D0
A(1,4)=0.D0
A(2,1)=-.2951D0
A(2,2)=-.9362D0*UHAT**2+.207D-1
A(2,3)=-.9362D0*UHAT
A(2,4)=-.1299D1*UHAT
A(3,1)=0.D0
A(3,2)=0.D0
A(3,3)=.D0
A(3,4)=1.D0
A(4,1)=.12D-1
A(4,2)=-.5742D0*UHAT
A(4,3)=-.5742D0*UHAT**2-.2961D0
A(4,4)=-.2091D1
II=0
JJ=0
LL=0

```

```

SH000850
SH000860
SH000870
SH000880
SH000890
SH000900
SH000910
SH000920
SH000930
SH000940
SH000950
SH000960
SH000970
SH000980
SH000990
SH001000
SH001010
SH001020
SH001030

```

```

COMPUTE THE B MATRIX

```

```

DO 1 J=1,2
B(1,J)=0.D0
B(3,J)=2.D0
1 CONTINUE
B(2,1)=-.2964D0*UHAT**2
B(2,2)=-.1624D0*UHAT**2
B(4,1)=-.3706D0*UHAT**2
B(4,2)=.1452D0*UHAT**2

```

```

SH001040
SH001050
SH001060
SH001070
SH001130
SH001140
SH001150
SH001160

```

```

READ TIME PARAMETERS--TI,DT,TF

```

```

12 READ(5,1100) TI,DT,TF
WRITE(6,1105) TI,DT,TF
TEST=TF/(4.D0*DT)
PRMT(1)=TF
PRMT(2)=TI
PRMT(3)=-DT
PRMT(4)=1.D0-5
DO 2 I=1,I0
TEMP1(I)=0.D0
Y(I)=0.D0

```

```

SH001320
SH001330
SH001340
SH001350
SH001360
SH001370
SH001380
SH001390
SH001090
SH001100

```



SH001110  
SH001120  
SH001130

SH001400  
SH001410  
SH001420  
SH001430  
SH001440

SH001450  
SH001460  
SH001470  
SH001480

SH001162  
SH001485  
SH001530

SH001540  
SH001550  
SH001560  
SH001570  
SH001580  
SH001590  
SH001600

SH001770

SH001775  
SH001780  
SH001790

SH001170

```

DERY(I)=.1D0
2  CONTINUE
  WRITE(6,1110)

READ Q MATRIX ROW BY ROW

DO 3 I=1,4
  READ(5,1200) (Q(I,J),J=1,4)
  WRITE(6,1111) (Q(I,J),J=1,4)
3  CONTINUE
  WRITE(6,1210)

READ R MATRIX ROW BY ROW

DO 4 I=1,2
  READ(5,1112) (R(I,J),J=1,2)
  WRITE(6,1205) (R(I,J),J=1,2)
4  CONTINUE

READ WHETHER CONTROL SYSTEM IS DESIRED OR NOT

READ(5,1452) NKNTL
IF(NKNTL.EQ.0) GO TO 13
WRITE(6,1005)

COMPUTE THE CONSTANT K MATRIX

CALL DTRAN(B,BT,4,2)
CALL DRINV(R,RI)
CALL DMPRD(RI,BT,RIBT,2,2,4)
CALL DMPCG(B,RIBT,P,4,2,4)
CALL DHPCG(P,MT,Y,DERY,10,IHLF,FCT,OUTP,AUX)
WRITE(6,1300) IHLF
LL=4

READ TYPE OF CONTROL SYSTEM TO USE

READ(5,1451) KNTRL

READ WHETHER OR NOT THE CONTROLS ARE SATURATED

READ(5,1451) KSAT
IF (KNTRL) 8,9,10
8  WRITE(6,1465)

COMPUTE THE G MATRIX

CP(1,1)=0.4907D0

```

\*\*\*

\*\*\*

\*\*\*

\*\*\*

\*\*\*

\*\*\*

\*\*\*





SH001180  
SH001190  
SH001200  
SH001210  
SH001220  
SH001230  
SH001240  
SH001250  
SH001260  
SH001270  
SH001280  
SH001290  
SH001300  
SH001310  
SH001800  
SH001810  
SH001820  
SH001830  
SH001490  
SH001500  
SH001510  
SH001520  
SH001832  
SH001610  
SH001620  
SH001630  
SH001640  
SH001650  
SH001660  
SH001670

SH001680  
SH001690  
SH001700  
SH001710  
SH001720  
SH001730  
SH001734

SH001740  
SH001750

```

CP(1,2)=-0.503D-1
CP(2,1)=-0.503D-1
CP(2,2)=0.2865D0
DO 6 I=1,2
  K=2*I
DO 6 J=1,2
  BP(I,J)=B(K,J)
6 CONTINUE
CALL DRINV(BP,BPI)
CALL DMPRD(BPI,CP,GM,2,2,2)
DO 7 I=1,2
  DO 7 J=1,2
    G(I,J)=-GM(I,J)
7 CONTINUE
GO TO 121
9 WRITE(6,1466)
GO TO 121
10 WRITE(6,1467)
  M=2
  IF(R(1,1).LT.0.9D0) M=0
  IF(R(1,1).LT.0.4D0) M=-2
  CALL EST(A2,B2,E2,D2,M)
  GO TO 121
121 PRMT(1)=TI
  PRMT(2)=TF
  PRMT(3)=DT
  DO 5 I=1,6
    DERY(I)=1.D0/5.D0
5 CONTINUE
  WRITE(6,1250)

**
**
**
  READ SHIP'S NON-DIMENSIONAL INITIAL CONDITIONS
13 READ(5,1200) (Y(I),I=1,4)
  WRITE(6,1350) UHAT,(Y(I),I=1,4)
  Y(5)=0.D0
  Y(6)=0.D0
  II=0
  JJ=0
  IF(NKNTL.EQ.0) WRITE(6,1468)

**
**
**
  READ SEA CONDITION
  READ(5,1451) ISEA
  IF(ISEA.EQ.0.D0) GO TO 119

**
**
**
  READ NON-DIMENSIONAL OCEAN WAVELENGTH

```



SH001750

SH001840

READ(5,1461) WLHAT

COMPUTE THE WAVE FORCES (ZHATW) AND MOMENTS (MHATW)

IF(ISEA) 100,119,110

FOLLOWING SEA

```
100 PSI=0.D0
WRITE(6,1470) WLHAT
WEFRQ=DSQRT(2.D0*PI/WLHAT)-2.D0*PI*UHAT/WLHAT*DCOS(PSI/DEG)
IF(UHAT.GT.1.1D0) GO TO 101
A1=0.408926D0-0.294982D0*WLHAT+0.591889D-1*WLHAT**2-0.510023D-2*
WLHAT**3+0.2318D-3*WLHAT**4-0.539434D-5*WLHAT**5+0.505979D-7*
WLHAT**6
B1=-0.350088D0+0.147652D0*WLHAT-0.164184D-1*WLHAT**2+0.887811D-3*
WLHAT**3-0.254773D-4*WLHAT**4+0.3331D-6*WLHAT**5-0.109496D-8*
WLHAT**6
D1=-1.39117D0+0.597654D0*WLHAT-0.768856D-1*WLHAT**2+0.539146D-2*
WLHAT**3-0.214538D-3*WLHAT**4+0.451631D-5*WLHAT**5-0.389348D-7*
WLHAT**6
E1=0.388758D0-0.274848D0*WLHAT+0.550417D-1*WLHAT**2-0.465091D-2*
WLHAT**3+0.204644D-3*WLHAT**4-0.456401D-5*WLHAT**5+0.407234D-7*
WLHAT**6
GO TO 120
101 A1=0.626065D0-0.453279D0*WLHAT+0.91014D-1*WLHAT**2-0.776281D-2*
WLHAT**3+0.348576D-3*WLHAT**4-0.803407D-5*WLHAT**5+0.750506D-7*
WLHAT**6
B1=-0.507524D0+0.222259D0*WLHAT-0.273648D-1*WLHAT**2+0.170222D-2*
WLHAT**3-0.576673D-4*WLHAT**4+0.966982D-6*WLHAT**5-0.584761D-8*
WLHAT**6
D1=-2.33443D0+0.971726D0*WLHAT-0.12184D0*WLHAT**2+0.830526D-2*
WLHAT**3-0.32266D-3*WLHAT**4+0.6696D-5*WLHAT**5-0.575847D-7*
WLHAT**6
E1=0.766135D0-0.492584D0*WLHAT+0.100878D0*WLHAT**2-0.900991D-2*
WLHAT**3+0.424255D-3*WLHAT**4-0.102077D-4*WLHAT**5+0.986452D-7*
WLHAT**6
GO TO 120
```

AHEAD SEA

```
110 PSI=180.D0
WRITE(6,1475) WLHAT
WEFRQ=DSQRT(2.D0*PI/WLHAT)-2.D0*PI*UHAT/WLHAT*DCOS(PSI/DEG)
IF(UHAT.GT.1.1D0) GO TO 111
A1=0.502667D0-0.364173D0*WLHAT+0.798172D-1*WLHAT**2-0.766724D-2*
WLHAT**3+0.385676D-3*WLHAT**4-0.983189D-5*WLHAT**5+0.100043D-6*
WLHAT**6
```



```

B1=-0.547692D-1+0.662901D-2*WLHAT+0.12247D-2*WLHAT**2-0.245175D-3*
  WLHAT**3+0.144963D-4*WLHAT**4-0.395096D-6*WLHAT**5+0.416539D-8*
  WLHAT**6
D1=1.04556D-0-0.442992D-0*WLHAT+0.528556D-1*WLHAT**2-0.33672D-2*
  WLHAT**3+0.119255D-3*WLHAT**4-0.218464D-5*WLHAT**5+0.15902D-7*
  WLHAT**6
E1=-0.551822D+0.224035D-0*WLHAT-0.290222D-1*WLHAT**2+0.227802D-2*
  WLHAT**3-0.104387D-3*WLHAT**4+0.256714D-5*WLHAT**5-0.259431D-7*
  WLHAT**6
GO TO 120
111 A1=0.714126D-0.531282D-0*WLHAT+0.11505D-0*WLHAT**2-0.107728D-1*
  WLHAT**3+0.529087D-3*WLHAT**4-0.13218D-4*WLHAT**5+0.13215D-6*
  WLHAT**6
B1=0.155114D-0-0.964082D-1*WLHAT+0.163468D-1*WLHAT**2-0.127389D-2*
  WLHAT**3+0.472894D-4*WLHAT**4-0.787404D-6*WLHAT**5+0.405063D-8*
  WLHAT**6
D1=1.81165D-0-0.776761D-0*WLHAT+0.949809D-1*WLHAT**2-0.62921D-2*
  WLHAT**3+0.237888D-3*WLHAT**4-0.483654D-5*WLHAT**5+0.411761D-7*
  WLHAT**6
E1=-0.45764D+0.11325D-0*WLHAT+0.23954D-2*WLHAT**2-0.15712D-2*
  WLHAT**3+0.854828D-4*WLHAT**4-0.263091D-5*WLHAT**5+0.299181D-7*
  WLHAT**6
GO TO 120

```

\*\*\*

CALM SEA

```

119 WRITE(6,1480)

```

```

A1=0.D0
B1=0.D0
D1=0.D0
E1=0.D0
A2=0.D0
B2=0.D0
D2=0.D0
E2=0.D0
WEFR0=0.D0

```

\*\*\*

COMPUTE THE TIME HISTORIES OF THE SHIP'S RESPONSES

```

120 CALL DHPG (PRVT,Y,DERY,6,IHLF,FCT,OUTP,AUX)
  WRITE(6,1300) IHLF
  WRITE(6,1485) JX,JU,JT
  NK=NK-1

```

\*\*\*

RETURN FOR MORE DATA IF ANOTHER RUN IS CALLED FOR

```

IF(NK.GT.0) GO TO 11
LL=10

```

```

SH002590
SH002600

```

```

SH002450
SH002460
SH002470
SH002480
SH002490
SH002500
SH002510
SH002520
SH002530
SH002540

```

```

SH002550
SH002560
SH002570
SH002580

```





PRINT OR PLOT OUTPUT AS DESIRED

STOP  
SEND





```

**      **      **
SUBROUTINE DTRAN(X,Y,M,N)
THIS SUBROUTINE TAKES THE TRANSPOSE OF AN (M X N) MATRIX X AND RETURNS IT
IN AN (N X M) MATRIX Y. (DOUBLE PRECISION)
SH002980

IMPLICIT REAL*8 (A-H,O-Z)
DIMENSION X(M,N),Y(N,M)
DO 1 I=1,M
DO 1 J=1,N
Y(J,I)=X(I,J)
1 CONTINUE
RETURN
END
SH002990
SH003000
SH003010
SH003020
SH003030
SH003040
SH003050
SH003060

**      **      **
SUBROUTINE DMPRD(A,B,C,L,M,N)
THIS SUBROUTINE PERFORMS THE DOUBLE PRECISION MATRIX MULTIPLICATION
A(L X M)*B(M X N)=C(L X N)
SH003100

IMPLICIT REAL*8 (A-H,O-Z)
DIMENSION A(L,M),B(M,N),C(L,N)
DO 1 I=1,L
DO 1 J=1,N
C(I,J)=0.D0
DO 1 K=1,M
1 C(I,J)=C(I,J)+A(I,K)*B(K,J)
RETURN
END
SH003110
SH003120
SH003130
SH003140
SH003150
SH003160
SH003170
SH003180
SH003190

**      **      **
SUBROUTINE FCT(X,Y,DERY)
THIS SUBROUTINE CONTAINS THE DIFFERENTIAL EQUATIONS TO BE SOLVED BY THE IBM
SUBROUTINE DHPG.
SH003230

IMPLICIT REAL*8 (A-H,O-Z)
REAL*8 JU,JX,JT,MHATW
COMMON A(4,4),B(4,2),F(2,4),P(4,4),Q(4,4),RIBT(2,4),TEST,TEMP1(10)
*,R(2,2),G(2,2),DEG,U(2,1),JU,JX,JT,MHATW,ZHATW,WEFRQ,A1,B1,D1,E1,
*A2,B2,D2,E2,KNTRL,KSAT,NKNTRL,NK,I1,JJ,LL
DIMENSION XT(1,4),QX(4),UT(1,2),RU(2,1),V(2),Y(1),DERY(1)
IF(LL.GT.2) GO TO 2
DIFFERENTIAL EQUATIONS FOR SOLVING THE CONSTANT K MATRIX.
SH003240
SH003250
SH003260
SH003270
SH003280
SH003290
SH003300
SH003310
SH003320
SH003330

DERY(1)=-2.D0*(A(2,1)*Y(2)+A(4,1)*Y(4))-Q(1,1)+P(2,2)*Y(2)**2
*+(P(2,4)+P(4,2))*Y(2)*Y(4)+P(4,4)*Y(4)**2

```



```

DERY(2)=-Y(1)-A(2,2)*Y(2)-A(4,2)*Y(4)-A(2,1)*Y(5)-A(4,1)*Y(7)
      -Q(1,2)+P(2,2)*Y(2)+P(2,4)*Y(7)+P(4,2)*Y(4)*Y(5)
      +P(4,4)*Y(7)
DERY(3)=-A(2,3)*Y(2)-A(4,3)*Y(4)-A(2,1)*Y(6)-A(4,1)*Y(9)-Q(1,3)
      +P(2,2)*Y(2)*Y(6)+P(2,4)*Y(9)+P(4,2)*Y(4)*Y(6)
      +P(4,4)*Y(9)
DERY(4)=-A(2,4)*Y(2)-Y(3)-A(4,4)*Y(4)-A(2,1)*Y(7)-A(4,1)*Y(10)
      -Q(1,4)+P(2,2)*Y(2)*Y(7)+P(2,4)*Y(10)+P(4,2)*Y(4)*
      Y(7)+P(4,4)*Y(10)
DERY(5)=-2.*D0*(Y(2)+A(2,2)*Y(5)+A(4,2)*Y(7))-Q(2,2)+P(2,2)*Y(5)**2
      +(P(2,4)+P(4,2))*Y(5)*Y(7)+P(4,4)*Y(7)**2
DERY(6)=-Y(3)-A(2,3)*Y(5)-A(2,2)*Y(6)-A(4,3)*Y(7)-A(4,2)*Y(9)
      -Q(2,3)+P(2,2)*Y(5)*Y(6)+P(2,4)*Y(9)+P(4,2)*Y(6)*Y(7)
      +P(4,4)*Y(9)
DERY(7)=-Y(4)-A(2,4)*Y(5)-Y(6)-A(2,2)+A(4,4)*Y(7)-A(4,2)*Y(10)
      -Q(2,4)+P(2,2)*Y(5)*Y(7)+P(2,4)*Y(10)+P(4,4)*Y(7)
      *Y(10)+P(4,2)*Y(7)**2
DERY(8)=-2.*D0*(A(2,3)*Y(6)+A(4,3)*Y(9))-Q(3,3)+P(2,2)*Y(6)**2
      +(P(2,4)+P(4,2))*Y(6)*Y(9)+P(4,4)*Y(9)**2
DERY(9)=-A(2,4)*Y(6)-A(2,3)*Y(7)-Y(8)-A(4,4)*Y(9)-A(4,3)*Y(10)
      -Q(3,4)+P(2,2)*Y(6)*Y(7)+P(2,4)*Y(9)+P(4,2)*Y(7)*
      Y(9)+P(4,4)*Y(10)
DERY(10)=-2.*D0*(A(2,4)+P(4,2)*Y(7)+Y(9)+A(4,4)*Y(10))-Q(4,4)+P(2,2)*Y(7)*
      *2+(P(2,4)+P(4,2))*Y(7)*Y(10)+P(4,4)*Y(10)**2
      RETURN

```

# STATE EQUATIONS FOR THE SEMISUBMERGED SHIP

```

2  ZHATW=A1*DCOS(-WEFRQ*X)+B1*DSIN(-WEFRQ*X)
   MHATW=E1*DCOS(-WEFRQ*X)+D1*DSIN(-WEFRQ*X)
   IF(NKNTL.EQ.0) GO TO 8
3  U(1,1)=F(1,1)*Y(1)+F(1,2)*Y(2)+F(1,3)*Y(3)+F(1,4)*Y(4)+G(1,1)*
   *ZHATW+G(1,2)*MHATW
   U(2,1)=F(2,1)*Y(1)+F(2,2)*Y(2)+F(2,3)*Y(3)+F(2,4)*Y(4)+G(2,1)*
   *ZHATW+G(2,2)*MHATW
   GO TO 6
4  U(1,1)=F(1,1)*Y(1)+F(1,2)*Y(2)+F(1,3)*Y(3)+F(1,4)*Y(4)
   U(2,1)=F(2,1)*Y(1)+F(2,2)*Y(2)+F(2,3)*Y(3)+F(2,4)*Y(4)
   GO TO 6
5  V(1)=A2*DCOS(-WEFRQ*X)+B2*DSIN(-WEFRQ*X)
   V(2)=E2*DCOS(-WEFRQ*X)+D2*DSIN(-WEFRQ*X)
   U(1,1)=F(1,1)*Y(1)+F(1,2)*Y(2)+F(1,3)*Y(3)+F(1,4)*Y(4)+V(1)
   U(2,1)=F(2,1)*Y(1)+F(2,2)*Y(2)+F(2,3)*Y(3)+F(2,4)*Y(4)+V(2)
   GO TO 6
8  U(1,1)=0.D0
   U(2,1)=0.D0
   GO TO 10

```

\*\*\*







```

IF(CHECK.GE.1.D-2) GO TO 9
1 CONTINUE
II=II+1
IF(II.GE.TEST) GO TO 2
RETURN
9 TEMPI(I)=Y(I)
II=0
RETURN

```

\*\*\*

STORE THE STEADY-STATE VALUES IN THE MATRIX GAIN(I,J)

```

2 PRMT(5)=2.D0
KJ=-1
DO 4 I=1,4
KJ=KJ+1
IF(I.EQ.4) KJ=2
DO 4 J=1,4
IJ=I+J+KJ
IF(I.EQ.1) IJ=J+KJ
KMAT(I,J)=-Y(IJ)
KMAT(J,I)=KMAT(I,J)
4 CONTINUE
DO 8 I=1,4
DO 8 J=1,4
GAIN(I,J)=-KMAT(I,J)
8 CONTINUE

```

\*\*\*

COMPUTE THE CONSTANT STATE VECTOR FEEDBACK MATRIX F

```

CALL DMPRD(RIBT,KMAT,F,2,4,4)
WRITE(6,60)
DO 5 I=1,2
WRITE(6,55) (I,J,F(I,J),J=1,4)
5 CONTINUE
DO 7 I=1,4
WRITE(6,60)
WRITE(6,65) (I,J,GAIN(I,J),J=1,4)
7 CONTINUE
RETURN
20 IF(LL.GT.5) GO TO 30
IF(JJ.LT.1) GO TO 21
JJ=JJ+1
IF(JJ.GE.14) JJ=0
RETURN
21 II=II+1
JJ=JJ+1
IF(NK.LT.2) GO TO 23

```

\*\*\*

SH004110  
SH004120  
SH004130  
SH004140  
SH004150  
SH004160  
SH004170  
SH004180

SH004190  
SH004200  
SH004210  
SH004220  
SH004230  
SH004240  
SH004250  
SH004260  
SH004270  
SH004280  
SH004290  
SH004300  
SH004310  
SH004320  
SH004330

SH004340  
SH004350  
SH004360  
SH004370  
SH004380  
SH004390  
SH004400  
SH004410  
SH004420  
SH004430  
SH004440  
SH004450  
SH004460  
SH004470  
SH004480  
SH004490  
SH004500  
SH004510





RUN #1 TIME HISTORIES--

\*\*\*\*\*

X1=>HEAVE VELOCITY  
X2=>HEAVE VELOCITY  
X3=>PITCH VELOCITY  
X4=>PITCH VELOCITY  
X5=>ELEVATOR CONTROL SURFACE  
X6=>CANARD CONTROL SURFACE

X1(I1)=Y(1)  
X2(I1)=Y(2)\*DEG  
X3(I1)=Y(3)\*DEG  
X4(I1)=Y(4)\*DEG  
X5(I1)=U(1,1)\*DEG  
X6(I1)=U(2,1)\*DEG  
TIME1(I1)=X  
GO TO 25

SH004520  
SH004530  
SH004540  
SH004550  
SH004560  
SH004570  
SH004580  
SH004590

RUN #2 TIME HISTORIES--

\*\*\*\*\*

X7=>HEAVE VELOCITY  
X8=>HEAVE VELOCITY  
X9=>PITCH VELOCITY  
X10=>PITCH VELOCITY  
X11=>ELEVATOR CONTROL SURFACE  
X12=>CANARD CONTROL SURFACE

23 X7(I1)=Y(1)  
X8(I1)=Y(2)\*DEG  
X9(I1)=Y(3)\*DEG  
X10(I1)=Y(4)\*DEG  
X11(I1)=U(1,1)\*DEG  
X12(I1)=U(2,1)\*DEG  
TIME2(I1)=X

SH004600  
SH004610  
SH004620  
SH004630  
SH004640  
SH004650  
SH004660

COMPUTE THE PERFORMANCE MEASURE JT (J TOTAL)

\*\*\*\*\*

25 JX=JX+Y(5)  
JU=JU+Y(6)  
JT=JX+JU  
IF(I1.EQ.1000) PRMT(5)=1.D0  
RETURN

SH004670  
SH004680  
SH004690  
SH004700  
SH004710

THIS PART OF THE PROGRAM MAY BE USED FOR PRINTING OR PLOTTING THE OUTPUT.  
NPS SUBROUTINE DRAW WAS USED DURING THE INVESTIGATION.

\*\*\*\*\*

30 READ(5,90) TITLE  
CALL DRAW(I1,TIME1,X1,1,0,LABEL,TITLE,10,,2,3,RT,2,0,8,4,0,Z)  
CALL DRAW(I1,TIME2,X7,3,0,LABEL,TITLE,10,,2,3,RT,2,0,8,4,0,Z)  
READ(5,90) TITLE

SH004840  
  
SH004880



```

CALL DRAW(I1, TIME1, X3, 1, 0, LABEL, TITLE, 10, 10, 1, RT, 2, 0, 8, 4, 0, Z)
CALL DRAW(I1, TIME2, X9, 3, 0, LABEL, TITLE, 10, 10, 1, RT, 2, 0, 8, 4, 0, Z)
WRITE(6, 86) I1
FORMAT(4(4X, 'F(', I1, ', ', I1, ') = ', D16.8), /, /)
FORMAT(4(4X, 'K(', I1, ', ', I1, ') = ', D16.8), /, /)
FORMAT(4(4X, 'T9, 'TIME1', T28, 'HEAVE', T40, 'HEAVE VELOCITY', T64, 'PITCH',
84 * T76, 'PITCH VELOCITY', T97, 'ELEVATOR', T117, 'CANARD', /, /)
FORMAT(7(F16.8, 2X))
FORMAT(20X, 'I1 = ', I4)
FORMAT(6A8)
FORMAT(A4)
RETURN
END

```

SH005100  
SH005110  
SH005120  
SH005130  
SH005140  
SH005150  
SH005160  
SH005170  
SH005210  
SH005220  
SH005240  
SH005250

SH005290

THIS SUBROUTINE COMPUTES THE DOUBLE PRECISION INVERSE OF A (2 X 2) MATRIX A  
AND RETURNS THE RESULT IN THE (2 X 2) MATRIX B.

```

IMPLICIT REAL*8 (A-H, C-Z)
DIMENSION A(2,2), B(2,2)
DEL=A(1,1)*A(2,2)-A(1,2)*A(2,1)
B(1,1)=A(2,2)/DEL
B(1,2)=-A(1,2)/DEL
B(2,1)=-A(2,1)/DEL
B(2,2)=A(1,1)/DEL
RETURN
END

```

\*\*\*\*\*

SH005300  
SH005310  
SH005320  
SH005330  
SH005340  
SH005350  
SH005360  
SH005370  
SH005380

SH005420

THIS SUBROUTINE RETURNS THE COEFFICIENTS OF THE COMMAND SIGNAL V(T) WHEN  
UAT IS 1.0

SH005430  
SH005440

THE R MATRIX IS ONE TENTH OF THE IDENTITY MATRIX

```

1 A=0.1913560000*DSIN(3.204156965D0)
B=-0.1913560000*DCOS(3.204156965D0)
C=0.17333513D0*DSIN(0.477839366D0)
D=-0.17333513D0*DCOS(0.477839366D0)
RETURN

```

\*\*\*\*\*



\*\*\*

THE R MATRIX IS ONE HALF OF THE IDENTITY MATRIX

```
2  A=0.12337738D0*DSIN(3.405767837D0)
   B=-0.12337738D0*DCOS(3.405767837D0)
   C=0.10170269D0*DSIN(0.342135621D0)
   D=-0.10170269D0*DCOS(0.342135621D0)
   RETURN
```

\*\*\*

THE R MATRIX IS THE IDENTITY MATRIX

```
3  A=0.9399569D-1*DSIN(3.432566603D0)
   B=-0.9399569D-1*DCOS(3.432566603D0)
   C=0.7081240D-1*DSIN(0.218452002D0)
   D=-0.7081240D-1*DCOS(0.218452002D0)
   RETURN
   END
```

SH005500  
SH005510  
SH005520  
SH005530  
SH005540

SH005550  
SH005560  
SH005570  
SH005580  
SH005590  
SH005600



## LIST OF REFERENCES

1. Naval Undersea Research and Development Center Technical Note TN-414, Naval Feasibility Study of the NUC Semi-Submerged Ship Concept, Part 1, by T. G. Lang, September 1970.
2. Abkowitz, M. A., Stability and Motion Control of Ocean Vehicles, M.I.T. Press, 1969.
3. Naval Undersea Research and Development Center Technical Note TN-582, Dynamics and Control of a Twin-Hulled Semisubmerged Ship, by D. T. Higdon, 1 August 1971.
4. Ward, J. R. and Strum, R. D., The Signal Flow Graph in Linear Systems Analysis, Prentice-Hall, 1968.
5. Kirk, D. E., Optimal Control Theory, An Introduction, Prentice-Hall, 1970.
6. Kalman, R. E., "Contributions to the Theory of Optimal Control," Bol. Soc. Mat. Mex., 1960.
7. Athans, M. and Falb, P.L., Optimal Control, p. 773, 801, McGraw-Hill, 1966.
8. Hsu, J.C. and Meyer, A.U., Modern Control Principles and Applications, p. 342, McGraw-Hill, 1968.





# INITIAL DISTRIBUTION LIST

	No. Copies
1. Defense Documentation Center Cameron Station Alexandria, Virginia 22314	2
2. Library, Code 0212 Naval Postgraduate School Monterey, California 93940	2
3. Professor Donald E. Kirk, Code 52 Ki Department of Electrical Engineering Naval Postgraduate School Monterey, California 93940	4
4. Professor Harold A. Titus, Code 52 Ts Department of Electrical Engineering Naval Postgraduate School Monterey, California 93940	6
5. Dr. Donald T. Higdon Advanced Concepts Group Naval Undersea Research and Development Center San Diego, California 92106	1
6. LT Gilbert F. Monell, Jr., USN 3508 Schoolhouse Lane Harrisburg, Pennsylvania 17109	1



Unclassified

Security Classification

## DOCUMENT CONTROL DATA - R &amp; D

(Security classification of title, body of abstract and indexing annotation must be entered when the overall report is classified)

1. ORIGINATING ACTIVITY (Corporate author)		2a. REPORT SECURITY CLASSIFICATION	
Naval Postgraduate School Monterey, California 93940		Unclassified	
		2b. GROUP	
3. REPORT TITLE			
AUTOMATIC CONTROL SYSTEMS FOR LONGITUDINAL MOTION OF SEMISUBMERGED SHIPS			
4. DESCRIPTIVE NOTES (Type of report and inclusive dates)			
Electrical Engineer Thesis; September 1972			
5. AUTHOR(S) (First name, middle initial, last name)			
Gilbert Finley Monell, Jr. Lieutenant, United States Navy			
6. REPORT DATE		7a. TOTAL NO. OF PAGES	7b. NO. OF REFS
September 1972		113	8
8a. CONTRACT OR GRANT NO.		9a. ORIGINATOR'S REPORT NUMBER(S)	
b. PROJECT NO.			
c.		9b. OTHER REPORT NO(S) (Any other numbers that may be assigned this report)	
d.			
10. DISTRIBUTION STATEMENT			
Approved for public release; distribution unlimited.			
11. SUPPLEMENTARY NOTES		12. SPONSORING MILITARY ACTIVITY	
		Naval Postgraduate School Monterey, California 93940	
13. ABSTRACT			
<p>Optimal control theory is used to develop three automatic control systems for the longitudinal motion of a semisubmerged ship. A linearized mathematical model of the ship motion is used and the control problem is treated as a linear regulator. Simulations of the ship's longitudinal motions, utilizing the three control systems, are compared for various sea conditions. It is concluded that if the wave forces and moments are known or are estimated as functions of time, a suboptimal controller is the best controller. However, if a frequency domain approach is used to estimate the wave forces and moments, the complexity of a suboptimal controller approaches that of an optimal controller and the difference between the two is negligible. Preliminary work on three techniques for estimating the forces and moments is presented.</p>			



14 KEY WORDS	LINK A		LINK B		LINK C	
	ROLE	WT	ROLE	WT	ROLE	WT
Semisubmerged Ship Optimal Control Suboptimal Control Linear Regulator Estimator Observer						



5 NOV 74  
25 MAY 76  
12 MAR 79

22793  
23200  
25275

Thesis  
M673  
c.1

Monell

Automatic control systems for longitudinal motion of semisubmerged ships.

137134

5 NOV 74  
25 MAY 76  
12 MAR 79

22793  
23200  
25275

Thesis  
M673  
c.1

Monell

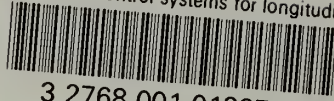
Automatic control systems for longitudinal motion of semisubmerged ships.

137134



thesM673

Automatic control systems for longitudin



3 2768 001 01227 1

DUDLEY KNOX LIBRARY